ETALON

D 4.1 Trackside Energy harvester solutions report

Due date of deliverable: 30/04/2018

Actual submission date: 28/05/2018

Leader of this Deliverable: Jan Smilek, Brno University of Technology

Reviewed: Yes

Project funded from the European Union's Horizon 2020 research and innovation programme		
Dissemination Level		
PU	Public	X
CO	Confidential, restricted under conditions set out in Model Grant Agreement	
CI	Classified, information as referred to in Commission Decision 2001/844/EC	

Document status		
Revision	Date	Description
1	01.03.18	First draft of Trackside Energy harvester solutions
2	06.04.18	Contribution of chapters Physical principles of energy harvesting and Trackside energy harvesting design options
3	10.04.18	Update of Vibration energy harvesting technologies and analysis of preselected energy harvesting systems
4	13.04.18	Update of Trackside energy harvesting design
5	19.04.18	Contribution to the finalization of analyses and pre-selection
6	26.04.18	Preliminary version for WP4 partners
7	26.04.18	Chapter Conclusion was added
8	26.04.18	Revised document
9	27.04.18	Final draft version ready for TMT revision
10	16.05.18	Post-TMT revision of the document
11	25.05.18	Final version
12	28.05.18	Quality Check

Start date of project: 01/09/2017 Duration: 30 months

REPORT CONTRIBUTORS

Name	Company
Jan Smilek	BUT
Zdenek Hadas	BUT
Pavel Tofel	BUT
Cristian Ulianov	UNEW
Paul Hyde	UNEW
Yao Dong Wang	UNEW
Boru Jia	UNEW
David Vincent	PER

EXECUTIVE SUMMARY

This report presents the outcomes of a survey of the energy harvesting-based power source capabilities for trackside smart object controllers. The objectives of this deliverable were set as follows:

- Determine the requirements and define railway track parameters
- Perform a survey of potentially available energy conversion principles
- Research currently existing TEH solutions and evaluate their feasibility and readiness level for the given application
- Identify suitable principles and candidates to be implemented, including their potential limitations
- Deliver an educated recommendation for a future trackside energy harvesting system

The aforementioned objectives have all been successfully achieved within the planned timeframe.

Track environment was analysed, defining the basic railway parameters that can be used for later modelling and simulations of TEH performance. The potential sources of input energy for conversion were found in the trackside environment: mechanical movements of the track parts, energy of the air flow caused either by the passing train or by the regular winds, energy of the passing train itself, and solar energy. Each of these sources provide potentially significant levels of ambient energy available for extraction and conversion into electricity, without negatively affecting the environment, including, but not limited to the track dynamic parameters.

The piezoelectric effect, electromagnetic induction, electrostatic conversion, magnetostriction, and triboelectric effects are introduced from both historical and functional points of view as exploitable electromechanical energy conversion methods. Furthermore, photovoltaic and thermoelectric effects are presented as potentially feasible energy conversion methods for other than mechanical energy conversion into electricity.

A survey of existing energy harvesting solutions that were designed for, or can be adapted for the trackside environment was concluded. The reported solutions use most of the energy conversion methods presented in previous chapters of the report, with the exceptions of electrostatic and thermoelectric conversion, which are not feasible for the trackside environment due to their working characteristics and requirements (priming voltage, scalability, temperature gradient). The majority of the electromechanical harvesting solutions found exploit electromagnetic energy conversion with different excitation types, such as direct excitation through relative movement of railway and/or train parts, vibrations, or air flow energy harvesting utilising wind turbines.

From the technology readiness level point of view, the most advanced reported solutions for TEH are wind turbines and solar panels. Displacement-based electromagnetic TEHs exploiting geared generators also report generally high technology readiness levels, compared to all piezoelectric, triboelectric or even vibration-based electromagnetic harvesters.

During the pre-selection of feasible trackside energy harvesting solutions, the strengths and weaknesses of different design options were investigated, and four basic approaches were selected for further consideration: a variable reluctance harvester, and a displacement-based harvester

utilizing a relative movement of track parts, both of them selected for their promising power output capabilities; a vibration harvester for its maintenance-free operation, and solar panels, considered mainly for the high technology readiness level and easy scalability. Theoretical power outputs of these TEH solutions were then analysed using estimated available input energy levels to determine the most feasible candidate for powering the smart trackside object controller. The analyses indicate, that:

- A variety of technologies is available to meet a range of energy demand types that may be distributed down the track.
- Energy harvesting technologies in direct contact with the track and/or rolling stock (wheels) have the advantage of offering the opportunity for a self-contained, compact system.
- Inertial/resonant energy harvesters have a low impact on track and rolling stock, but only offer low output power (milliwatts as the train passes over).
- Conventional energy harvester systems (solar, wind) provide more power but are more vulnerable to the environment (weather, theft, vandalism). A higher cost for the installation is driven by the mounting infrastructure for the units and higher energy storage requirements. Trackside combined harvesting installations do indicate appropriate solutions may be implemented, however.
- Track and wheel coupled harvester designs may use a common mechanical format with a variety of transduction techniques. For simplicity, we have focused on linear electromagnetic energy conversion.

Presented in the following document is an outline of some available energy harvesting technologies, with sufficient background information and output analysis to, in the first instance, guide further work in this project, and ultimately guide development of energy harvester powered object controllers by demonstrating opportunities and limitations of energy harvesting in this environment.

TABLE OF CONTENTS

LIST OF FIGURES

LIST OF TABLES

LIST OF PARTICIPANTS

NO	LEGAL NAME	SHORT NAME
3	ARDANUY INGENIERIA SA	ARDANUY
7	Perpetuum Limited	PER
8	University of Newcastle upon Tyne	UNEW
9	VYSOKE UCENI TECHNICKE V BRNE	BUT

TRACKSIDE ENERGY HARVESTER SOLUTIONS REPORT

1 INTRODUCTION

1.1 THE ETALON PROJECT

The ETALON project focus is the development and/or adaptation of energy harvesting technologies for powering trackside and on-board signalling and communication devices. The project scope is addressed by two work-streams. The first is the development of competitive solutions for enhancing train integrity functionalities, including provision of a suitable energy supply for on board train integrity devices. This is particularly targeted at cases where trains do not have any power supply available on the vehicles (e.g., freight trains). Emphasis is also placed on considering the proposition of a robust communication system that will overcome on-board communication issues within the rail environment. The second work-stream focuses on the development of competitive energy harvesting solutions for enhancing trackside object controller deployment, with the vision to minimising trackside infrastructure, especially cabling. Specifically relevant to the S2R, the ETALON project Technical Objectives are to:

1: Identify, adapt and validate effective solutions for on-board Train Integrity radio communication systems (including antennas suitable to be installed in the queue of a very long train);

2: Identify, adapt and validate effective energy generation solutions for feeding on-board Train Integrity systems;

3: Identify the most suitable energy harvesting solution for new trackside Object Controllers, considering both a technical and economic point of view;

4: Demonstrate the efficiency of proposed energy harvesting solutions for trackside Object Controllers, ensuring appropriate safety considerations; As a result of these activities, ETALON will specify and develop energy harvesting solutions to support on-board train integrity and trackside object controllers which are economically viable and suitable for application, particularly considering modern radio communication requirements and safety critical aspects. The prototypes will be tested and validated in controlled as well as real environments.

1.2 PURPOSE OF THIS DOCUMENT

This report is meant to provide an overview of potential trackside energy harvester solutions, both available (with or without adaptation) and early concepts requiring development. This deliverable should serve as a comprehensive guide to trackside energy harvesting solutions, providing the reader with an overview of potentially exploitable energy conversion methods, and their current stages of development, at different TRL levels.

Based on the data processing and transmission requirements established in cooperation with D2.1, some of the presented technologies are expected to be rejected at this stage, and the theoretical and practical limitations of others are to be identified.

Furthermore, the report is meant to compare the feasible energy harvesting approaches and to provide initial analyses of pre-selected candidates for the trackside application so that a suitable TEH system can be developed within the project.

1.3 LIST OF ABBREVIATIONS

Abbreviation	**Meaning**
EH	Energy Harvester
FOM	Figure Of Merit
IC	Integrated Circuit
LCC	Life-Cycle Cost
MEMS	Micro Electro Mechanical System
MMR	Mechanical Motion Rectifier
MPPT	Maximum Power Point Tracking
OC	Object Controller
PEH	Piezoelectric Energy Harvester
TEH	Trackside Energy Harvesting
TENG	Triboelectric NanoGenerator
TRL	Technology Readiness Level

2 TRACKSIDE ENERGY HARVESTING

2.1 ENERGY HARVESTING

2.1.1 Introduction to Energy Harvesting technologies

The basic idea of energy harvesting is based on converting some type of available ambient energy into usable electrical energy using some device (energy harvester). For nearly 40 years energy harvesting has been investigated as a possible source of power for wireless applications, which would be for one reason or another difficult to connect to the power grid. These applications currently include mainly wireless sensor nodes in industrial structural or health monitoring systems [1], aerospace [2] or transportation [3]. Available power is a crucial limiting factor for independent devices, and most of the mentioned applications rely on the battery or another source as a primary source of power. Energy harvesting, if implemented, serves mostly as a secondary power source meant to extend the service life until the next battery replacement or recharge. With the ongoing miniaturisation of the electronic devices, their increasing power efficiency and decreasing power consumption however, the energy harvesters could serve as the primary power source for some ultra-low power applications (Figure 1).

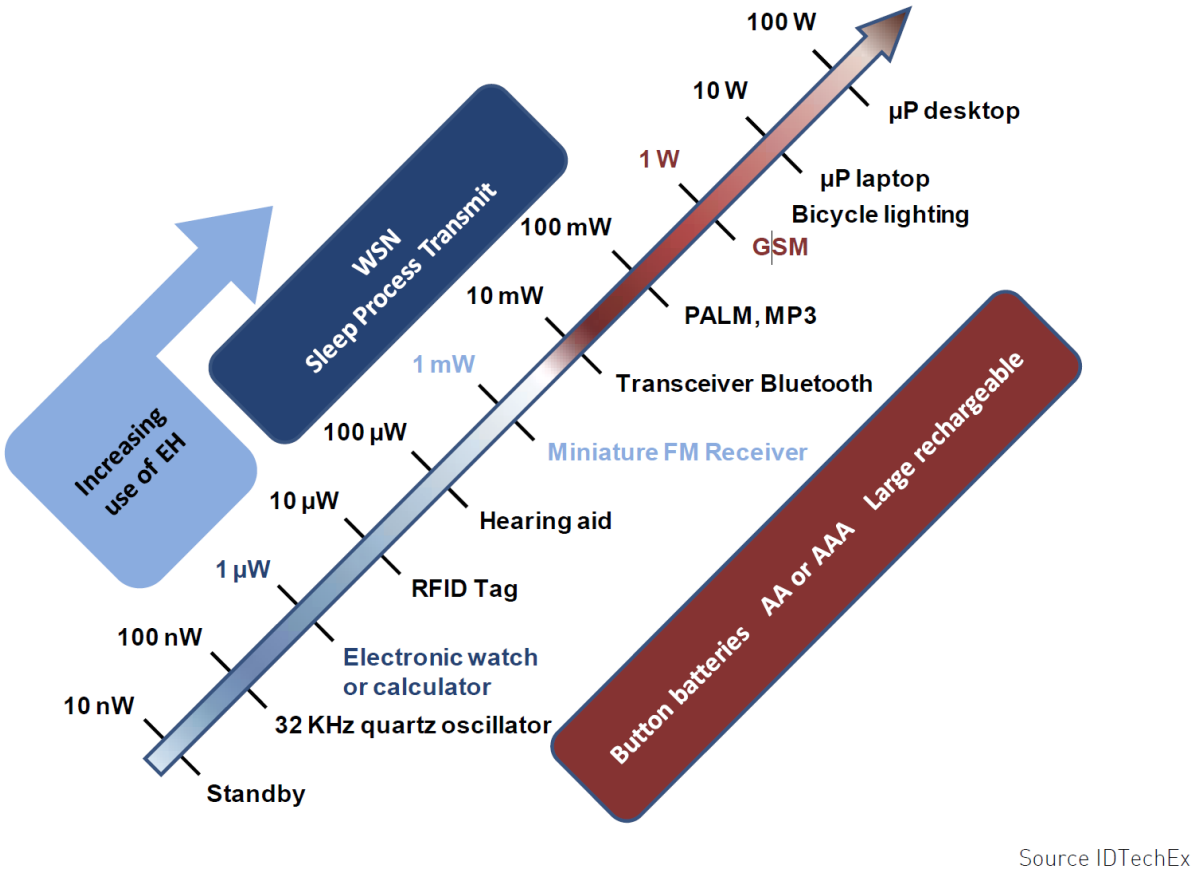

Figure 1 Power consumption and sources for current and future electronic applications

2.1.2 Development of TEH system

A preliminary analysis and a feasibility study of an energy harvesting solution are necessary development steps in the design of these autonomous systems. Mathematical models of employed physical principles can be used for the feasibility study of useful energy harvesting systems, which respects the nature and amount of ambient energy in the given industrial application. In case of preliminarily analysed output power being in accordance with the power requirements the development cycle can lead to a successful design of an energy harvesting system.

The model for the track side preliminary analysis can then be extended and models of geometry and used materials for a chosen design solution can be created for the design of a lab prototype. When the model is verified with respect to a lab test, the energy harvester design can be optimised using advanced optimisation tools [4] for maximising the harvested energy. New innovative energy harvesting systems, nanomaterials, smart materials [5], and structures [6] can be also integrated into energy harvesting devices if the original design cannot provide appropriate results. Complex mathematical and simulation models have very important roles during the development of energy harvesting devices in both industrial and railway trackside applications. The waterfall development diagram, shown in Figure 2, can be used to describe development steps for the design of fully autonomous energy harvesting systems.

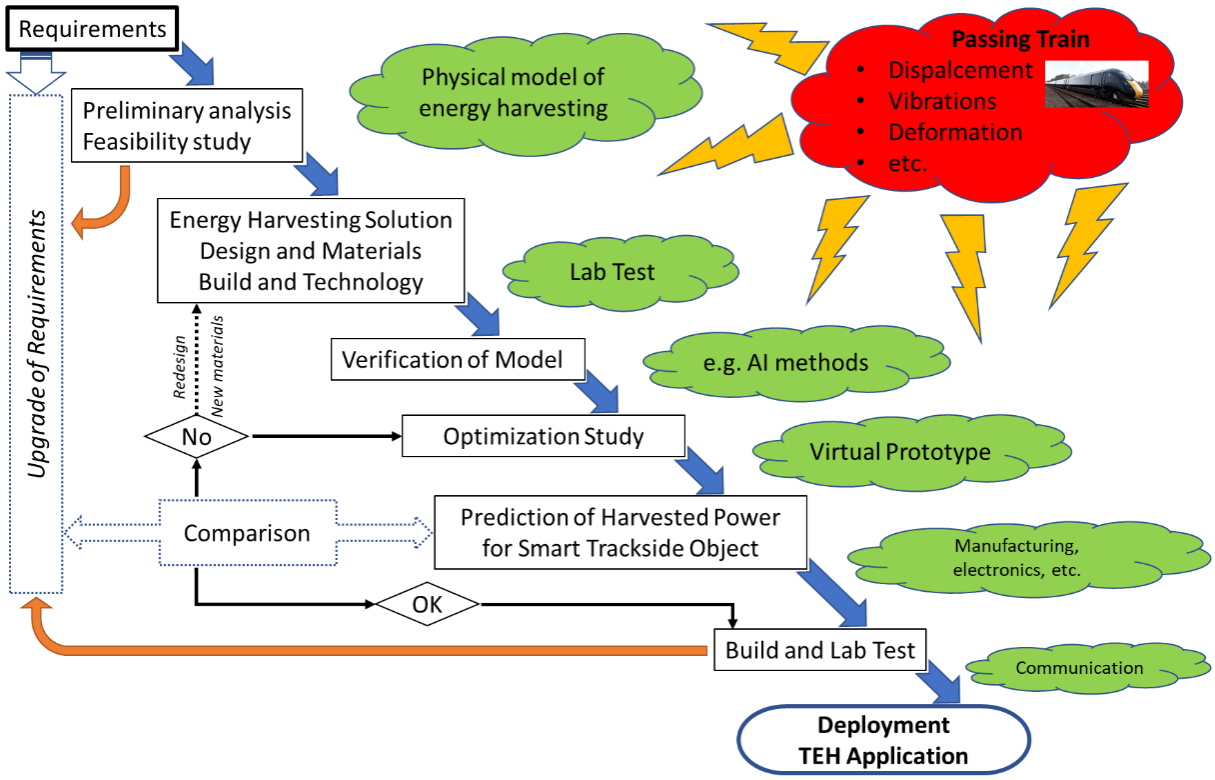

Figure 2 Waterfall Development Diagram of Energy Harvesting System for Trackside Application

2.2 POTENTIAL ENERGY HARVESTING SOLUTIONS FOR THE TRACKSIDE

Wind and solar power stations are commonly used as autonomous sources of energy for various remote electronic applications. These technologies can be exploited for the trackside power source solution, too. Kinetic energy in a form of mechanical deformation, vibrations, and shocks; and thermal energy in a form of waste heat sources are exploitable inputs for autonomous power sources in several engineering applications related to energy harvesting. However, the amount of harvested energy is usually very low, and the output electrical power has to be predicted and compared with the power requirements of intended ultra-low power applications.

The waste heat sources are not readily available in the trackside environment. However, they could be useful for on-board solution (e.g. waste heat caused by friction). On the other hand, a passing train provides a non-negligible source of input mechanical energy, which could be converted into electricity by various transducer setups (Figure 3).

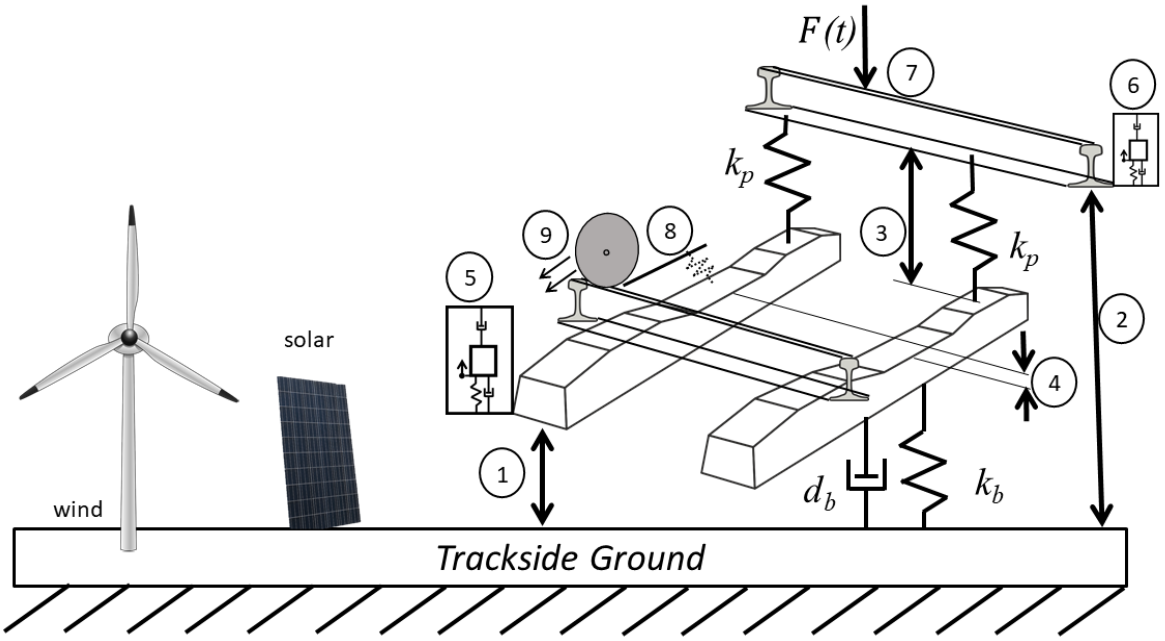

Figure 3 Potential trackside energy harvesting technologies

Potential trackside energy harvesting technologies:

- Commercial solar and wind power station (sections 4.4, 4.5)
- Displacement, strain and deformation energy harvesting – type 1, 2, 3, 4, 7, 8 (section 4.1)
- Vibration energy harvesting – type 5, 6 (section 4.3)
- Change of magnetic field by passing wheel – 9 (section 4.2)

2.3 TRACKSIDE ENERGY HARVESTER APPLICATION CONSIDERATIONS

2.3.1 Railway network parameters

The parameters in the railway environment which affect energy harvesting vary according to the particular location, the construction of the infrastructure, and the type and frequency of railway traffic. A set of values for the parameters at a particular location or case will be referred to collectively as the conditions. Different physical principals of energy harvesting are affected by differently (or hardly at all) by variations in the particular parameters. The conditions can be categorised into the following categories

- Route geographic conditions (mostly affect environmental energy harvesting methods, such as solar and wind):
    - The orientation and position of the location; railway routes are generally linear in nature, the general direction of the line of track means that the track and trackside environment will be aligned in certain directions. Solar based energy harvesting methods in particular need to be aligned with the sun the, layout of the available trackside land might affect the installation (such as two panels side by side, or separated along the trackside so they don't shade each other. Also the geographic position of the location affects the solar exposure throughout the year and the pattern of wind conditions.
    - The ground profile and vegetation of the location; railway track is nominally level compared to most types of construction however the ground on either side can be level, steeply sloped (or have built structures) either above or below the track (either side of the same location can vary from the other), of the track can be in a tunnel or on a bridge. Similarly the height of vegetation cover on the track side can vary. These factors affect the incident solar and wind energy at the trackside, the local landscape increasing the exposure or sheltering/shading the energy harvester compared to a flat open site.
- Railway infrastructure characteristics (greatest effect on energy harvesting based on train induced vibration and displacement):
    - Track construction, components and materials; different types of rail, fixing, and rail support (sleepers etc.) affect the dynamic behaviour of the track and therefore the dissipation of the energy imparted by a passing train, which in turn affects the quantity and form (in terms of frequency and amplitude for example) of energy available at a location for the energy harvesters to collect. Stiffer, more ridged track will generally have lower displacements and lower amplitude higher frequency vibrations than more flexible track. Also the quality of the maintenance of the alignment affects the interaction between the train and the track and hence the energy input to the track, well maintained track with little deviation from the nominal route will result in lower force interactions than poorly maintained track with higher deviations from the nominal route. Other features such as switches and crossings present a disturbance to the support of the rail, leading to impacts and locally higher energy input into the track. If the track has overhead electrical power supply and other structures such as

signalling equipment, these might affect the incident solar radiation depending on the relative positions.
    - Track support and ground conditions; different track support systems and materials (generally ballast), and substructure affect the dynamic behaviour of the track in a similar way to the track construction, and has a similar effect on energy harvesters.
- Railway traffic characteristics, traffic pattern (greatest effect on energy harvesting based on train induced vibration and displacement, and train aerodynamics based wind generators):
    - Type of train; different train types and consists have different lengths, numbers of wheels, load characteristics and vehicle dynamics, as well as operational characteristics (most notably speed). Locomotives and loaded freight vehicles are generally heavier than passenger vehicles and therefore impart larger displacements and more energy to the track, however freight trains and stopping passenger trains generally run slower than express passenger trains. The faster the train is travelling the higher the energy input into the track and the higher the frequency of the vibrations and displacements.
    - Traffic frequency and type; different locations will have different traffic patterns with different numbers of passenger trains (express and stopping services) and freight trains, and therefore different numbers of each vehicle type passing each day. This means that the energy input, and therefore the energy it is possible to harvest, will be dependent on the traffic.

2.3.2 Expected conditions for TEH systems

The railway network parameters for each location where TEH systems are to be installed would have to be assessed for each installation, alternatively locations with similar characteristics could be grouped into categories and suitable TEH harvester installations determined for each category. To allow the evaluation of the effectiveness of different energy harvester concepts and designs a generic example scenario is defined here, this will enable the evaluation to be carried out with a set of parameters which have values of an appropriate order of magnitude, with the understanding that the energy harvesting performance will vary at locations with different conditions according to the effects of the variations of each parameter described in section 2.3.1. The conditions for the example scenario are as follows:

- Geographic conditions: Central Europe, track running East to West, level ground clear to horizon.
- Railway infrastructure conditions: Electrified straight track, maintained to UIC QN1 (good) track geometry quality, 60kg/m rail, welded rail, Pandrol clips, under rail pads, concrete sleepers, on ballast, and with good sub-ballast ground support.
- Railway traffic pattern; medium density mix traffic pattern with the following daily trains:
    - 6 Express passenger trains (140km/h) consisting of one loco and 8 passenger vehicles
    - 8 Stopping passenger trains (100km/h) consisting of 4 vehicle units
    - 4 Loaded freight trains (60km/h) consisting of locomotive and 20 loaded freight wagons

- 4 Un-loaded freight trains (60km/h) consisting of locomotive and 20 un-loaded freight wagons
  - The characteristics of the vehicles are as follows:
    - Locomotive: 4 axle Bo'Bo' 85tonnes
    - Express passenger vehicle: 4 axle (2 bogies) 40tonnes
    - Stopping passenger vehicle: 4 body, 5 bogie electric passenger multiple unit total weight 205tonne
    - Loaded freight wagon: 4 axle (2 bogies) 80tonnes
    - Un-loaded freight wagon: 4 axle (2 bogies) 20tonnes

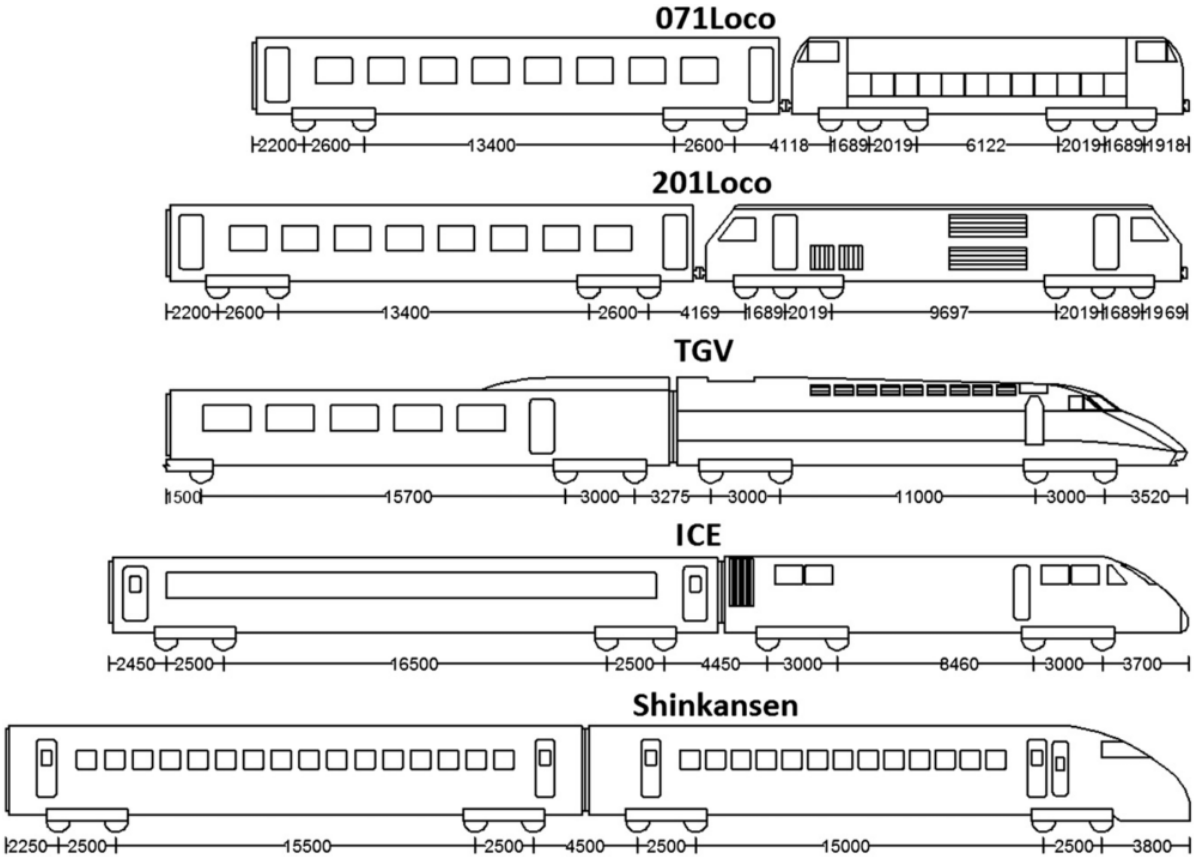

Figure 4 Illustration of train fleet with first carriage including axle spacing [7]

2.3.3 Reliability, cost and maintenance considerations

In addition to the physical environment and the practical viability of a TEH design, the reliability, cost and maintenance requirements of the TEH (and track) need to be considered, this includes the following considerations:

- Be at least as reliable as current power supply
- Lower life cycle costs considering procurement, installation and maintenance
- Easily maintainable at track-side, self-diagnostic and easy to inspect, components or modules should be easily replaceable to minimise downtime and time staff on site to correct faults.
- The extent to which the TEH device impacts maintenance of the track and railway infrastructure, such as inspections, tamping, and rail-grinding.
- Vulnerability to theft, and other external factors such as extreme winds and flooding
- Vulnerability to theft

3 ENERGY TRANSDUCTION PHYSICAL PRINCIPLES

3.1 PIEZOELECTRIC CONVERSION

3.1.1 Physical principle and operation modes

Piezoelectric materials have the property of converting a mechanical stress or strain applied to them into electric field or electric displacement on them and vice versa. Conversion from mechanical to electrical energy is called the direct piezoelectric effect, the conversion from electrical into mechanical domain is known as reverse piezoelectric effect [8]. The piezoelectric phenomenon is based on the fundamental structure of a crystalline network. Certain crystalline structures have a charge balance with polarization, which must be oriented in one direction to produce piezoelectric behaviour of the material. Piezoelectric effect is expressed by constitutive equations [9]:

$$T_p = c_{pq}^E \cdot S_q - e_{kp} \cdot E_k$$

$$D_i = e_{iq} \cdot S_q + \epsilon_{ik}^S \cdot E_k$$

Where $\boldsymbol{T_p}$ is stress component (in newtons per square meter), $\boldsymbol{c_{pq}^E}$ is elastic stiffness constant for constant electric field (in newtons per square meter), $\boldsymbol{S_q}$ is strain component (no unit), $\boldsymbol{e_{kp}}$ is piezoelectric constant (in coulombs per square meter), $\boldsymbol{E_k}$ is electric field component (in volts per meter), $\boldsymbol{D_i}$ is electric displacement component (in coulombs per square meter), $\boldsymbol{\epsilon_{ik}^S}$ is permittivity component for constant strain (in farads per meter) and $\boldsymbol{_{i,k,p,q}}$ are direction indexes (no unit). Direction 3 is defined as the direction, in which the material is polarized. These equations can also be expressed in alternative forms by equivalent modifications of them to express another variable than in the aforementioned form. Alternative forms are used e.g. in publication [8]. Piezoelectric constant $\boldsymbol{e_{kp}}$ varies for alternate forms to $\boldsymbol{d_{kp}}$, $\boldsymbol{g_{kp}}$, $\boldsymbol{h_{kp}}$ (in meter per volt = coulomb per newton, volt meter per newton = square meter per coulomb, volt per meter = newton per coulomb, respectively), where the form of $\boldsymbol{d_{kp}}$ is commonly used.

These equations express piezoelectric effect in 6 directions [9] and could be used to model precise sensors or actuators [10]. However, only two modes are important for energy harvesting [11]: mode 33 and mode 31, depicted in Figure 5. In these modes, the external force is applied only in one direction, which is the most common case in energy harvesting devices.

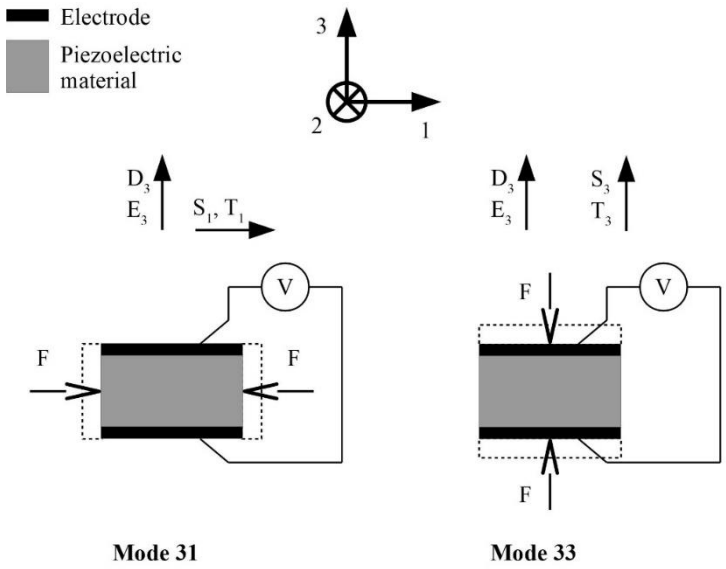

Figure 5 Diagram of piezoelectric material working modes

In both modes (33 and 31) the electric displacement, electric field and final voltage on electrodes are in direction 3 in which the piezoelectric material is polarized. Mechanical stress and strain is always in one direction. In mode 33 the stress, strain and external force are in the same direction as the voltage (direction 3); and in mode 31 the stress, strain and external force are in perpendicular direction 1 (Figure 6). These modes are the simplest case. However, they are precise enough to model the energy harvesting system, and as such they will be used in the following chapters.

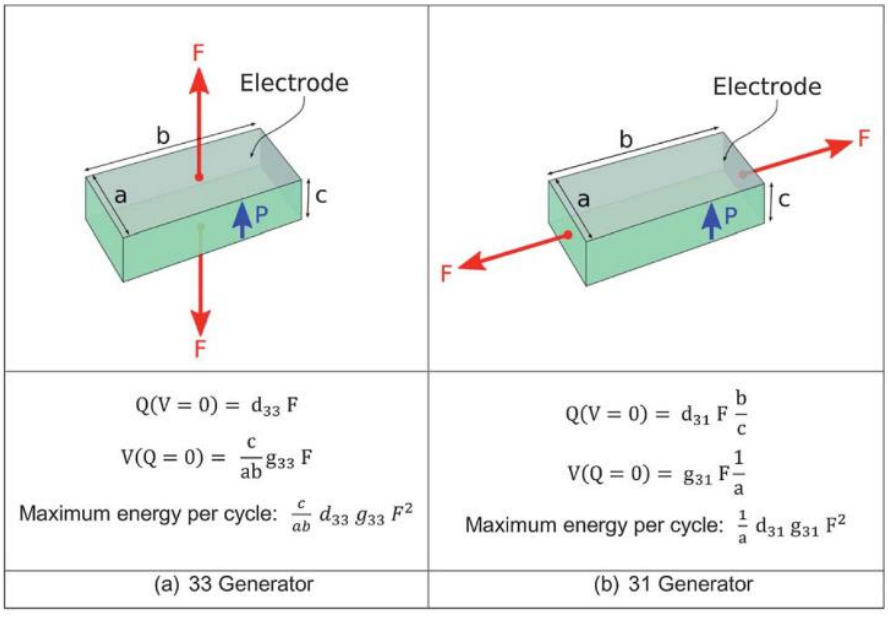

Figure 6 (a) 33 and (b) 31 piezoelectric stress driven generator configurations. Q and V are the electric charge and voltage respectively, F is the applied force, P is polarization direction, d_{33} and d_{31} are the piezoelectric charge coefficients, g_{33} and g_{31} are the piezoelectric voltage coefficients. [5]

3.1.2 Materials

Piezoelectric material properties directly affect the electrical power output of given piezoelectric energy harvester. For selection and comparison of piezoelectric materials a figure of merit (FOM) is used [12]–[14]:

$$FOM = g \cdot d = \frac{d^2}{\varepsilon^T}$$

Where g and d are the piezoelectric constants defined in the previous chapter and ε^T is permittivity as in previous chapter, but here it is for constant tension. By this way a selection of various type of piezoelectric materials for PEH might be considered with point of view on theoretical level of power output from PEH. The FOM calculated for different commercial piezoelectric products are shown in Table 1. The results of the FOM are compared in Figure 7. Highest values are obtained for single crystals based on PMN-PT. Fabrication cost, rigidity and brittleness are main disadvantages of PMN-PT single crystals ceramics [15].

Table 1 The FOM calculated for examples of different piezoelectric materials

Company	Note	Material	d_{33} [pC/N]	g_{33} [10^{-3}Vm/N]	FOM [10^{-12}]
		PZT-2	152	38	5.79
		PZT-8	225	25	5.71
Ferroperm	Hard PZT	Pz28	275	31	8.63
Ferroperm	Soft PZT	Pz29	574	22	12.97
	Soft	BCZT-Ce	500	14	7.05
	Soft	BaTiO3	145	13	1.89
		PVDF	33	330	10.89
CTS	Single crystal	PMN-28PT	1190	24	29.09
CTS	Single crystal	PMN-32PT	1620	26	42.36
CTS	Single crystal	PIN33-PMN-PT	1338	33	44.63
Del Piezo	BiT	DL-10	21	18	0.38
Del Piezo	PT	DL-20	72	40	2.88
Del Piezo	BT	DL-21	140	13	1.91
Del Piezo	Lead Metaniobate	DL-31	90	33	3.05
Del Piezo	Lead Metaniobate	DL-33	62	40	2.48
Del Piezo	Hard PZT	DL-40	145	47	6.81
Del Piezo	Hard PZT	DL-48	365	15	5.69
Del Piezo	Soft PZT	DL-50HD	430	25	10.75
Del Piezo	Soft PZT	DL-61HD	810	13	11.25
Noliac		NCE41	310	25	7.75
Noliac		NCE51/NCE51f	443	26	11.51
Noliac		NCE55	670	19	12.73
Noliac		NCE80	270	28	7.56

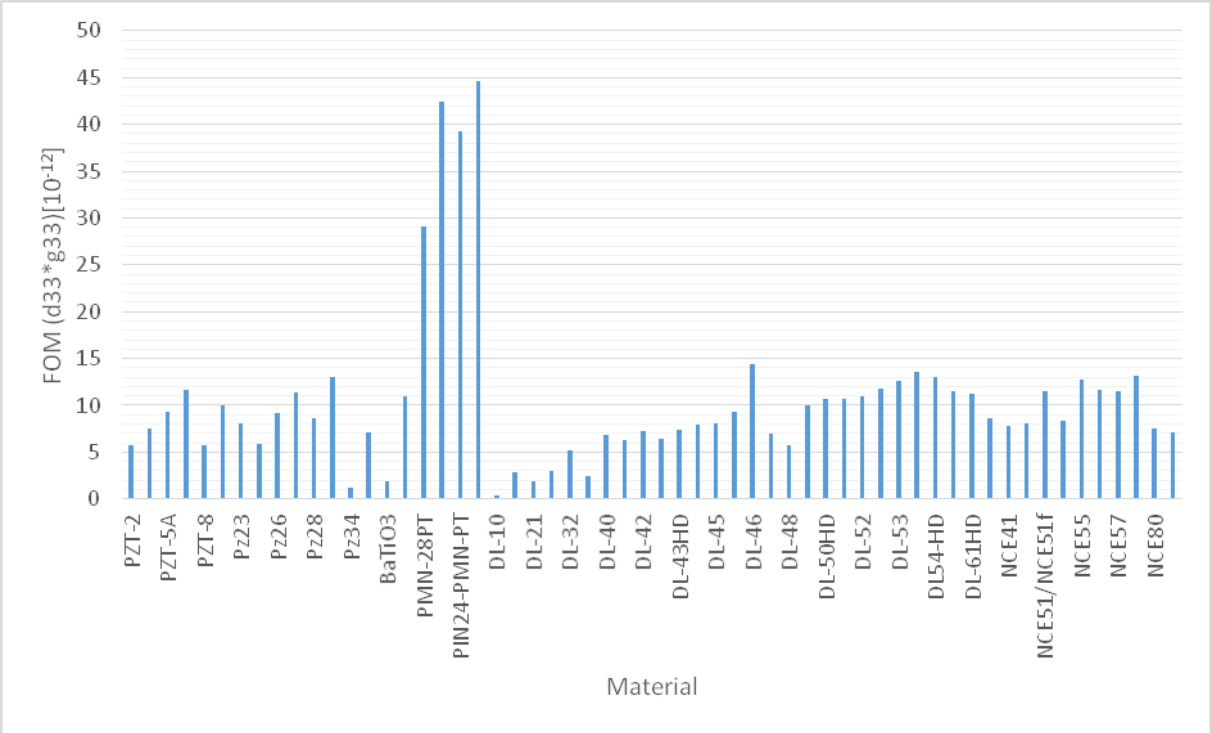

Figure 7 FOM values for chosen piezoelectric materials

3.1.3 Piezoelectric cantilever – mode 31

The most common setting of a piezoelectric energy harvesting device for vibration operation is bimorph cantilever beam [16]–[18], shown in Figure 9. This cantilever configuration is described as one degree of freedom mechanical oscillator with piezoelectric coupling for mode 31 [19] through coupled differential equations [20]:

$$m \cdot \ddot{z} + d \cdot \dot{z} + k \cdot z + \Theta \cdot v = F_{ext}$$

$$\dot{v} = \frac{1}{C} \cdot (\Theta \cdot \dot{z} - i)$$

Where *z* is tip displacement (in meters), *m* is weight of tip mass (in kilograms), *d* is mechanical damping (in newton seconds per meter), *k* is mechanical stiffness (in newtons per meter), Θ is piezoelectric coupling coefficient (in newtons per volt), F_{ext} is external force (in newtons), *C* is capacitance of piezoelectric layers (in farads) and *i* is electric load current (in amperes). These equations flow from fundamental piezoelectric equations and parameters are calculated from piezoelectric constants and dimensions or from experiment.

External force could be from arbitrary source. Mostly, this type of harvester is excited by vibrations of the base structure. Then the force is expressed by simple equation [19]:

$$F_{ext} = -m \cdot a_{base}$$

Where a_{base} is acceleration of the base structure (ms^{-2}). This is contactless type of energy harvesting in point of view on moving mass. In this type of energy harvesting the frequency of excitation vibrations is important. If the excitation frequency is the same as the resonance frequency of the harvester, the harvested power is high. Otherwise, however, the harvested power is significantly lower than in the resonance operation. This issue is demonstrated on piezoelectric vibration energy harvester frequency response, showed in Figure 8. It is widely discussed in [19].

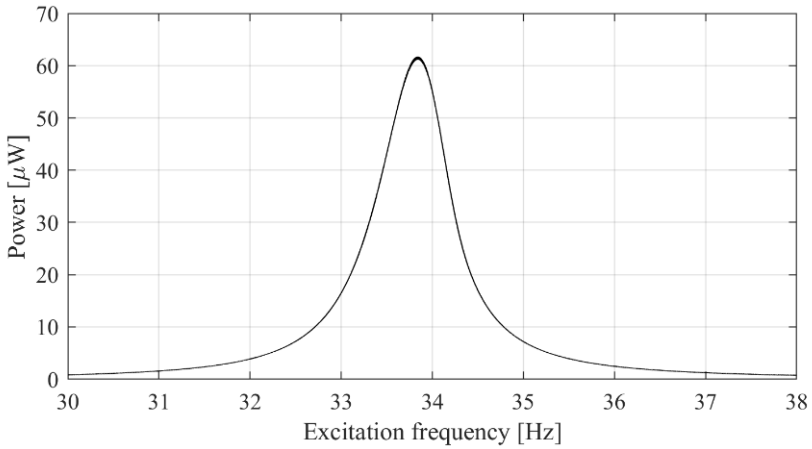

Figure 8 Output harvested power for excitation by acceleration

The external force could be also acting directly on the moving proof mass (exciting it by pressing with a mechanism), however there is a risk of the cantilever snapping, and there are better ways for exploiting the direct excitation, as presented in the next chapter.

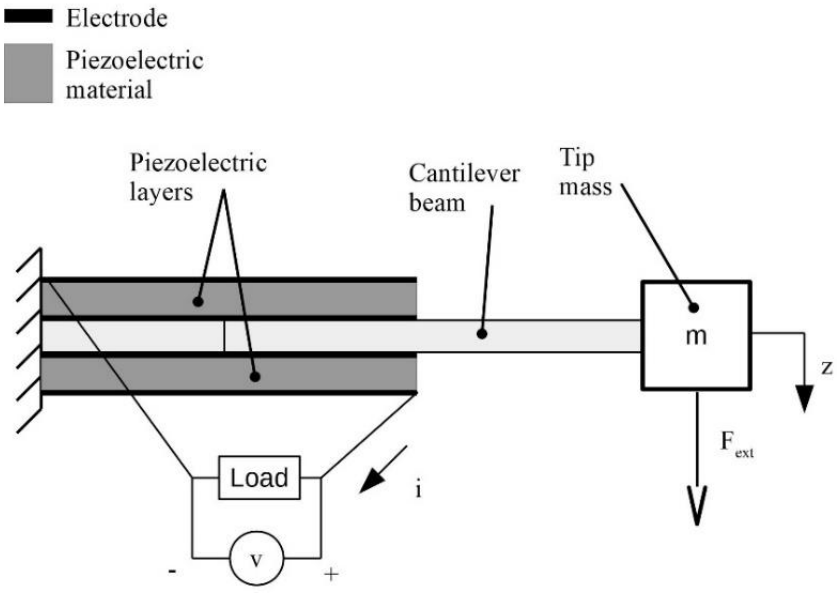

Figure 9 Piezoelectric vibration energy harvester design

3.1.4 Piezoelectric stack – mode 33

Piezoelectric stacks are used mainly for direct energy harvesting from displacement - meaning from direct contact with any mechanism. The stack is composed from piezoelectric elements operating in mode 33 (Figure 10) and could be described by the same differential equations as the cantilever harvester from previous capture. However, when the harvester is excited by displacement, the excitation force is high and for piezo stack the mass is low in comparison with the excitation force and the high stiffness of the stack, so the equations could be reduced to form:

$$d \cdot \dot{z} + k \cdot z + \Theta \cdot v = F_{ext}$$

$$\dot{v} = \frac{1}{C} \cdot (\Theta \cdot \dot{z} - i)$$

From the modified equations it is clear that in this type of harvesting the frequency of external force with respect to the harvester resonant frequency is not important. The harvested power is in this case affected only by the integral of excitation force, and by the parameters of the piezo stack.

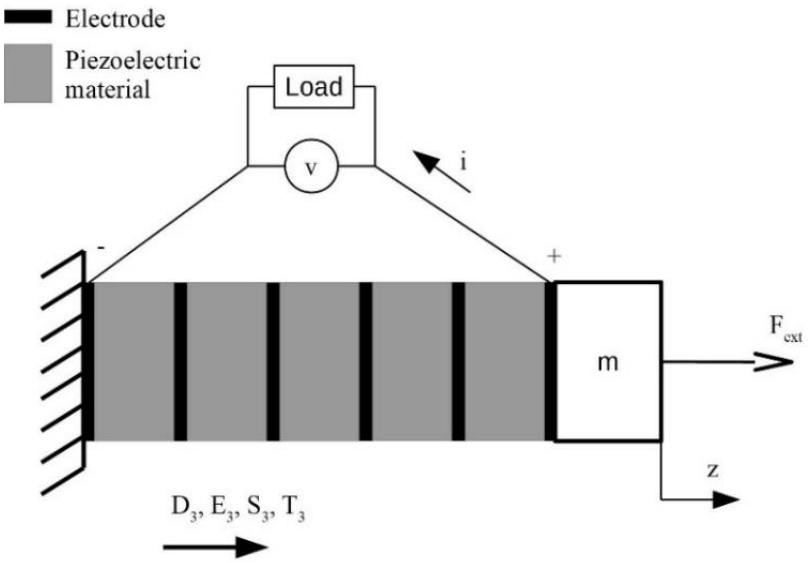

Figure 10 Piezoelectric stack harvester

3.2 ELECTROMAGNETIC INDUCTION

Electromagnetic or magnetic induction is the production of an electromotive force (EMF, unit: voltage) across an electrical conductor in a changing magnetic field. In 1831, Michael Faraday discovered that, by varying magnetic field with time, an electric field could be generated. The phenomenon is known as electromagnetic induction. The EMF generated by Faraday's law of induction due to relative movement of a circuit and a magnetic field is the phenomenon underlying electrical generators. When a permanent magnet is moved relative to a conductor, or vice versa, an electromotive force is created. If the wire is connected through an electrical load, current will flow, and thus electrical energy is generated, converting the mechanical energy of motion to electrical energy.

Faraday showed that no current is registered in the galvanometer when bar magnet is stationary with respect to the loop. However, a current is induced in the loop when a relative motion exists between the bar magnet and the loop. In particular, the galvanometer deflects in one direction as the magnet approaches the loop, and the opposite direction as it moves away. Faraday's experiment demonstrates that an electric current is induced in the loop by changing the magnetic field. The coil behaves as if it were connected to an EMF source. Experimentally it is found that the induced EMF depends on the rate of change of magnetic flux ∅ through the *N* turns of the coil:

$$emf = \frac{d\psi}{dt} = N \cdot \frac{d\emptyset}{dt}$$

Faraday's law of electromagnetic induction states that an electrical current will be induced in any closed circuit when the magnetic flux through a surface bounded by the conductor changes. This applies whether the field itself changes in strength or the conductor is moved through it. The EMF generated by Faraday's law of induction due to relative movement of a circuit and a magnetic field is the phenomenon underlying electrical generators. When a permanent magnet is moved relative to a conductor, or vice versa, an electromotive force is created. If the wire is connected through an electrical load, current will flow, and thus electrical energy is generated, converting the mechanical energy of motion to electrical energy.

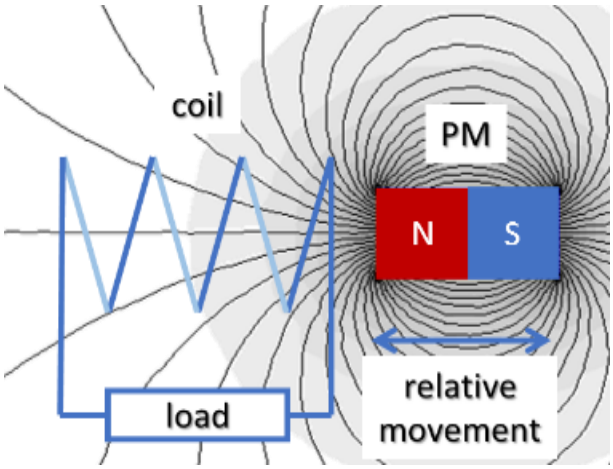

Figure 11 Electromagnetic induction principle

One of the most important applications of Faraday's law of induction is to generators and motors. A generator converts mechanical energy into electric energy. A linear alternator is most commonly used to convert back-and-forth motion directly into electrical energy. In an electromagnetic generator, permanent magnets are used to produce strong magnetic field and a coil is used as the conductor. Either the permanent magnet or the coil is fixed to the frame while the other is attached to the inertial mass. The relative displacement caused by the vibration makes the Kinetic Energy Harvesting transduction mechanism work and generate electrical energy. The induced voltage, EMF, across the coil is proportional to the strength of the magnetic field, the velocity of the relative motion and the number of turns of the coil. An electromagnetic generator is characterised by high output current level at the expense of low voltages.

3.3 ELECTROSTATIC CONVERSION

The principle of electrostatic energy conversion lies in exploiting a capacitor with variable capacitance value. The two electrodes of the capacitor, separated by air, vacuum or any dielectric material, move with respect to each other due to mechanical excitation. That leads to a change either in the active surface of the electrodes, or their distance from each other, causing a variation in the capacitance [21]. The electrostatic harvesters can be divided into two main groups: electret-free devices and electret-based devices. The difference between the two groups lies in usage (or lack of) the electret material between the electrodes, which eliminates the need for priming voltage to provide the initial energy for conversion.

The electret-free devices are passive structures that require additional electrical energy to convert mechanical energy into electricity. Most common working cycles (Figure 12) employed are the voltage-constrained and charge-constrained cycles. A correct synchronization of the energy extraction with capacitance variation is necessary in order to exploit the relative movement of the electrodes for generating electricity.

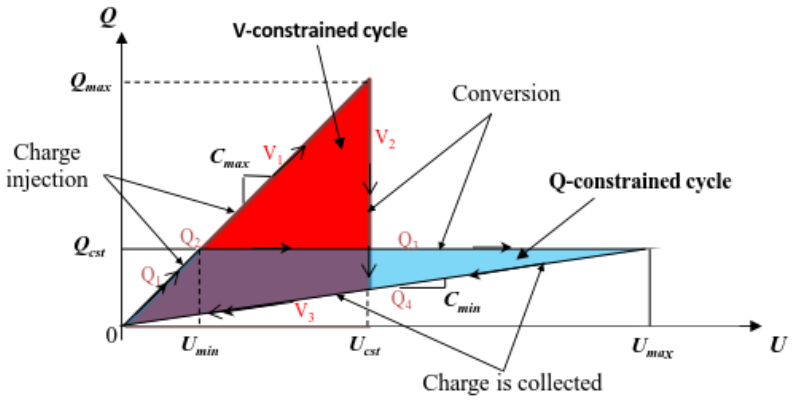

Figure 12 Electret-free devices possible working cycles [21]

The total amount of energy converted per cycle is equal to:

$$E_Q = \frac{1}{2} Q_{const}^2 \left(\frac{1}{C_{min}} - \frac{1}{C_{max}}\right)$$

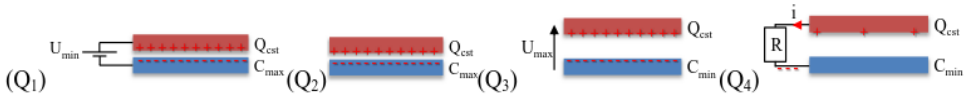

Figure 13 Principle of charge-constrained electrostatic EH operation [21]

For charge-constrained cycle (Figure 13); and to:

$$E_U = U_{const}^2 (C_{max} - C_{min})$$

For voltage constrained cycle (Figure 14).

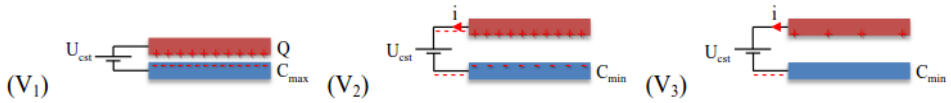

Figure 14 Principle of voltage-constrained electrostatic EH operation [21]

The electret-based devices (Figure 15) are in principle similar to electret-free harvesters, the main difference being a layer of electret material added to one or both electrodes, polarizing it. These devices therefore do not rely on initial electrical energy as the structure deformation directly induces an output voltage, much like in piezoelectric materials.

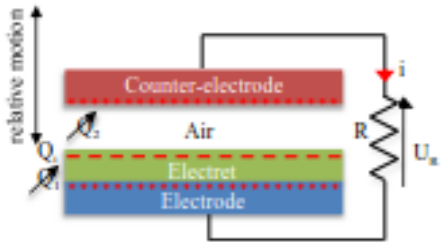

Figure 15 Diagram of electret-based energy harvester [21]

The electrostatic conversion principle is used mainly in MEMS sensors, actuators, and energy harvesters. The most common topologies of the harvesters employ the comb structure of the electrodes to maximise their surface (Figure 16).

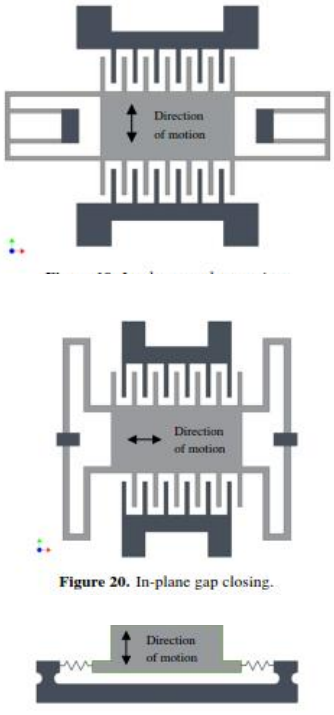

Figure 16 Example of common electrostatic EH topology [22]

3.4 MAGNETOSTRICTION

A characteristic property of magnetostrictive materials is that a mechanical strain will occur if they are subjected to a magnetic field in addition to strain originated from pure applied stresses, Figure 17. Also, their magnetisation changes due to changes in applied mechanical stresses in addition to the changes caused by the changes of the applied magnetic field, see Figure 18. These dependencies can be described by mathematical functions:

$$\varepsilon = \varepsilon(\sigma, H)$$

$$B = B(\sigma, H)$$

where, ε, σ, H and B be the strain, the stress, the applied magnetic field strength, and the magnetic flux density, respectively.

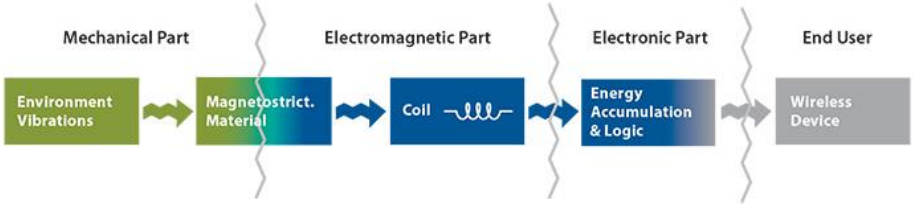

Figure 17 Magnetostriction energy harvester as combination of smart material and electromagnetic induction

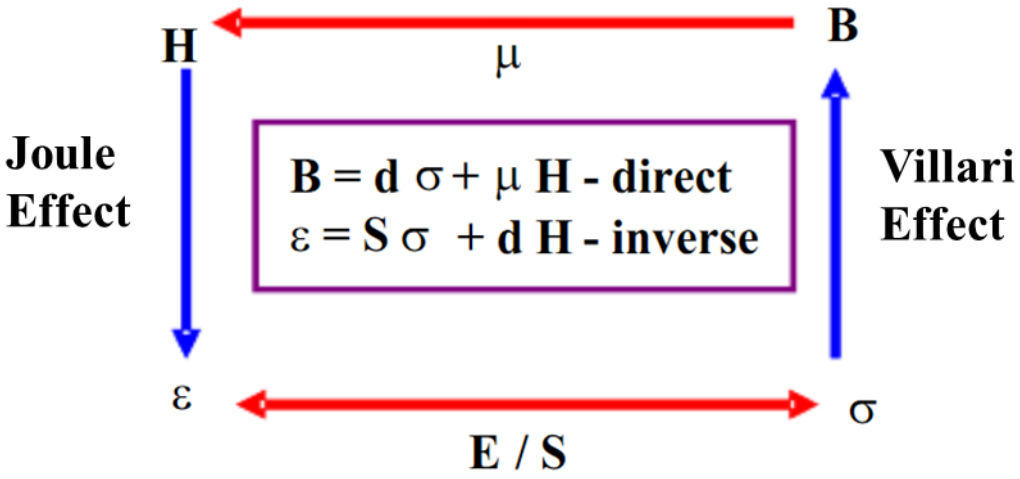

Figure 18 Coupled field effects for actuators and harvesters [23]

Taking into account the fact that the most important mode of operation of magnetostrictive materials is the longitudal one, the linearization of the differential response of strain and magnetisation leads to the following equations of magnetomechanical coupling:

$$\varepsilon = S^H \sigma + d_{33} H$$

$$B = d_{33}^* \sigma + \mu^\sigma H$$

Here $S^H = \frac{\partial \varepsilon}{\partial \sigma_{|H=const}} = \frac{1}{E^H}$ where E^H be the Young's modulus at constant applied magnetic field strength, $d_{33} = \frac{\partial \varepsilon}{\partial H_{|\sigma=const}}$ be the magnetostrictive strain derivative (linear coupling coefficient), $d_{33}^* = \frac{\partial B}{\partial \sigma_{|H=const}}$ be the parameter of magnetomechanical effect, $\mu^\sigma = \frac{\partial B}{\partial H_{|\sigma=const}}$ be the magnetic permeability at a constant stress [24].

Commonly used magnetostrictive materials include following:

- Terfenol-D alloy (Td0.3Fe0.7Dy1.9) [25]
- Galfenol - Iron–gallium alloys (Fe1-xGax, 0.14<x<0.3) [26]
- Metglas 2605SC (Fe81B13.5Si3.5C2)

Giant magnetostrictive materials exhibit a variety of interesting effects [25]. Direct and inverse magnetostrictive effects are applicable to actuator and sensor modes of operation. Most actuator applications rely on Joule effect, where magnetostriction change is induced in the direction of the applied magnetic field. Sensor applications and this study utilise its inverse effect, known as Villari effect (inverse magnetostriction effect), in which change in magnetisation is induced due to applied stress. The change in magnetic permeability is then picked up by a solenoid coil surrounding the material (Figure 19).

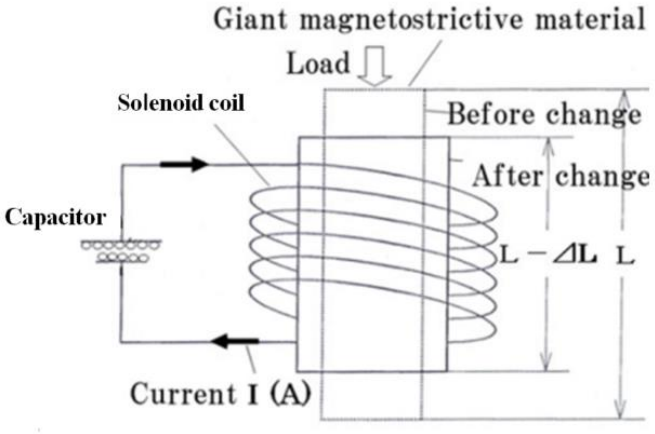

Figure 19 Principle of a Villari effect [25]

3.5 TRIBOELECTRIC EFFECT

Triboelectric nanogenerators (TENG) are based on two principles such as triboelectric effect and electrostatic induction. Theory of this type of energy harvesters is described by many researches as can be seen for example from these authors [27][28][29][30], and follows from structure of TENG device. Basically, the contact potential difference V_c is given by [31]:

$$V_c = V_{1/2} = -\frac{(\phi_1 - \phi_2)}{e}$$

Where $V_{1/2}$ is the contact potential difference of metal 1 against metal 2, e is the elementary charge.

The amount of the transferred charge is equal to the product potential difference and the capacitance between the two bodies and is given by:

$$\Delta q_c = C_0 V_c$$

Where C_0 is the capacitance between the bodies at the critical separation distance where the charge transfer is cut off.

Different metals and dielectric materials can donate or accept electrons in different amounts. This can be arranged in an order known as triboelectric series [32].

TENG has shown advantages such as high output voltages, high energy-conversion efficiency, abundant choices of materials, scalability and flexibility [33]. Four basic modes of TENG have been developed: Vertical contact separation (CS) mode [34], [35], [29], Lateral sliding (LS) mode [36], [37], [38], Single-electrode (SEC) mode [39], [40], Freestanding triboelectric-layer (CFT) mode [41], [42], [43]. Design of TENG and its application follows from the chosen mode. Illustration of different structures of TENG is shown in Figure 20.

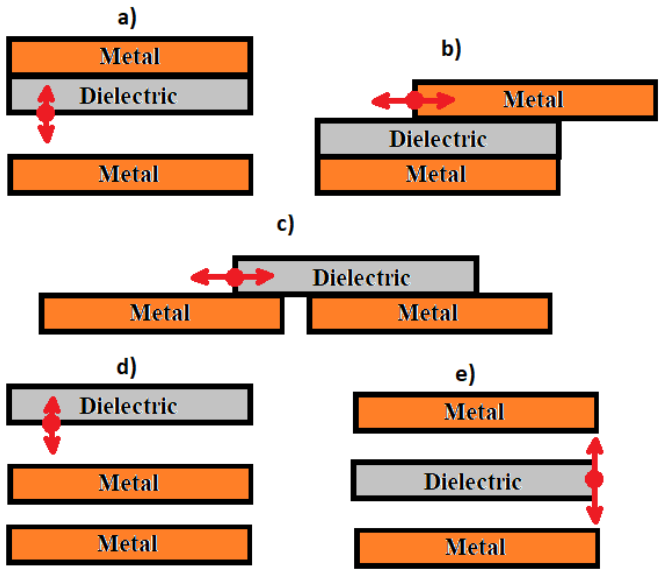

Figure 20 Illustration of symbols in 5 structures of TENG. a) Vertical contact-separation mode, b) Lateral sliding mode, c) Sliding freestanding triboelectric-layer structure, d) Single-electrode contact structure, e) Contact freestanding triboelectric-layer structure. [33]

A standard method to quantitatively evaluate TENG's performance from structures and materials points of view have been proposed by these authors [33], [28]. Output energy per cycle can be optimised by connecting a matched load resistance [38]. Necessary to say that the maximised output

energy per cycle can be achieved in open-circuit condition. A largest possible output energy per cycle can be expressed as [33]:

$$E_m = \frac{1}{2} Q_{SC,\max}\left(V_{OC,max} + V'_{max}\right)$$

Where $Q_{SC,max}$ is a maximum short-circuit transferred charge, $V_{OC,max}$ is a maximum open-circuit voltage and V'_{max} is a maximum achievable absolute voltage at $Q=Q_{SC,max}$. A dimensionless structural figure of merit (FOM_S) of TENG'S operating in cycles for maximised energy output can be expressed:

$$FOM_S = \frac{2\varepsilon_0}{\sigma^2}\frac{E_m}{Ax_{max}}$$

Where ε_0 is the permittivity of the vacuum, x_{max} is maximal displacement and A is a triboelectrification area. The σ^2 is a component related to the material properties and then the performance FOM (FOM_P) can be defined as:

$$FOM_P = FOM_S \cdot \sigma^2 = 2\varepsilon_0 \frac{E_m}{Ax_{max}}$$

The $FOM_{S,max}$ for different structures of TENG is reported in literature [33]. Data are extracted from FEM simulations with the same surface charge density σ and area A. It can be concluded that the best configuration of TENG is the contact-mode freestanding structure with FOM_S point of view. The contact-mode freestanding structure can be an effective energy harvester for vibration with the capability of non-contact operation [28]. A principle of working the contact-mode freestanding structure is shown in Figure 21. The absolute charge density of different materials is important too, and its method of measuring is reported by these authors [33]. The standard evaluation of the material FOM is performed by measuring triboelectric surface charge density via contacting the materials with liquid metals for example. The absolute charge density measured by contacting different materials with solid gallium and liquid galinstan is reported in literature [33].

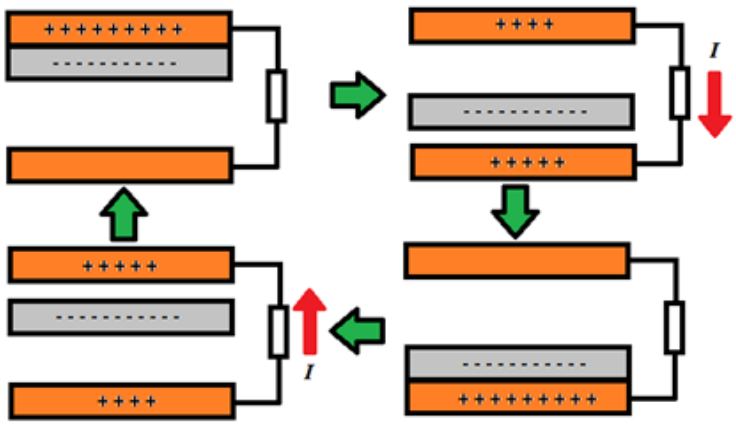

Figure 21 A contact-mode freestanding triboelectric structure of TENG. Schematic diagram of TENG and its principle of working. [33]

3.6 PHOTOVOLTAIC EFFECT

The photovoltaic effect occurs when photons are absorbed at a junction between two dissimilar materials (a heterojunction), inducing a voltage. The absorbed photons produce free charge carriers, i.e. electrons and holes, however, the induced voltage in the heterojunction causes the charge carriers to move apart, resulting in current flow in an external circuit. Materials used for fabricating such heterojunctions are generally semiconductors, which are responsive to light of various wavelengths. As seen in the figure below, a typical photovoltaic device mainly consists of a large area semiconductor p-n junction. A photon impinging on the junction is absorbed, when the energy is higher/equal to the semiconductor's bandgap energy, it will cause a valance band electron to be excited into the conduction band. This will leave behind a hole, thus creating a mobile electron-hole pair. If the electron-hole pair is located within the depletion region of the p-n junction, then the existing electric filed will either sweep the electron to the n-type side or the hole to the p-type side. The generated current can be written [44] as:

$$I = I_s \left[e^{\frac{qV}{kT}} - 1 \right]$$

Where q is the electron charge, k is the Boltzmann's constant, and T is the temperature of the p-n junction in Kelvin.

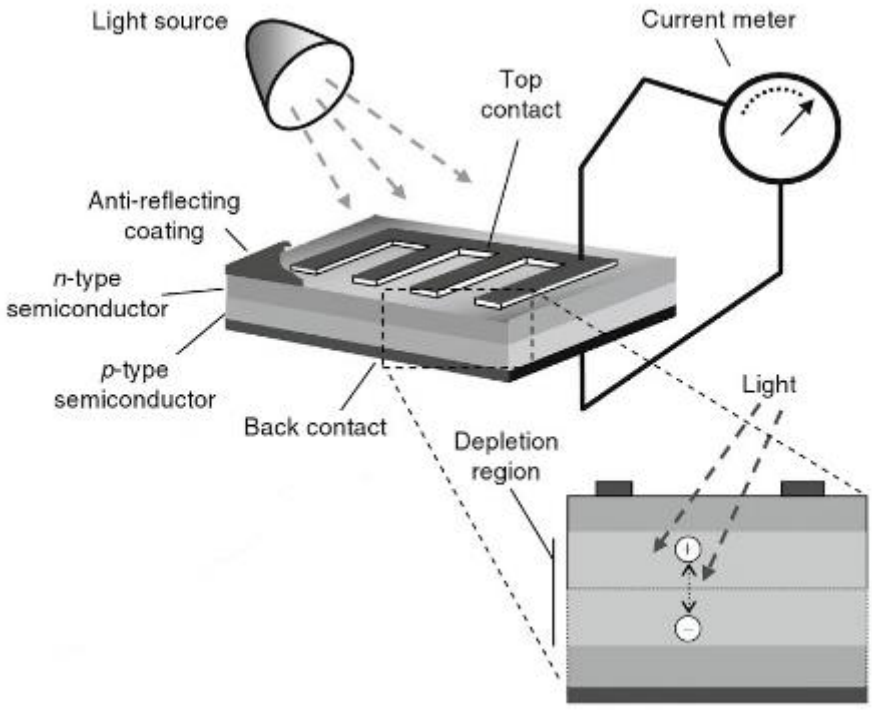

Figure 22 Illustration of photovoltaic effect [45]

3.7 THERMOELECTRIC CONVERSION

The thermoelectric generators consist of a thermoelectric module, a heat source (hot side) and a heat sink (cold side). The thermoelectric module is depicted in Figure 23. This module is a semiconductor device which ensures the conversion of temperature difference to the electromotive force utilising the Seebeck Effect. This phenomenon is based on diffusion of electrons through an interface between two different materials – usually semiconductors. The diffusion is achieved by applying heating at the junction of the materials which make a thermocouple.

When considering generated open circuit voltage on the output terminals of thermoelectric generator is linearly dependent on the temperature difference between hot and cold sides of the thermoelectric module:

$$U_{oc} = \alpha_{\Sigma}.(T_h\text{-}T_c)U_{oc} = \alpha_{\Sigma}.(T_h\text{-}T_c)U_{oc} = \alpha_{\Sigma}.(T_h\text{-}T_c)$$

where U_{oc} is open-circuit voltage, α_{Σ} net Seebeck coefficient of the module (component parameter), T_h temperature of the hot site, and T_c temperature of the cold side.

As the thermoelectric module behaviour can be described as a voltage source with internal resistance, the maximum power achievable from the module can be expressed as:

$$P_{MPP} = \frac{[\alpha_{\Sigma}.(T_h\text{-}T_c)]^2}{4R_{TEM}}$$

where P_{MMP} is the maximum achievable power, and R_{TEM} is the thermoelectric module internal resistance. Other symbols correspond to the previous notation. Such a situation shown in Figure 23 occurs when the generator's load (R_L) is matched with generator's internal resistance (R_{TEM}). The load equal to the internal resistance of a module is called the match load.

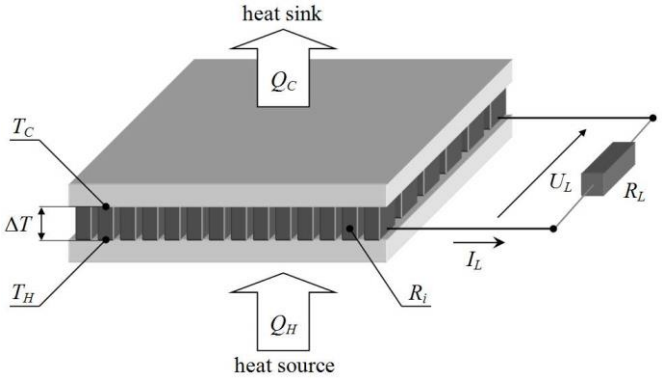

Figure 23 Thermoelectric EH module

The sources of thermal gradient are very limited in the trackside environment. The use of TEGs in trackside energy harvesting is therefore limited, even though in some specific applications it might be feasible.

4 TRACKSIDE ENERGY HARVESTER DESIGN OPTIONS

In this section the design options related to the practical methods and arrangements for capturing the different types of energy input via the related physical principles of energy harvesting in the trackside environment is discussed. This includes readily exploitable solutions where off-the-shelf components can be selected for combination into an installation, solutions which are nearly exploitable or used in other environments which could be adapted to the railway environment, and emerging solutions which are still in the laboratory testing phases of development.

4.1 DISPLACEMENT HARVESTERS

4.1.1 Linear displacement electromagnetic generator concept

The linear generators generate electricity from the relative movement of the components using the electromagnetic effect. A schematic representation of a linear generator is shown in Figure 24, a mover with magnet oscillates along a liner axis within a coil of wire (stator coil) to induce current in the wire. Linear generators use the same electromagnetic principals as rotary generators where the magnets rotate about a central axis and induce current in coils arranged around the outside (other configurations are possible), however linear generators are potentially more suitable for some applications as they do not require complex mechanisms to transfer linear motion into rotary motion to harvest energy. A few examples of linear generator applications and concepts are shown in the following sub-sections.

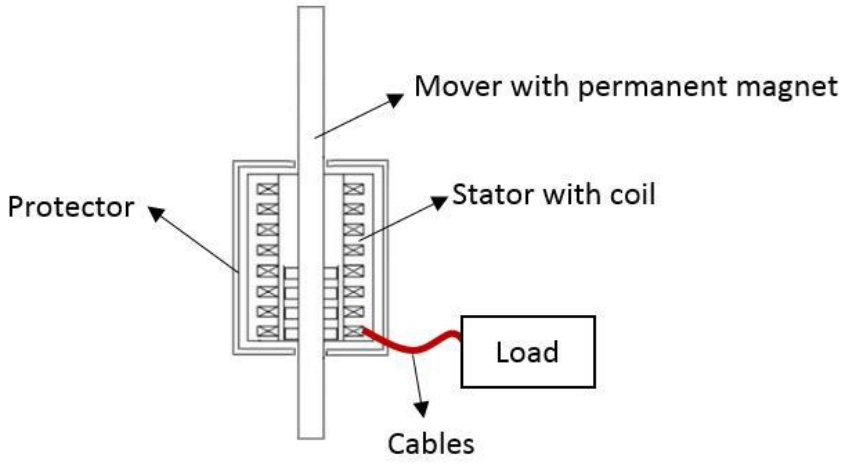

Figure 24 Schematic representation of a linear electric generator

4.1.1.1 Example application - Linear generator embedded into a road speed bump

The general architecture of a renewable road tunnel high voltage kinetic energy harvesting system, as shown in below (Figure 25), has four main parts: a speed bump, suspension, generator, and power storage modules. Acting as the energy input, the speed bump module harvests the kinetic energy of the speed bump's upward or downward motion. The suspension module drives the speed bumps upwards after the vehicle departs. The suspension damps the redundant vibration, which

increases the time to reset the mover. The linear generators generate electricity from the kinetic energy collected by the speed bumps. The power storage module rectifies the current and then stores the electrical energy in batteries ready for lighting, tunnel ventilation, charging for electric vehicles, etc. A peak voltage of 194 V and an average voltage of 55.2 V are generated from the prototype when the vehicle moves at 40 km/h. The achieved high power voltage indicates that the proposed high voltage kinetic energy harvesting system is acceptable for use in facilities in so-called 'renewable road tunnels'. It provides a cost-efficient power source for areas where power cannot be delivered economically and for electrical supply to intelligent transportation systems as well.

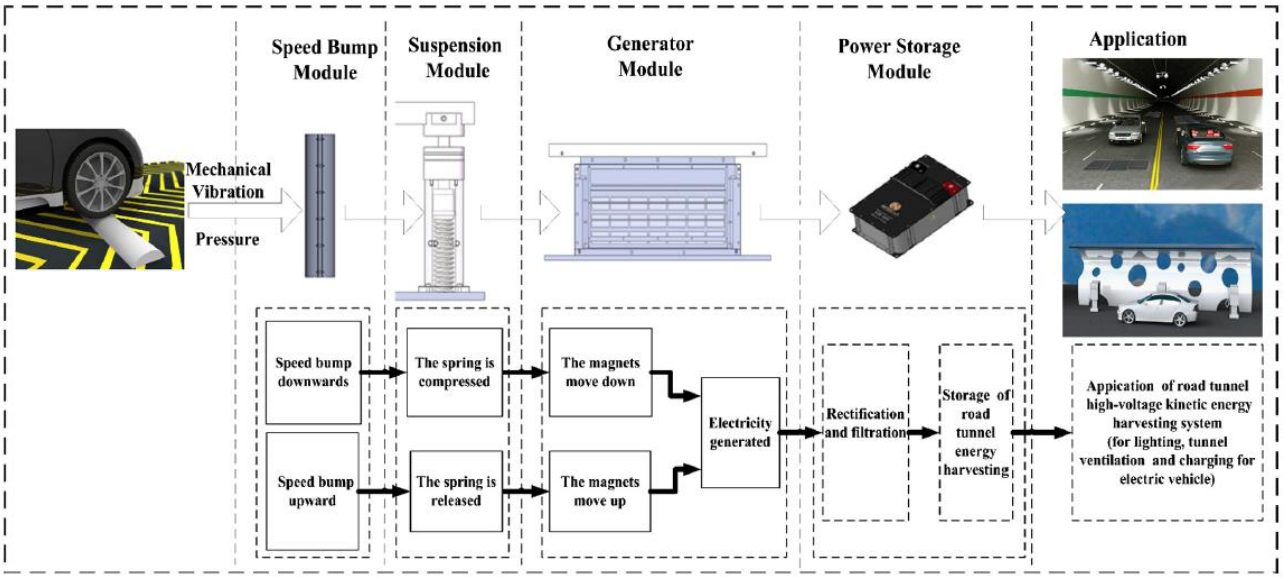

Figure 25 Linear generator embedded into a road speed bump [46]

4.1.1.2 Linear Generator Concepts Integrated into Railway Infrastructure

This group of outline concepts, for integrating linear generators into railway infrastructure, illustrated in Table 2 below, are based on the principal of capturing energy from displacements induced by either the train itself, or the movement of the track under the train and transferring those displacements to a linear generator.

Table 2 Concepts for integration of linear generators into railway infrastructure

Concept Number	Concept drawing	Description
1.1		• contactor (part which makes contact with the wheel) is mounted next to the gauge face of the rail with the top just below the level of the running surface of the rail • as the wheel of a train passes, the flange of the wheels (which projects below the running surface of the rail) make contact with the contactor displacing it downwards • motion is transferred directly to the linear generator
1.2	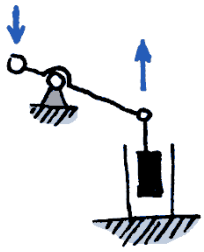	• contactor is mounted next to the gauge face of the rail with the top just below the level of the running surface of the rail • as the wheel of a train passes, the flange of the wheels make contact with the contactor displacing it downwards • motion transferred to linear generator via a lever • axis of the pivot for the lever is aligned with the axis of the rail
1.3	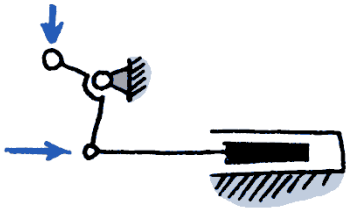	• contactor is mounted next to the gauge face of the rail with the top just below the level of the running surface of the rail • as the wheel of a train passes, the flange of the wheels make contact with the contactor displacing it downwards • motion transferred to linear generator via a lever • axis of the pivot for the lever is aligned with the axis of the rail • axis of motion of the generator coincides with the long axis of a sleeper
1.4	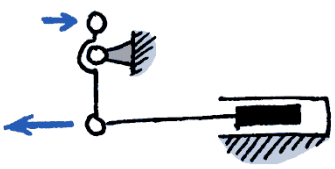	• contactor is mounted next to the outside face of the rail, projecting above the rail running head and makes contact with the outside edge of the wheel tread • wheels push the contactor ahead of them and downward as it pivots about the pivot

1.5		• motion is transferred via a lever to the linear generator • Concepts 1.4 and 1.5 Differ in the straight (1.4) or arced (1.5) shape of the linear generator
2.1		• displacement of the linear generator is derived from the displacement of the track (as the train passes) • lower stiffness sleeper-rail support (trackpad) • displacement of rail relative to sleeper transferred to linear generator via lever • pivot fixed to sleeper
2.2	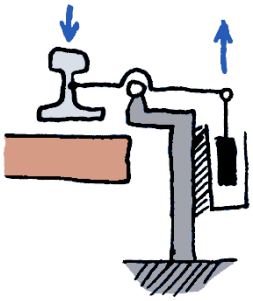	• displacement of the linear generator is derived from the displacement of the track • actuating arm fixed to rail • linear generator and the actuating arm pivot are mounted to a fixed base independent of the track • actuating arm transfers the displacement of the track to the linear generator
2.3	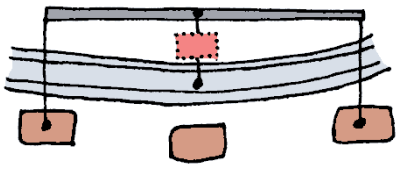	• displacement of the linear generator is derived from the displacement of the track • actuating arm is attached at each end to two sleepers, with a third unconnected sleeper in between • mid-point of the actuating arm attached to rail via a flexible link which includes a linear generator • waveform of track displacements causes differential displacement at the three fixing points causing flexible link (linear generator) to change length

4.1.2 Geared electromagnetic generators prototypes

A number of concepts and prototypes have been developed based on a device fitted to the track operating on the principal of transforming vertical displacement of the track caused by the passage of a train, via racks, gears and clutches, to a rotary motion to drive a rotary electromagnetic generator. The main distinguishing feature between the designs is whether the device is connected to some form of ground anchor to utilise the relative motion between the track and the ground, or if the device is only connected to the track and utilises the relative motion between different locations on the track.

4.1.2.1 Prototype developed by Southwest Jiaotong University, China

Author team from Southwest Jiaotong University, China, presented a portable high-efficiency electromagnetic energy harvesting system [47], depicted in Figure 26. It consists of two main parts: mechanical transmission and the electrical regulator. Authors describe the function of the device:

> *When a train rolls over a section of track, vertical displacements are induced by the weight of the train. Because of the elasticity of the rails, they vibrate. A rack that is fixed to the rail moves at the same amplitude and frequency as the rail. The rack harvests the vertical vibrational energy of the rail. The movement of the rack is amplified by a high-ratio gear set, thereby converting small displacements and velocities into high-speed rotation of a shaft connected to a generator. Two one-way bearings mounted on the shafts engage alternately to convert the bi-directional input displacement to unidirectional rotation to increase efficiency. The output shaft drives a DC generator in only one direction to generate power. The power is stored in the supercapacitors and can be drawn upon or stored for standby power in trackside applications such as crossing lights, switches and maintenance.* [47]

The peak voltage of 58 V at 1 Hz with a displacement of 2.5 mm was close to being practically useful for supplying rail-side applications, such as safety devices and emergency repairs in areas lacking power, indicated that the proposed energy-harvesting system has potential as a renewable alternative energy source.

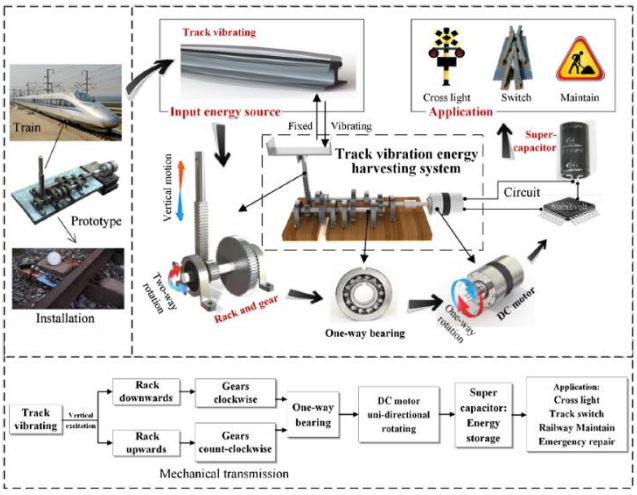

Figure 26 Design and prototype of the energy harvester with output energy peak voltage of 58 V at 1 Hz with a displacement of 2.5mm. [47]

4.1.2.2 Prototype developed by State University of New York at Stony Brook & Virginia Tech

A team from Stony Brook presented a preliminary prototype of mechanical rectifier based harvester [48]. Their lab results illustrate that sufficient power can be harvested as well as the features and benefits of the motion rectifier design, which is shown in Figure 27. They describe their harvester:

> *The harvester design mainly composed of a motion conversion mechanism, an electromagnetic generator, and a fly wheel. The bidirectional to unidirectional transmission includes three shafts, three spur gears, a pair of rack and pinion, and two roller clutches. The two racks move together in up and down direction. The roller clutches installed at the two input shafts control transmission of motion to the two large gears labelled gears 1 and 2. Both gears are only allowed to rotate in the counter-clockwise direction. This results in Shaft 3 rotating permanently in the clockwise direction. Shaft 3 engages the generator and flywheel through the bottom of the plate. (…)*
>
> *A properly designed mechanical based harvester has the potential to power major railway equipment and infrastructure, representing a safety benefit to areas lacking electrical infrastructure. (…) The preliminary prototype demonstrates the concept. However, the mechanical efficiency is still less than ideal, largely due to mechanical component friction.* [48]

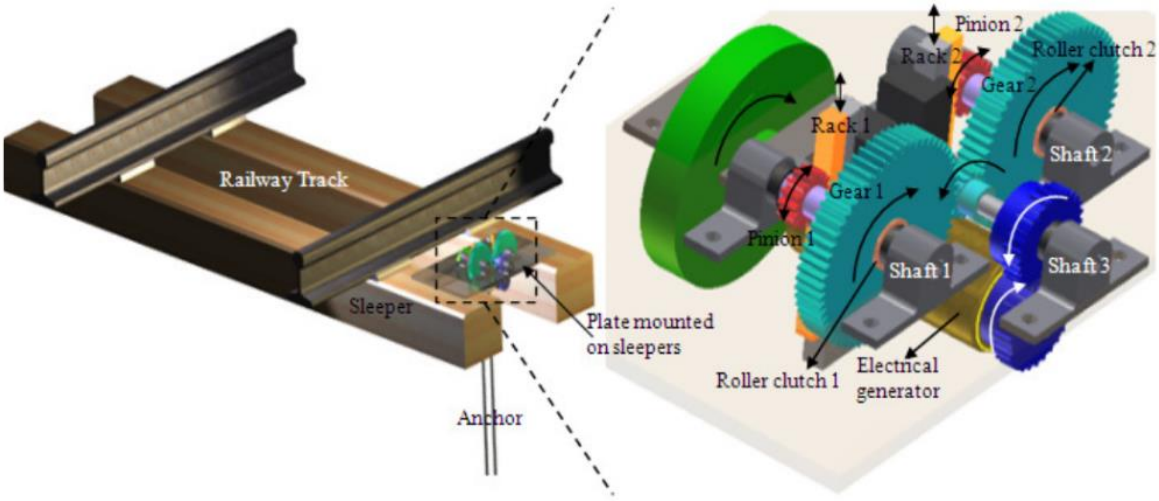

Figure 27 Electromagnetic Energy Harvesting from Train Induced Railway Track Displacement [48]

> *« Railway tracks of good quality have a track of displacement of around 0.25 inch for a moderately loaded passing train. A sinusoidal input at 1Hz and 0.25 inch amplitude is applied to the rack. (…) The power generated in this experiment is 1 Watt with 22.2% conversion efficiency. »* [48]

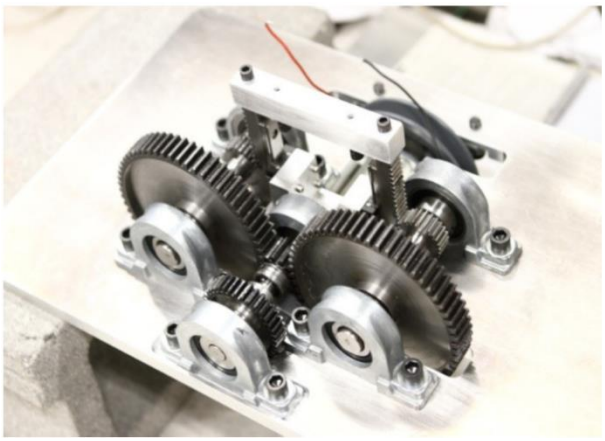

Figure 28 Full-scale prototype of the mechanical based harvester [48]

4.1.2.3 Prototype developed by Virginia Tech & State University of New York no.2

A novel direct motion-driven harvester (see Figure 29) has been reported [49] with anchorless mounting reveals higher power capacity without requiring special preparation during installation. Compared to any traditional anchor, this design is more practical, as it does not require the cement curing time, therefore not causing an interruption to the train operation. The authors write about the harvester:

> *To validate the installation and functionality of the proposed design under the real condition, an in-field test was conducted to the prototype at the Transportation Technology Center, Inc. (TTCI) test loop. The test train consisted of approximately 100 freight cars and ran at a constant speed of 64km/h (40mph). In all, the harvester experienced over 200 train passes over one night of test train operation before the data were recorded. (…)*
>
> *Anchorless mounting (Figure 30) enables the harvester to be easily and quickly installed on the traditional railway in 30 minutes, which shows its important practical value in field applications. The field tests show a quite high average power of 7W and a peak power of 56W. This shows the harvester design has very promising application for powering track-side electrical devices to assemble a self-powered setup. It also has the potential to power many railway trackside equipment and electrical infrastructures to improve railway safety, especially in remote areas or tunnels lacking viable power sources. The energy harvesting technique introduced in this work can also be extended into other energy harvesting fields to regenerate energy from pulse-like vibration*. [49]

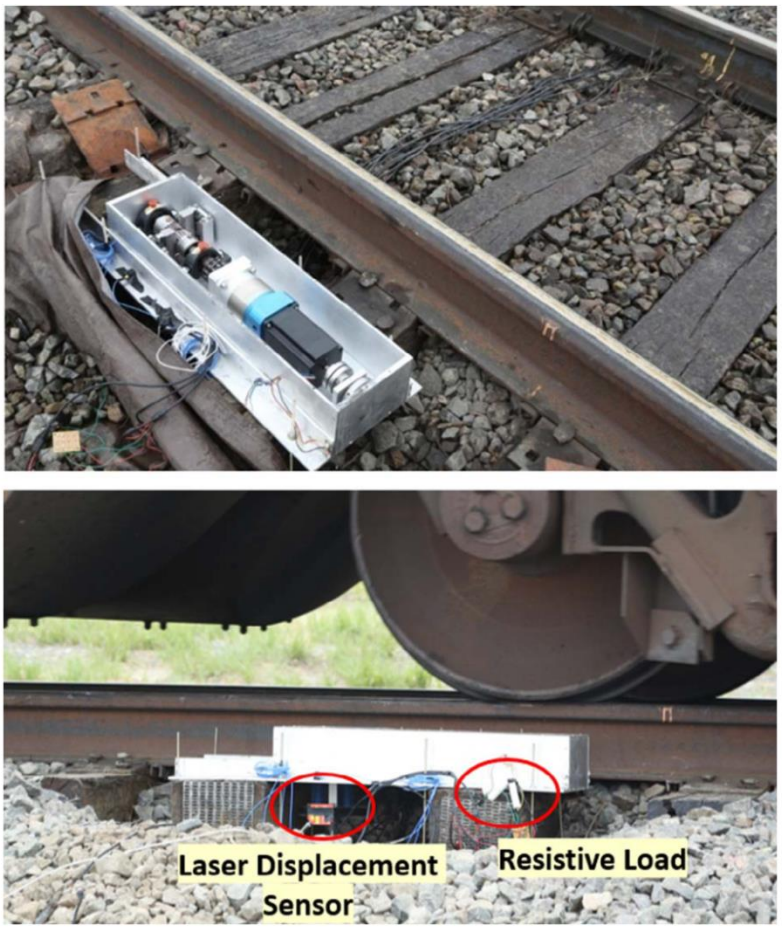

Figure 29 Harvester installed and tested at TTCI test track, with fully loaded freight train running at 64 km/h (40 mph) [49]

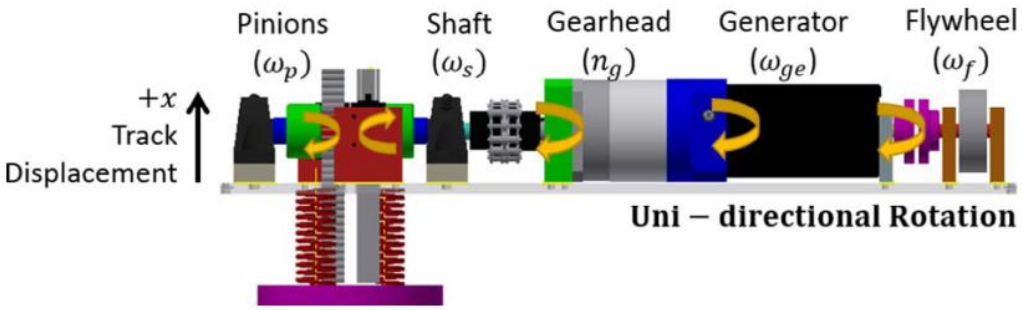

Figure 30 Dynamic model of the harvester. [49]

Table 3 Summary of field test result under different resistive load (data shows sum of all 3-phases from BLDC generator). [49]

Load resistance (Delta) (Ω)	Load resistance (eq. to Wye) (Ω)	Avg. power (W)	Peak power (W)	Measured disp. (mm)
4	1.3	4.1	16.6	4.4
8	2.7	5.5	29.0	4.8
16	5.3	6.7	50.4	5.1
50	16.7	**6.9**	**56.2**	5.7
150	50	3.5	22.9	5.9

4.1.2.4 Prototype developed by University of Nebraska-Lincoln

A theoretical study was presented by University of Nebraska, employing a cam mechanism to exploit a contact between a train wheel and a harvester mechanism to drive an electromagnetic generator [50].

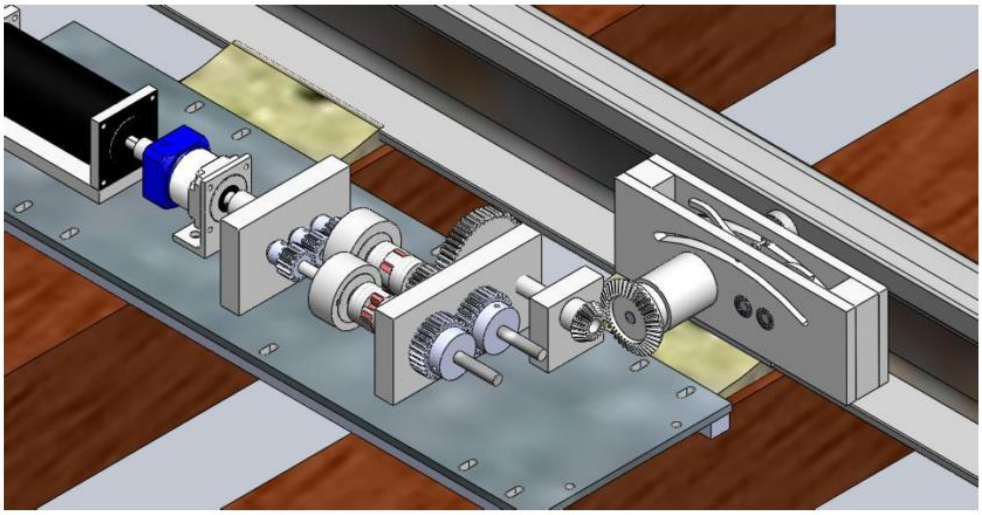

Figure 31 3D model of the mechanical device driven by the ramp-lever mechanism [50]

4.1.3 Piezoelectric linear harvesters concepts

4.1.3.1 Piezoelectric Drum - Shanghai University of Engineering Science

Authors from Shanghai University of Engineering Science presented the piezoelectric harvesting device [51] that is structurally simple. However, the position and topology of piezoelectric generator have huge impact to the energy harvesting. « *The displacement of the vibration can drive the piezoelectric energy harvester, see Figure 32, and supply power for wireless sensor network system, because some sensor only need to be activated when the train was nearby such as the locating*

system of trains. So it is meaningful to harvesting energy for track vibration as the assistance power source for the railway safety. » [51].

A proposed drum design [51] of the piezoelectric generator is installed under sleeper as shown in Figure 33. This method is simple, and avoids the need of changing the sleeper geometry. Lab test results, Figure 34, were compared with simulation, the comparison table is placed below.

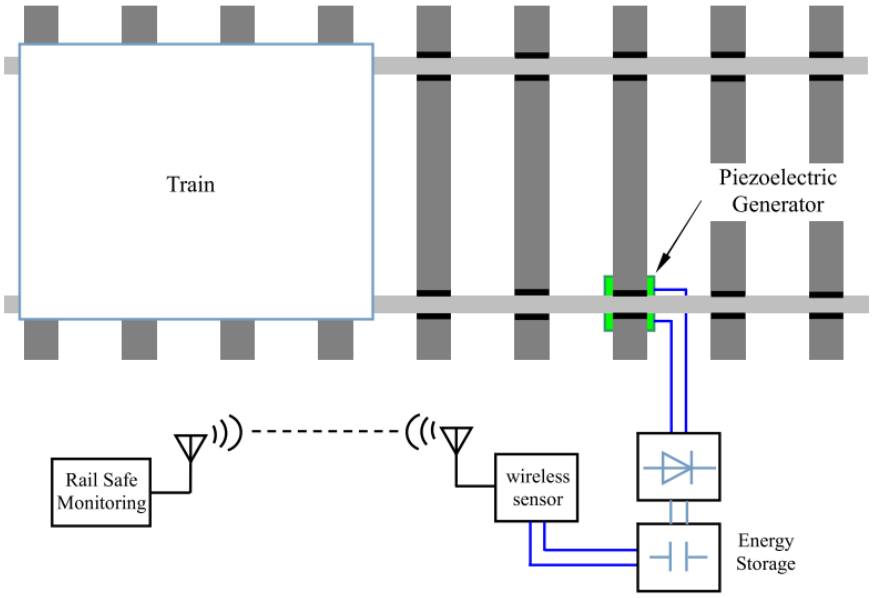

Figure 32 Design plan of the supply power for wireless sensor [51]

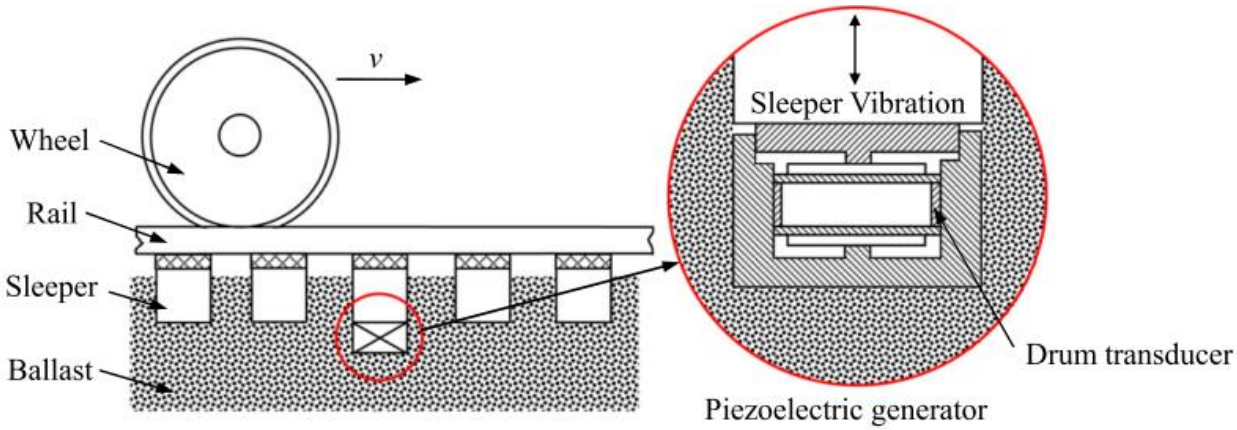

Figure 33 Location of piezoelectric drum generator [51]

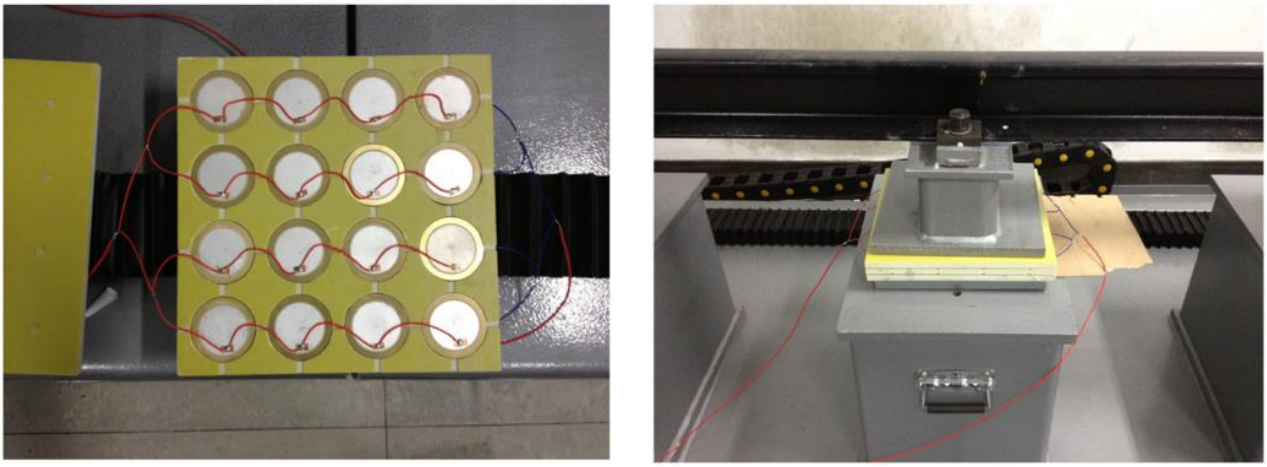

Figure 34 Piezoelectric drum transducer group and Installation location of the generator [51]

Table 4 Comparison results of simulation and experiment in real track condition. [51]

Results	Unit	Experiment	Conversion factor	Virtual experiment	Simulation	Error
Output voltage (rms)	V	15.6	$\alpha_V = 1$	15.6	16.5	9.62%
Output power (rms)	W	8.1×10^{-5}	$\alpha_P = 1200$	0.096	0.1	4.17%
Harvested energy	J	2.08×10^{-3}	$\alpha_E = 240$	0.49	0.38	24.32%

4.1.3.2 Piezoelectric patch and stacks

A study of a railway track structure with piezoelectric patch-type and stack-type energy harvesters [52] is depicted in Figure 35. «In the figure, a piezoelectric patch-type energy harvester is mounted at the bottom of a rail. A piezoelectric stack-type energy harvester is also installed at the bottom of the steel rail by a connecting device. Because the piezoelectric transducers are much smaller than the track structure as a whole, we neglect their effects on the whole track structure. » [52] However, significant electric outputs cannot be expected. Authors describe their device:

> *A stack-type piezoelectric transducer is placed at the bottom of a steel rail to harvest the mechanical energy induced by the moving train. A detailed installation schematic of the piezoelectric stack is exhibited in Figure 36. The piezoelectric stack device includes a displacement transmission rod, a compression spring, a force transmission unit, a piezoelectric stack, a whole metal shell, screw bolts and a wire hole. The transverse track displacement of the rail is converted into a force through the compression spring, and is then transferred to the piezoelectric stack. A schematic of this device and its photo are exhibited in Figure 37.* [52]

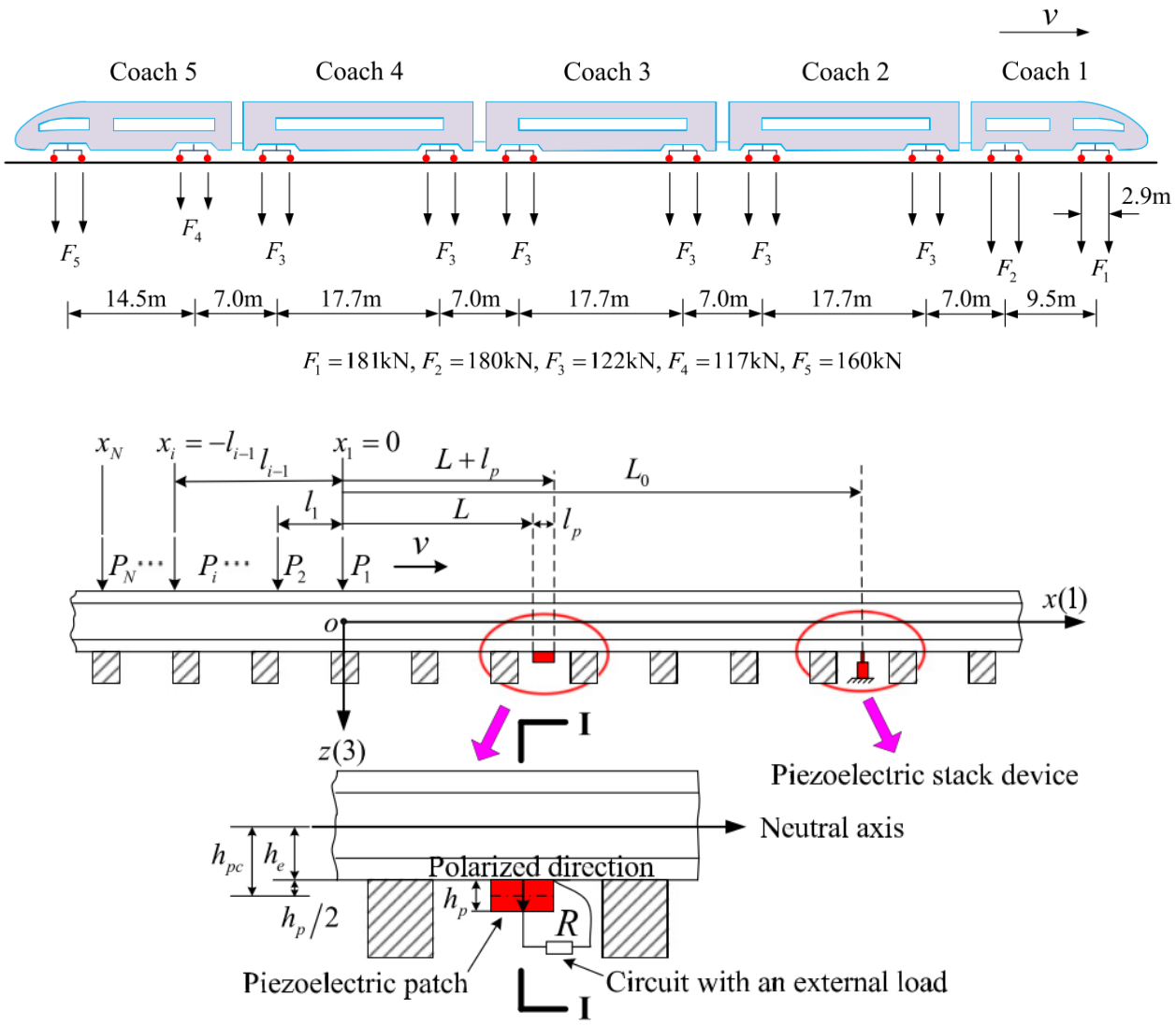

Figure 35 Schematic of railway track structure with piezoelectric energy harvesters [52]

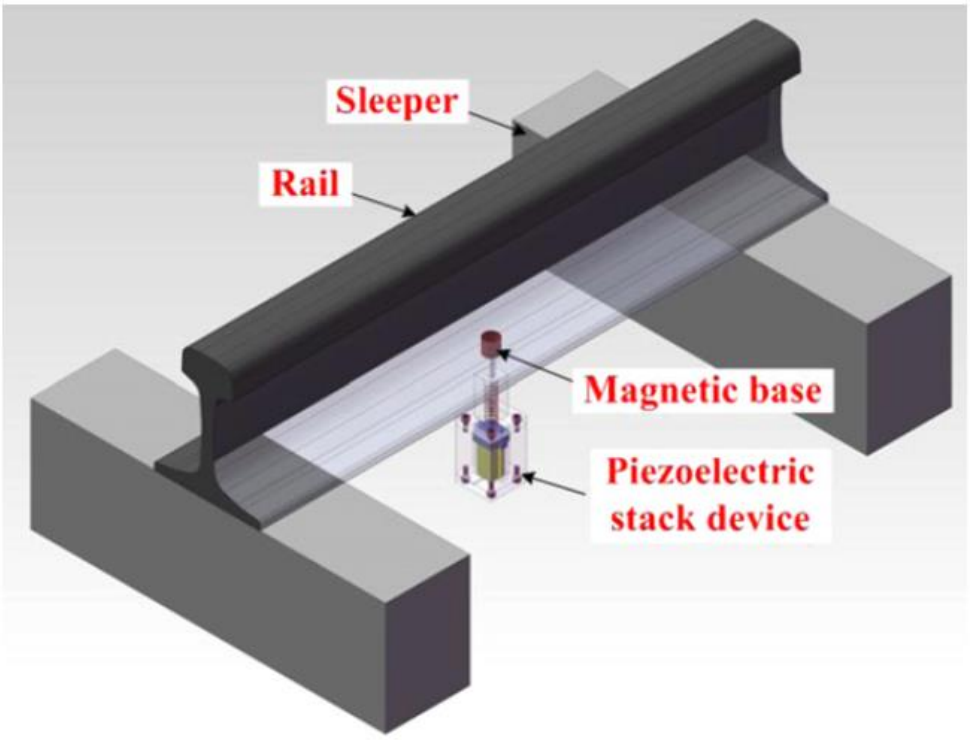

Figure 36 Installation schematic of piezoelectric stack. [52]

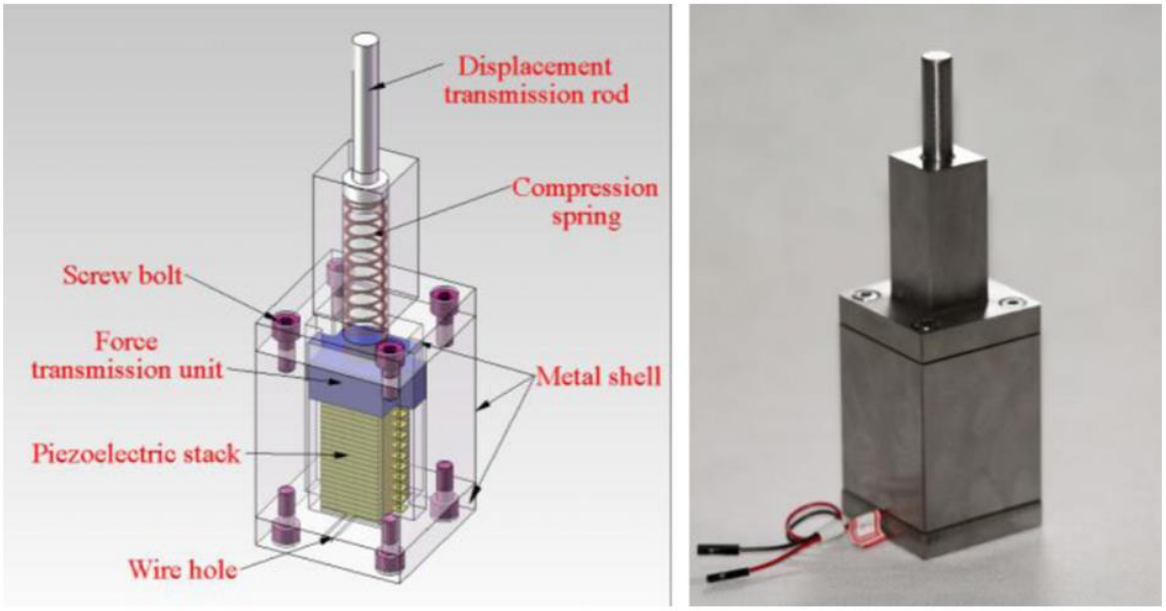

Figure 37 Schematic of a piezoelectric stack device and its photo. [52]

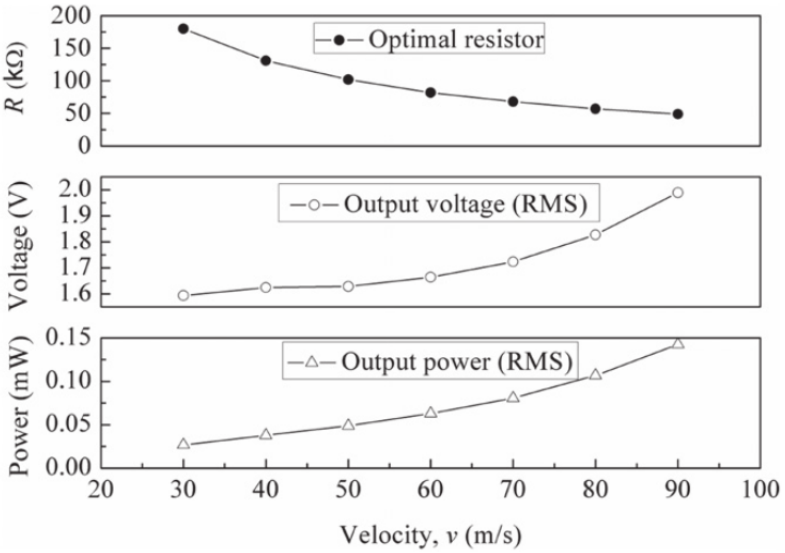

Figure 38 The optimal resistor and its corresponding output voltage and power change with the velocity of a passing train (stack). [52]

4.1.4 Magnetostrictive linear harvesters concept

4.1.4.1 Magnetostrictive Hammer Impact Device

Publication [53] describes that magnetostrictive materials potentially might be used for energy harvesting devices. The proposed devices, see Figure 39, are able to convert mechanical energy (with use of mechanical resonance) into electricity. The desired effect was obtained when the Terfenol-D rod was magnetically coupled with a powerful permanent magnet NdFeB. Terfenol-D bar under the influence of a mechanical stroke provides a strong mechanical signal (hammer blow to the bar) and simple magnetic circuit (coil and magnet) has allowed the electricity generation. This device could be placed under a rail with similar design as the previous energy harvester.

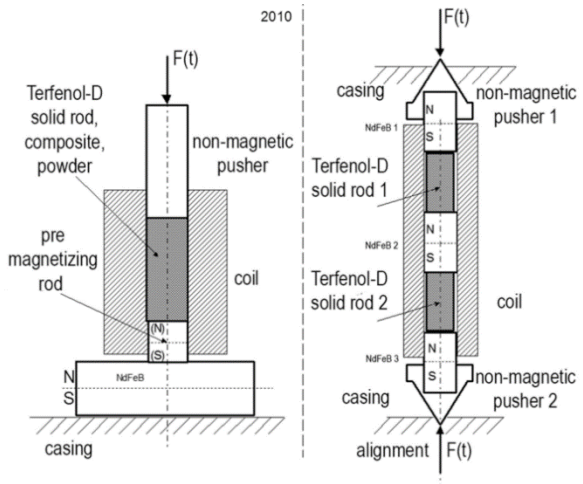

Figure 39 Two generations of Terfenol-D magnetostrictive harvester transducer [53]

4.2 VARIABLE RELUCTANCE HARVESTERS

4.2.1 Variable reluctance harvester concept

Electrical energy can be generated by an electromagnetic induction, caused by a change in magnetic reluctance induced by a passage of a train wheel, momentarily forming part of the magnetic circuit.

4.2.1.1 Example application developed by Harvester by University of Freiburg

The author team of University of Freiburg developed the variable reluctance harvester [54] and they claim that:

> *The results found within this study clearly show the applicability of variable reluctance harvesters as a train passage detector, or in any other environment with rotating or periodically moving ferromagnetic parts. With power outputs beyond the mW regime, energy-autonomous systems can be easily powered. The simulations of the output voltages have a higher slope than actually measured values, which has to be investigated in more detail in future work to figure out the relatively large deviation.* [54]

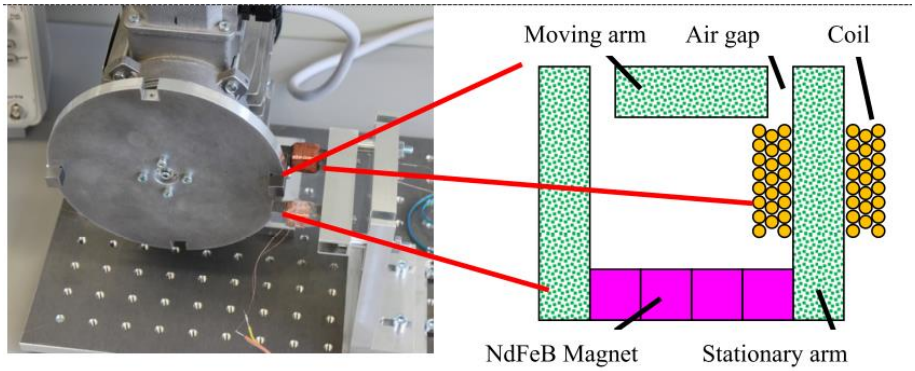

Figure 40 Test set-up for the harvester (left) and schematic top view of the reluctance circuit (right) [54]

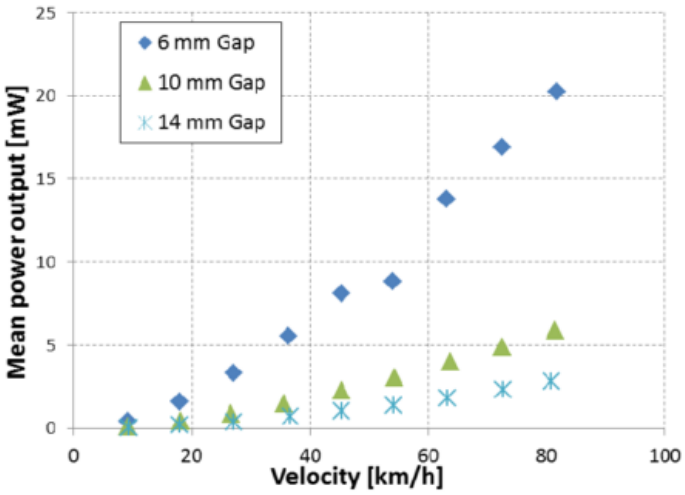

Figure 41 Measured mean power output with respect to the velocity for three different clearance widths between the moving and the static parts of the reluctance circuit. [54]

4.2.1.2 Variable reluctance harvester concept integration into railway infrastructure

Magnetic flux from a permanent magnet in the generator (Figure 42) (without the train wheel) passes through the fixed part of the magnetic circuit, rail and air gap. The value of magnetic flux density is minimal (B_{min}). When the train wheel is closing to generator, magnetic flux changing path over train and increasing to time, where whole train wheel is front of generator. Magnetic flux is closing over fixed part of magnetic circuit, rail, train wheel and shorter air gap. If the distance of wheel and generator's head isn't change, magnetic flux is constant and maxima (B_{max}). When train wheel is moving away, the magnetic flux is also decreasing to value B_{min}.

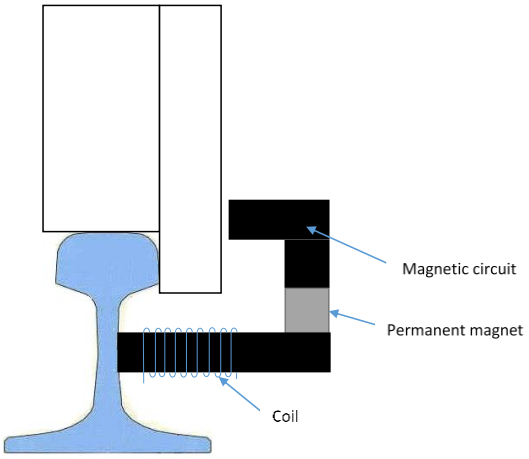

Figure 42 Variable reluctance energy harvester diagram

Magnetic flux density is shown in Figure 43.

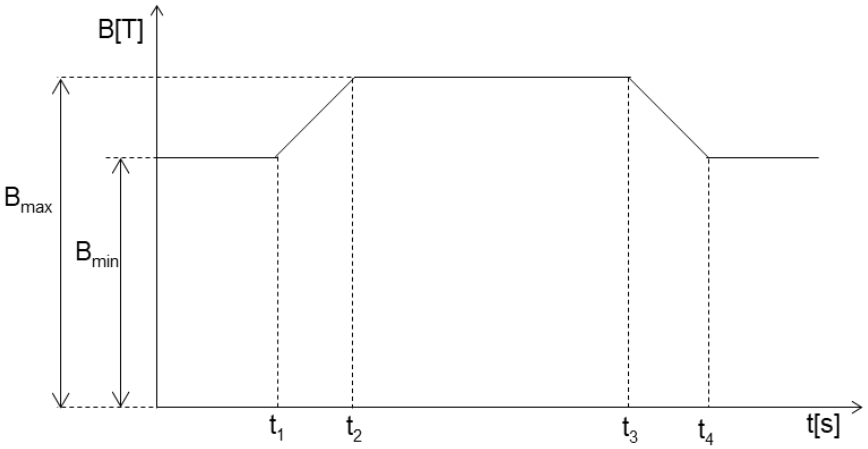

Figure 43 Magnetic flux density of system during passing train

For the induced voltage calculation it is necessary to start from the general equation for induced voltage:

$$u_i = \frac{d\psi}{dt} = N \cdot \frac{d\emptyset}{dt} = N \cdot S \cdot \frac{dB}{dt}$$

where N is number of turns, S is area of magnetic circuit and B is magnetic flux density.

For simplification it is supposed that increase of flux density is linear. On the base of this fact, induced voltage equation can be re-written to:

$$u_i = N \cdot S \cdot \frac{\Delta B}{\Delta t}$$

Analytic solution can be divided to three time part t_1-t_2, t_2-t_3, t_3-t_4.

Value of magnetic flux density change ΔB is possible to write as

$$\Delta B = B_{max} - B_{min}$$

For simplification can be supposed that train speed is constant, i.e. time part t_1-t_2 a t_3-t_4 is equal.

It can be write that:

$$\Delta t = t_2 - t_1$$

For particular time parts can be write that:

$$u_i = N \cdot S \cdot \frac{\Delta B}{\Delta t}, \qquad t_1 < t \leq t_2$$

$$u_i = 0, \qquad t_2 < t \leq t_3$$

$$u_i = N \cdot S \cdot \frac{-\Delta B}{\Delta t}, \qquad t_3 < t \leq t_4$$

Waveform of induced voltage is shown in Figure 44.

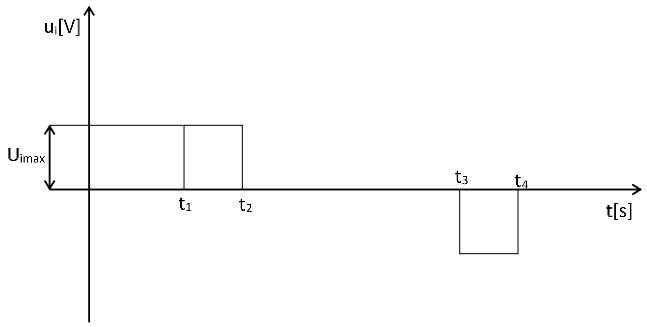

Figure 44 Waveform of Induced voltage during passing train

Value of generator's internal power during voltage pulse on pure resistance can be according to equation

$$P_i = \frac{U_{imax}^2}{R}$$

On the base of fact that output power is highest, when the load resistance is equal to internal coil resistance, output power is half against generator's internal power.

Energy generated by pass of one train wheel is calculated on the base of power during both voltage pulse:

$$E = 2 \cdot \frac{P_i}{2} \cdot \Delta t = P_i \cdot \Delta t$$

Value of magnetic flux density can be calculated by finite element method of by solving of equivalent magnetic circuit. Solution via equivalent magnetic circuit is not so much accurate, because main problem is calculation of reluctance between generator and rail, especially for stray flux.

Value of time is possible to be calculated on the base of train speed and assuming a simplification that the magnetic flux is starting to increase in the moment when the reluctance between the generator and a train wheel is lower than reluctance between the generator and the rail. Simply, this will happen in moment where distance of generator and wheel is lower than the distance between the generator and the rail.

4.3 VIBRATION ENERGY HARVESTERS

4.3.1 Inertial energy harvester working principle

Vibration (inertial) harvesters can be understood as accumulators of mechanical energy, which is being stored in the system as kinetic energy of the proof mass and potential energy in the spring element. During the operation a part of the accumulated mechanical energy is being extracted and converted into electrical energy by one of the transducing principles, using either electrodynamic or electrostatic damping force. Some part of the energy is inevitably lost due to the mechanical losses (Figure 45).

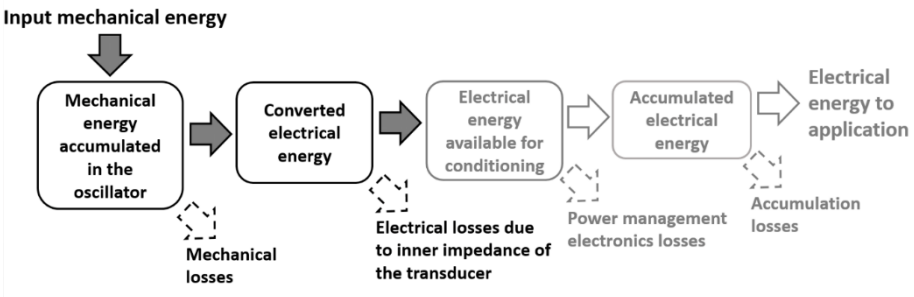

Figure 45 Energy flow in the inertial energy harvesters [55]

Let us assume that given 1 degree of freedom inertial harvester consisting of proof mass *m* with electrodynamic damping characteristics given by combination of mechanical and electrical damping d_m and d_e, respectively, contains linear stiffness *k* and is excited by vibrations of the frame $\ddot{z}$ (Figure 46).

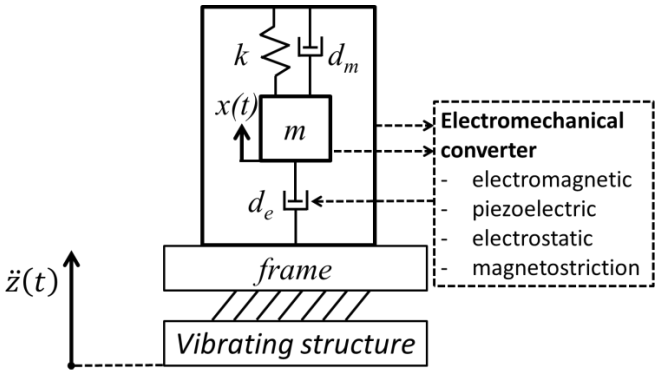

Figure 46 Inertial energy harvester spring mass damper model

Its dynamics is described by the well-known motion equation

$$\ddot{x} + \frac{[d_e + d_m]}{m}\dot{x} + \frac{k}{m}x = -\ddot{z}$$

where *x* represents the displacement of the proof mass. Natural frequency of such a system is found as $\Omega = \sqrt{\frac{k}{m}}$ and its damping ratio as

$$\xi = \frac{d_e + d_m}{2m\Omega}$$

The quality factor of the harvester is given by

$$Q = \frac{1}{2\xi} = \frac{m\Omega}{d_e + d_m}$$

The equation of motion can then be rewritten as

$$\ddot{x} + \frac{\Omega}{Q}\dot{x} + \Omega^2 x = -\ddot{z}$$

4.3.1.1 Harmonic excitation

In case of harmonic excitation $\ddot{z} = Av\cos(\omega t)$ the power output of the linear energy harvester is proportionally dependent on the square of the input acceleration magnitude Av of given frequency ω:

$$P_{el} = d_e \cdot \frac{\left(Av\frac{\omega}{\Omega^2}\right)^2}{\left[\frac{\omega(d_e + d_m)}{m\Omega^2}\right]^2 + \left[1 - \left(\frac{\omega}{\Omega}\right)^2\right]^2}$$

This formula can be used to calculate the frequency dependency of the power output of the system. By exploiting the superposition property of linear systems it is possible to calculate an estimate of a steady-state power output with arbitrary periodic input acceleration waveform by decomposing the input acceleration into harmonic components. It is obvious, that increasing the magnitude of input vibrations component with frequency equal to natural frequency of the harvester will lead to significant power generation improvement. Raising the magnitude of input vibrations is usually not feasible in real-life applications. However, the same effect can be achieved by proper orientation of the harvester.

4.3.1.2 Impulse excitation

In some applications the resonance operation of the inertial energy harvester is not possible due to discontinuous non-harmonic excitation waveforms. However, even such waveforms can provide sufficient input energy for inertial harvesters, assuming that the input acceleration spectrum contains frequency components on the same frequency, as the natural frequency of the harvester. An example of this can be seen in the impulse excitation of inertial energy harvester, as the (Dirac) impulse contains flat frequency spectrum, efficiently exciting the harvester with arbitrary natural frequency. Even though real-world acceleration pulses cannot be considered as Dirac impulses, but are in reality closer to rectangular or triangular pulses of finite length and magnitude. Frequency spectra of these pulses still contain multiple harmonic compounds depending on the shape of the pulse, which can be exploited for excitation of inertial energy harvester tuned to one of the frequencies present in the spectrum of the excitation waveform.

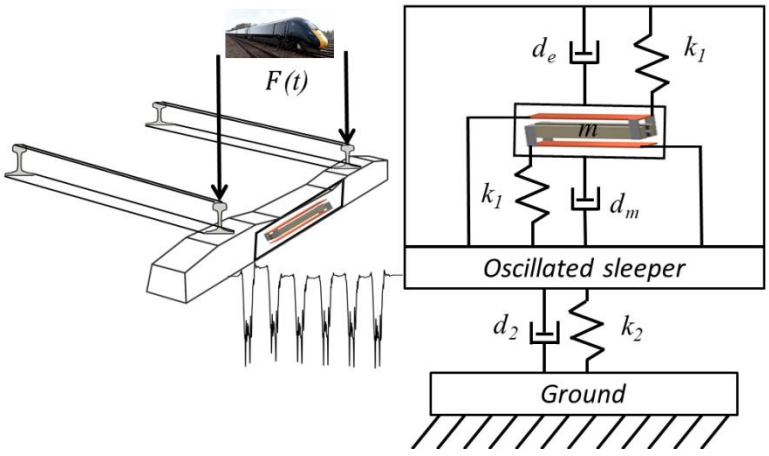

Figure 47 Pulse excitation of vibration energy harvester in trackside environment – integrated inside sleeper

4.3.1.3 Piezoelectric versus electromagnetic transducer

Research and development experience at Brno University of technology with vibration energy harvesting includes systems developed under several projects [2], which operates under resonance operation, the electromagnetic [56] and piezoelectric [57] vibration energy harvesters are used for wireless sensors [58], IoT applications [59], etc. The electromagnetic principle [60] is usually used for frequency in range of 10 – 50 Hz and output power is usually up to 80 mW. On the other hand, vibration piezoelectric harvesters [61] are suitable for higher operation frequencies in range 30 – 500 Hz with output power up to 5 mW. State of the art of kinetic energy harvesting systems for wide applications ranging from implanted devices and wearable electronic devices to mobile electronics and self-powered wireless network nodes was several times presented, e.g. by paper [62]. There is a comparison of several vibration energy harvesting systems with different physical principles, input vibrations, volumes, seismic mass, etc. It is very difficult to compare these systems and provide a transfer of this parameters in TEH application.

For this reason the analysis of both piezoelectric and electromagnetic principles with identical parameters in volume, seismic mass, input vibrations, resonance frequency and quality factor was done and presented [63]. Final output electric power of both systems is simulated and recommendation which type of energy harvester is suitable for employed applications. On the base of TEH application it is obvious that electromagnetic vibration energy harvester will provide higher outputs with respect of employed seismic mass and level of acceleration. The piezoelectric vibration harvesters are not suitable for vibration TEH.

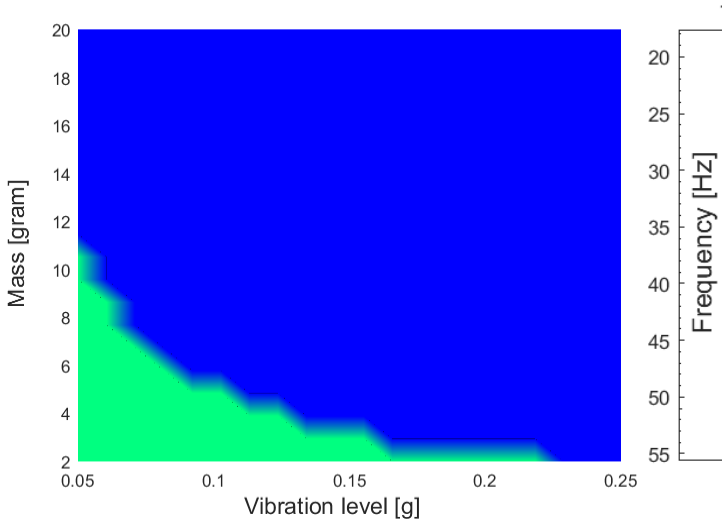

Figure 48 Comparison of resonance operation of piezoelectric and electromagnetic energy harvester simulations @ 0.1 g vibrations; green area – piezoelectric harvester provides higher power; blue area – electromagnetic harvester provides higher power

4.3.2 Review of electromagnetic vibration harvester concepts

4.3.2.1 Effect of speed variability for vibration energy harvesting in the UK

The paper [64] has investigated how much mechanical energy can potentially be harvested from the vertical vibration of a sleeper induced by trains passing at different speeds. To achieve this, a model of a track structure was combined with a model of an energy harvester. The models have been validated with experimental data from a site in the UK.

Oscillator parameter	Train speed [km/h]			
	162	180	195	200
Natural frequency [Hz]	13.72	15.14	16.57	16.86
Harvested energy [J]	0.14	0.18	0.26	0.27
Damping ratio	0.0045	0.0046	0.0043	0.0044
Relative displacement [mm]	4.52	4.54	5.05	5.02

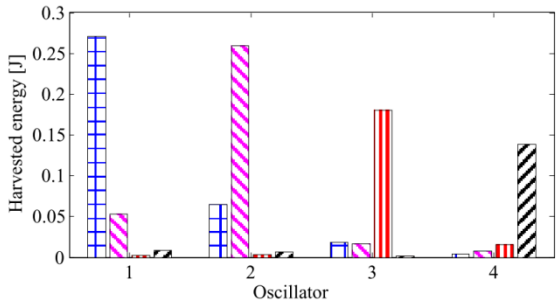

Train speeds: 200 km/h, 195 km/h, 180 km/h, and 162 km/h.

Figure 49 Energy harvested from harvesters with optimum parameters for a single passing train. Harvesters 1, 2, 3 and 4 are optimised for train speeds of 200, 195, 180 and 162 km/h respectively. [64]

4.3.2.2 Brno University of Technology

The validated model of track dynamics is very important for development of vibration TEH. A modern track provides a smooth track dynamics during a train passing while old regional line could be worn down and mechanical vibration of sleepers will be significantly higher and it could provide higher power density for vibration TEH. For this reason VUT used real vibration measurements for a lab analysis of vibration TEH. An experimental test of a sensitive electromagnetic resonator, which is described in detail by publication [65], with operation frequency 17 Hz (Figure 50) was done in VUT vibration lab. The harvester provides up to 35 mW of average power on load in resonance operation with 0.5 g magnitude of excitation acceleration. The tested resonance energy harvester is very sensitive for mechanical shock and it was fixed on a lab shaker and this device was excited by an acceleration measurement of the real sleeper during several train passing. The harvester operation under the real measured excitation was observed and analysed for different resistive load and output voltage on the resistive load of 3 kΩ is shown in Figure 50). Maximal harvested power was calculated for several types of passing train and position of energy harvester on trackside. The presented results correspond with average output power 2 mW during train passing and it could be useful for several low power sensing and monitoring applications. However this vibration energy harvesting system could be redesigned for trackside applications and also resized. Than higher power outputs

are expected and it has to be optimised [4] with respect to average speed of train and quality of trackside. This energy harvesting system could provide a maintenance free device and it could be integrated in a new generation of sleeper.

a) 

b) 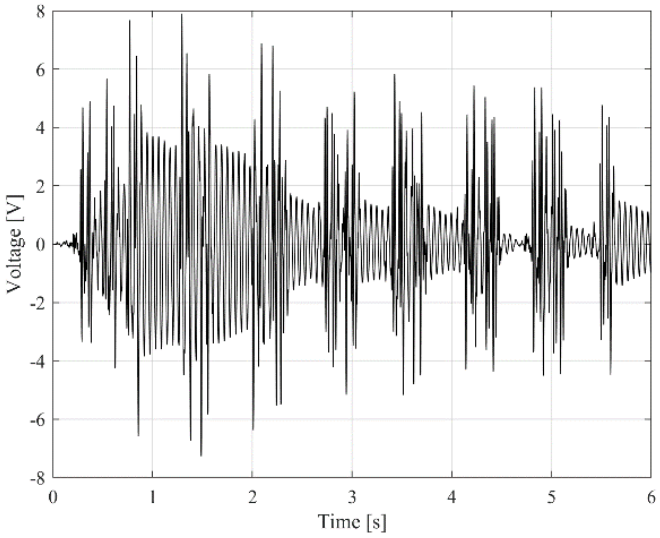

Figure 50 a) Tested electromagnetic vibration energy harvester 17 Hz; b) output voltage measurement during vibration excitation by measured vibration on sleeper – passing train with speed 130 km/h

4.3.2.3 ReVibe Energy

Swedish company ReVibe Energy focuses on development of electrodynamic vibration energy harvesters of various sizes. Their pilot project in cooperation with Deutsche Bahn AG includes adaptation of inhouse intertial energy harvesting units for the trackside environment. The aim of the project is to power up sensors attached to the track in order to monitor remote objects, such as railway switches. The ReVibe energy harvesters are inertial electrodynamic devices, which can provide up to 21 mW in resonance operation on 62.5 Hz at 0.4 g acceleration magnitude [66].

Fig. 51 ReVibe energy harvester mounted on track. [66]

4.3.2.4 Southwest Jiaotong University, Chengdu, China

The paper published by Southwest Jiaotong University [67] investigated the possibility of establishing a self-powered wireless sensor network by integrating the ZigBee stack protocol together with energy harvesting power source. The work was focused on the railway condition monitoring. Three types (Figure 52) of track-borne electromagnetic harvester were compared. It was found that energy harvesting by magnetic levitation is suitable for powering the ZigBee end device due to its wide frequency response.

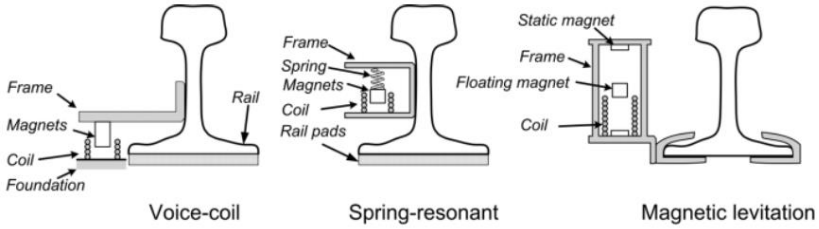

Figure 52 Illustration of types of track-borne electromagnetic energy harvester. [67]

The testing results indicated the resonance frequency of 6 Hz for the resonant electromagnetic harvester [68]. For the magnetic levitation one, it was capable of energy harvesting at a broadband low-frequency (3 Hz to 7 Hz) range with small railway vibration (0.6 mm to 1.2 mm). The induced voltage and power for the coil setup 4 at 1.2 mm rail displacement were Vp−p = 2.32 V, Pp−p = 119 mW at resistive load of 44.6 Ohm.

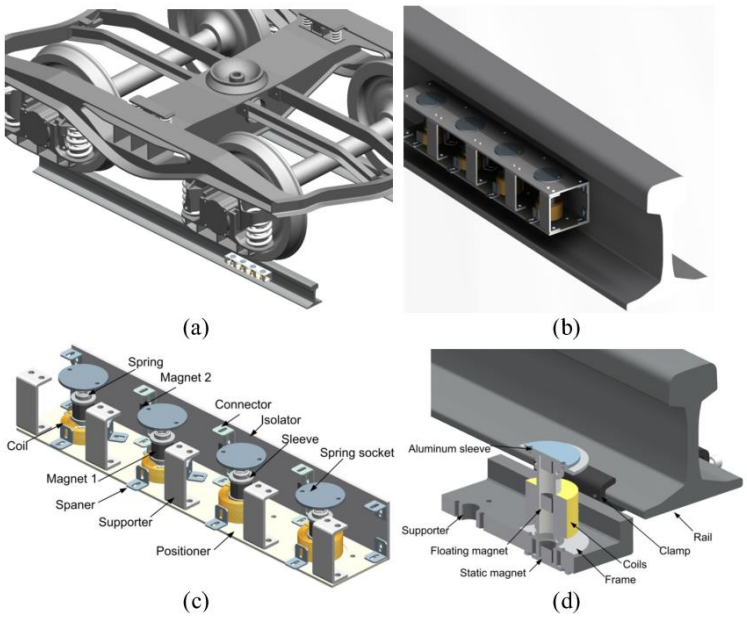

Figure 53 (a) Illustration of bogie-rail-harvester scales; (b) enlarged view of the harvester; (c) resonant harvester setup; (d) levitation device setup. [68]

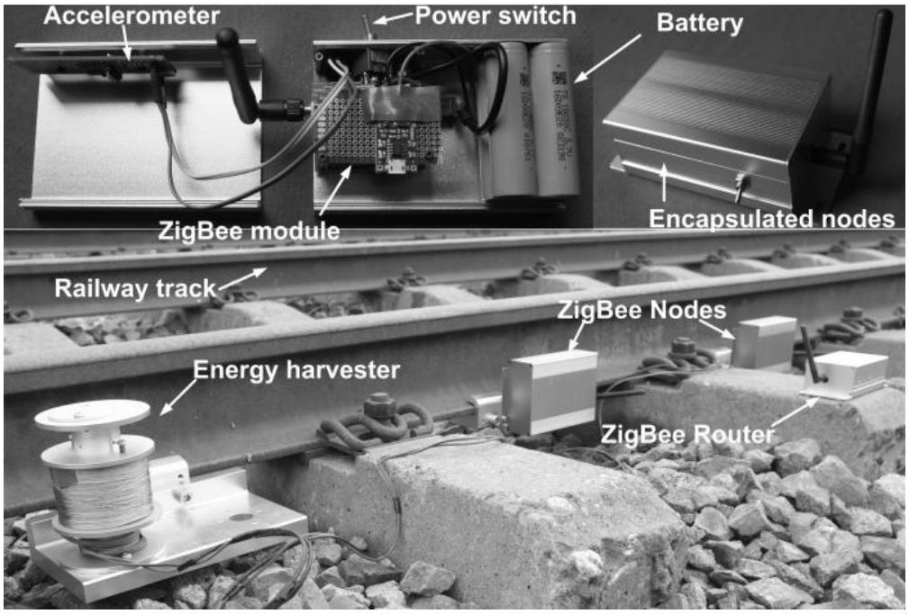

Figure 54 Encapsulated sensor node prototypes developed by SWJTU [67]

4.3.3 Piezoelectric vibration harvester concepts

4.3.3.1 School of Civil Engineering, Southwest Jiaotong University, Chengdu, China

The testing results of piezoelectric vibration cantilever harvester [69] indicated an energy harvesting at frequency of 5 Hz to 7 Hz. $P_{p\text{-}p}$ = 4.9 mW and $V_{p\text{-}p}$ = 22.1 V were achieved with a load impedance of 100 kOhm at rail vibration displacement of 0.2 mm to 0.4 mm, rail acceleration of 5 g with excitation frequency of 7 Hz.

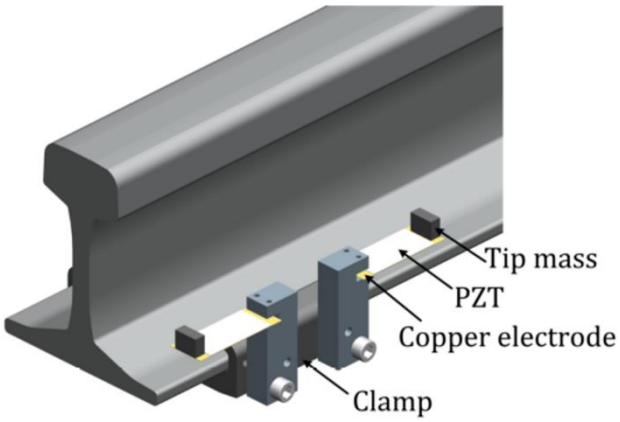

Figure 55 clamped cantilevered piezoelectric beam configuration [69]

4.3.3.2 Chinese Academy of Sciences

Generating electric energy from mechanical vibration using a piezoelectric circular membrane array is presented in the paper [45]. The resonance operation is assumed for test of 3 membrane array with a dimension ofΦ40mm×0.4mmresulted in an electrical power generation of 21mW through a resistor load of 11 kΩ.

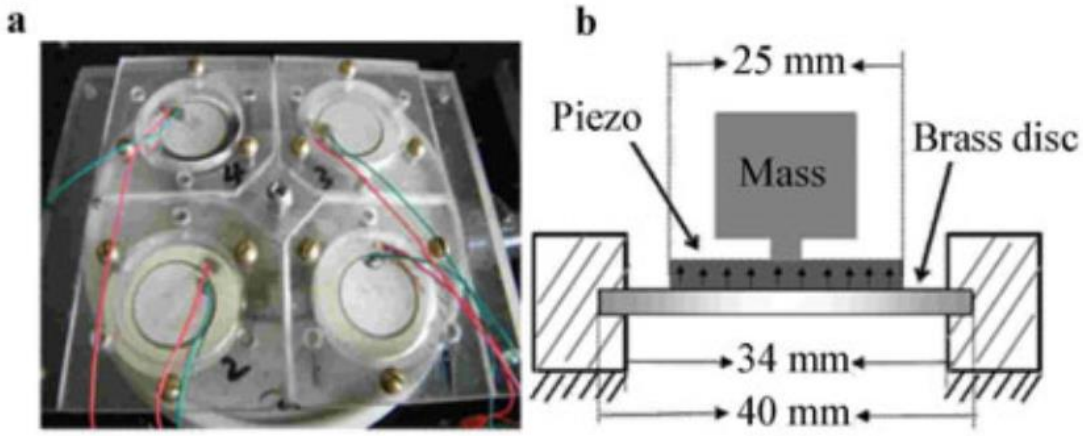

Figure 56 clamped cantilevered piezoelectric beam configuration [45]

4.3.4 Triboelectric vibration harvesters

Examples of reported power densities of harvesting vibration energy by TENG:

- Vertical Contact-Separation Mode, Operating frequencies 2 to 200 Hz with a wide working bandwidth of 13.4 Hz. The highest peak power density obtained for such a structure was 726.1 mW/m^2 [70].
- Contact Single-Electrode Mode. For large-scale applications with the highest peak power density 0.4 W/m^2 [71].
- Multilayer Structural TENG [72] with power density 104.6 W/m^2.
- Organic thin-film based TENG [73], with power density 60.2 mW/m^2.
- Rollable Paper Based TENG [74] with obtained power density 121 mW/m^2.
- TENG [75], Figure 50, reached up to 71.9 μA and 187.8 V at the resonance frequency of 13.9 Hz with the instantaneous power output of 9.3 mW and power density of 3.7 W/m2. This design concept could be used under sleeper with similar principle as is shown in Figure 51.

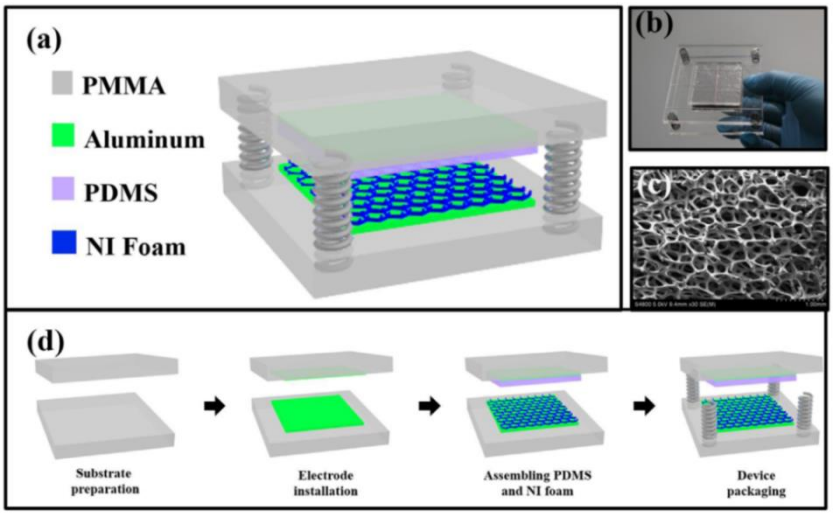

Figure 57 Porous micro-nickel foam based triboelectric nanogenerator. (a) Schematic and (b) photograph of a fabricated TENG. (c) An SEM image of porous micro-nickel foam. (d) Process flow for fabricating the porous nickel foam based TENG. [75]

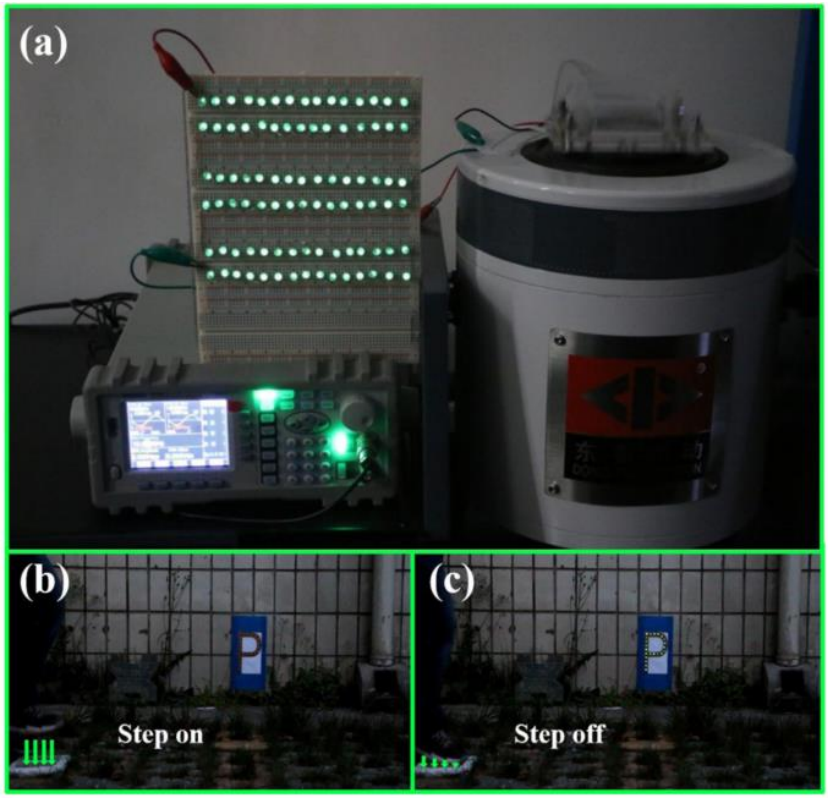

Figure 58 PMNF-based TENG as a sustainable power source. (a) TENG working on an electrodynamic shaker at the resonance vibration frequency of 13.9 Hz. About 100 LEDs light up simultaneously. (b) Setup in which the TENG acted as a direct power source for self-power pilot lamps and (c) when footstep fell on the TENG, simultaneously lighting up the pilot lamps in real time, promising a potential caution system of park or self-powered floor [75]

4.3.5 Power management electronics and storage for vibration energy harvesters

Vibration energy harvesters require specific power management solutions, due to their low outputs and their operation in resonant or transient modes. For this reason the electronics built from discrete elements is not usually feasible; instead, on-chip ultra-low power management solutions are being used.

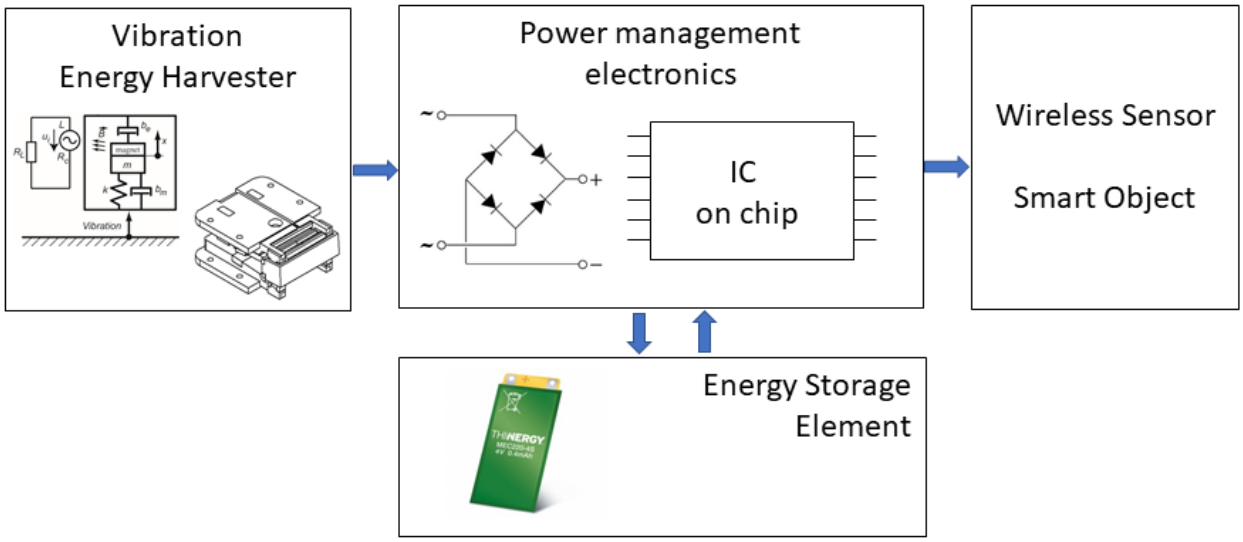

Figure 59 Schematic diagram of whole energy harvesting system

In recent years, with energy harvesting becoming an important research topic, the development of integrated circuits with low power consumption is needed. At present, a lot of ICs have been developed by commercial companies for this area. Most of them are adjusted for all kinds of energy sources such as mechanical, solar and thermal energy. Basic electronics for vibration energy harvester device is required and includes AC/DC conversion, DC/DC converter and energy storage. This part of the document describes how to find an appropriate power management chip and electronics for the vibration energy harvester device. General requirements for electronics are: rectification, optimal impedance load, optimal voltage adjustment, stabilisation of output voltage, electronics protection and energy storage. Figure 60. shows a block scheme of energy harvester (EH) with power management electronics and energy storage.

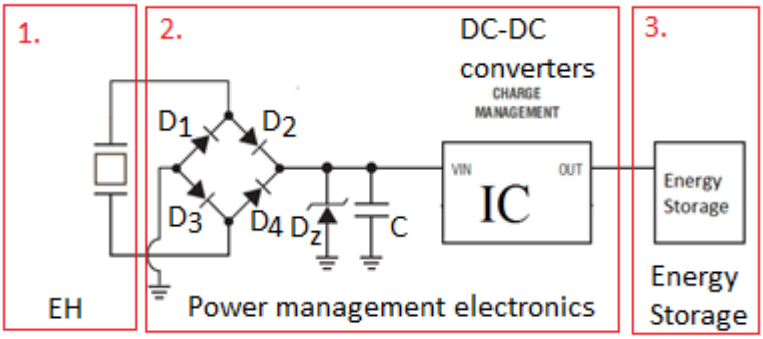

Figure 60 Block scheme of energy harvester with power management electronics and energy storage

The electronics results from the vibration environment in which the energy harvester will operate. The best solution is to use an accelerometer to evaluate the character of the vibration source. The accelerometer provides information about the character of vibration such as level and frequency of vibration and an optimal energy harvester may then be chosen for given vibration source. Dominant frequency of vibrations can be easily evaluated from accelerometer data by Fast Fourier Transform (FFT) method. Higher amplitude and frequency of vibrations generate more power from energy harvester. Also, it is important to know, whether the vibration energy is generated by continuous vibration or by shock impacts. The energy scavenging from continuously vibrating source is more effective than from irregular shocks applications. The energy harvester for mechanical vibration energy scavenging generates alternating current (AC) on its output. This signal cannot be stored to some battery or capacitor directly because only the mean current value at time can be stored at energy storage. In this case the AC current generated by EH has to be transformed to direct current DC and then the energy can be stored. The AC current is transformed to DC current by a rectifier. There are several types of rectifiers, but a full-wave rectifier employing four diodes is used in most of cases as is illustrated in Figure 60 (diodes D1, D2, D3 and D4). Then the energy from EH can be stored at capacitor *C*. The Zener diode D_z is connected as a protection of electronics for overvoltage. If EH operates the level of voltage on capacitor *C* is increasing until the voltage on the capacitor is saturated. This level of voltage is given by energy *E* which is delivered by EH over rectifier and by value of capacitance *C* as can be seen from equation for energy on capacitor:

$$E = \frac{1}{2}CV^2$$

From which the voltage V can be derived as:

$$V = \sqrt{\frac{2E}{C}}$$

This voltage V measured on capacitor C, when no load is connected, is called open circuit voltage (V_{oc}). For illustration of how to choose the level of capacitance C, Figure 61 shows the voltage and power measured on capacitor C with two different capacitances 1 μF (Figure 61 a) and 10 μF (Figure 61 b) where very low energy is delivered from energy harvester. Because of a small capacitance C

(Figure 61 a), the shape of behaviors is not linear (looks like saw blade) because a part of energy is lost from capacitor between each two cycles of EH but the voltage on capacitor is quickly saturated. Higher capacitance (Figure 61 b) smoothens the behavior but level of V_{oc} will be lower and take more time for saturation of the voltage on capacitor.

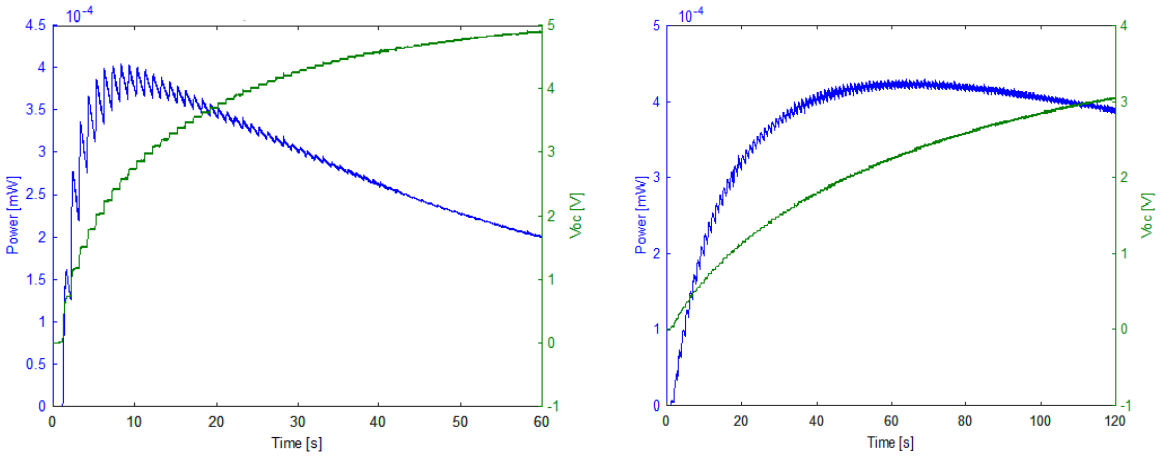

Power and Voc measured on capacitor C of capacitance 1 µF

Power and Voc measured on capacitor C of capacitance 10 µF

Figure 61 Power and Voc measured on capacitor C of capacitance 1 µF a 10 µF, where weak energy is delivered by energy harvester

If the energy delivered from EH is high, the high capacitance of C can be chosen as well. If the EH operates in shock application, this energy from capacitor can be used for some application directly. But as is described above, this way we can harvest only small amount of energy. If the continuous vibration mode of EH is used, the energy from EH can be gradually accumulated to the energy storage and if sufficient energy is accumulated, it can be used for some application. Energy from C needs to be gradually shifted to another energy storage, such as supercapacitor or battery.

Supercapacitor can be used for some applications during or briefly after the EH is operating. It can be used as a peak power source. Power management electronics for EH with supercapacitors is simple, only DC-DC converters such as charge pumps are used (for delivering a higher voltage to the supercapacitor) and electronics for stabilisation of output voltage, if it is required. This type of electronics is maintenance free.

If battery is used, the device has energy even the EH is not operating, but the power management electronics needs to contain electronic parts focused on correct battery charging and protection for controlling undervoltage and overvoltage levels. Batteries also generally require maintenance.

Power management electronics can be assembled by commercial electronic components (mostly for high power applications with power in range of tens watts and higher) or it can by purchased as a small SMD device where all electronics is integrated (for applications under ten watts of power).

4.3.5.1 Rectifiers

A rectifier is an electrical device that converts alternating current (AC) to direct current (DC). The standard AC/DC voltage conversion is consisted by diodes. Piezoelectric or electromagnetic energy harvester has typical AC output. Simulations of three basic types of rectifiers such as a full bridge (FB) rectifier (Figure 62), a voltage doubler (VD) (Figure 63) and cascade voltage (CD) multiplier (Figure 64) were performed with effort to obtain advantages and disadvantages of given rectifiers. Simulations were focused on possibilities of small AC voltage conversion to DC voltages with respect to small losses. The aim of this simulations was select the best circuit with the lowest power loss on diodes. For this experiment diodes with low voltage drop BAT54 (approximately 200 mV), Ir@10V = 25 µA, trr = 1,3 ns were used. This is crucial especially for the extremely low operation voltages. Diodes must be chosen with respect to low voltage drop for forward direction and low leakage current. The diode 54 is a Schottky Barrier Diode with low forward voltage, low capacitance and fast switching capability. Next suitable diode for energy harvesting circuit is BAV 199, a standard Si diode with high threshold voltage and minimal reverse current, fast switching capability, capacitance 2 pF.

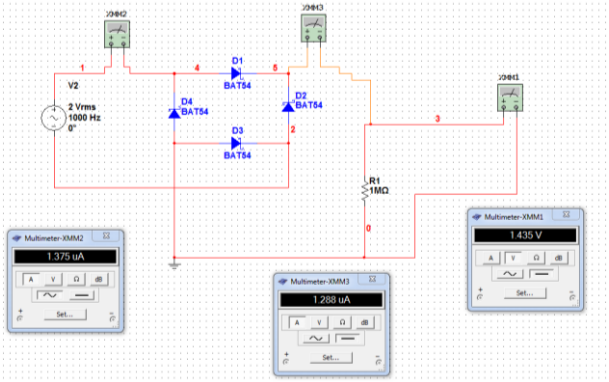

Figure 62 A full bridge (FB) rectifier simulation

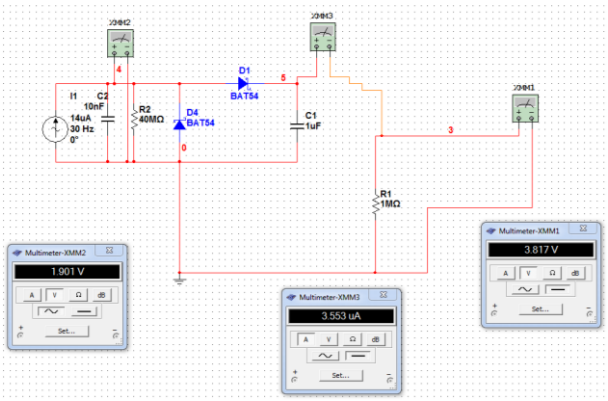

Figure 63 A voltage doubler (VD) rectifier simulation

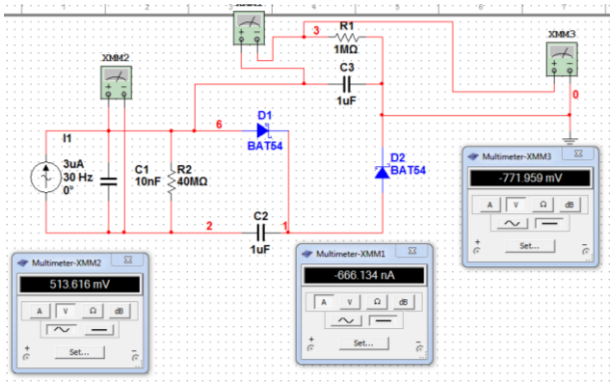

Figure 64 A cascade voltage multiplier (CD) rectifier simulation

Simulations were focused on power losses for diode BAT54 connected into different type of rectifiers. Output power in influence of output current for different input voltages of FB, VD and CD rectifier is shown in Figure 65. It can be observed that for extremely low output current from rectifier I_{out} < 0.5 nA and input voltage 0.5 V is better to used cascade type of VD then FB but for higher output current is necessary to use FB rectifier.

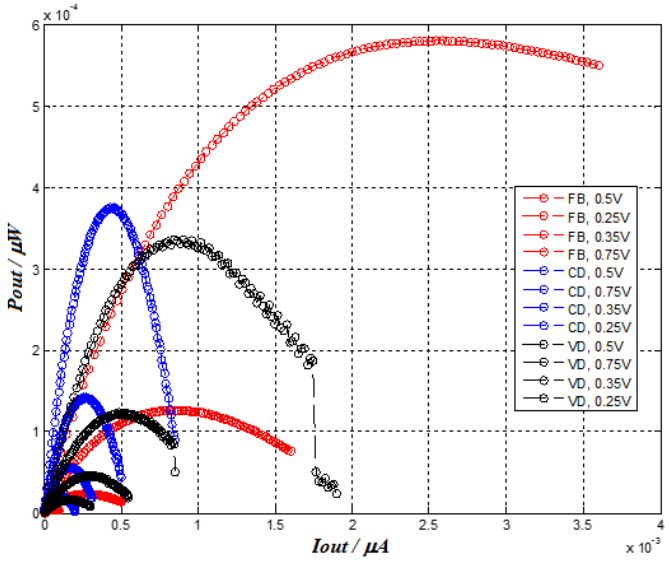

Figure 65 Output power as a function of output current for different types of rectifiers

Power loss on diodes in influence of output voltage for different input voltages of FB, VD and CD rectifier is shown in Figure 66. We can observe, that power loss on diodes increases very strongly for FB for lower voltages V_{out} < 0.5 V and is better to use a VD. If the output voltage from rectifier is higher than 0.5 V, a FB rectifier is the best choice.

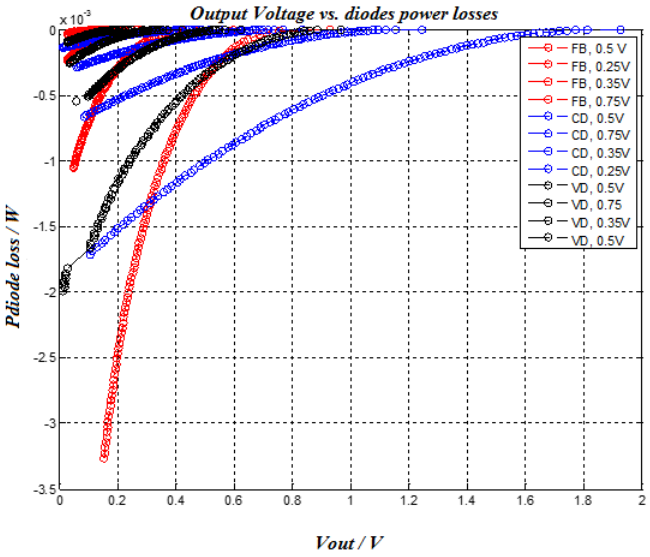

Figure 66 Power losses on diodes as a function of output voltage for different types of rectifiers

FB: high power for high current, low voltage – not applicable, low power loss for relatively high input voltage

CD: relatively fast increase of power for low current, high current is difficult to transfer to the output, uniform power loss, high output voltage, operates with low signals

VD: better results than FB connection for low output currents and voltages, electrical power transfer is higher compare it with CD but efficiency is lower, operates with low input voltages, higher power loss for high input voltage, low output voltage

Generally, the FB rectifier is used for most applications, because most of energy harvesters provide voltages higher than 0.5 V and currents above 0.5 nA. It is easy to integrate and it can be bought buy as a small SMD device, such as i.e. B05GF. As it was mentioned previously, the low forward voltage drop and low leakage current is important for such a device. Several researchers have been focusing on increasing the rectifier efficiency, because the energy loss during AC/DC conversion especially from piezoelectric harvester is not negligible. It is achieved using by switching devices. This requires next requirement on additional source of energy for current monitoring and controlling switching devices. A simplest method is based on controlled switching, where a switch is connected across the piezoelectric harvester driving a full-bridge rectifier [76]. More effective method is bias flip rectifier [76][77] and [78] where the method of performance of a piezoelectric energy harvesting system using the synchronised switch harvesting on inductor is based. Researchers [79][80] and [81][82] have developed a new power flow optimisation principle based on the extraction of the electric charge produced by a piezoelectric element, synchronised with the mechanical vibration operated at the steady state.

4.3.5.2 Optimal impedance load

To maximise transfer efficiency, the load must be matched to energy harvester's equivalent impedance. In practice, the energy harvester (EH) at a given amplitude and frequency, as well as the load impedance, can be thought of as a pair of simple (but unknown) resistances which make up a resistor divider. The power transfer between the two is optimised when their values match. This corresponds to the point at which the energy harvester's loaded voltage is equal to half its open-circuit voltage (Figure 67).

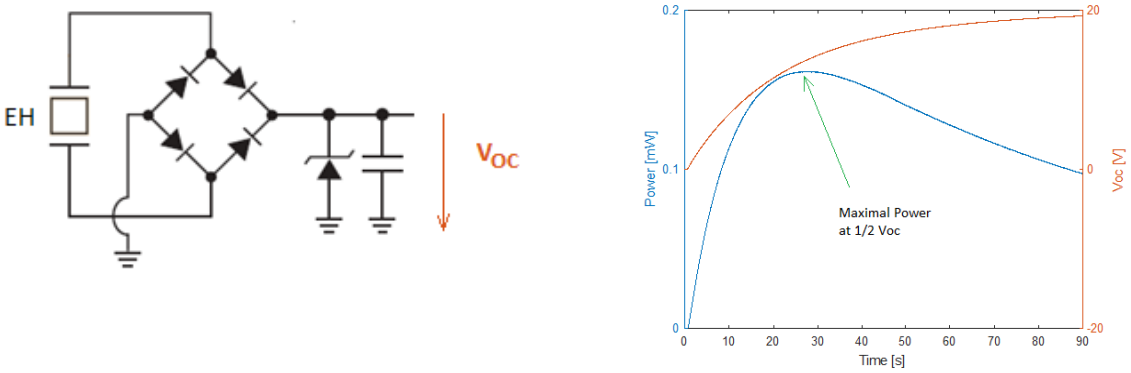

a) Basic topology of EH with rectifier and capacitor

b) Open circuit voltage and power measured on capacitor

Figure 67 Open circuit voltage and power measured on capacitor of basic circuit for energy harvester and capacitor

Thus, the impedance match can be optimised without formally measuring or knowing the impedance of the EH source. A few integrated circuits for energy harvesting have integrated a programmable MPPT sampling network to optimise the transfer of power into the device. Generally, sampling of the open circuit voltage is programmed using external resistors (mostly by two resistors) where values for both resistors must be equal and then half open circuit voltage is held on the main storage capacitor and optimal resistive load for piezoelectric harvester is performed. It promises a high-power efficiency of energy harvesting. Also, MPPT requires some energy for working. Efficiency of MPPT function is shown in Figure 68.

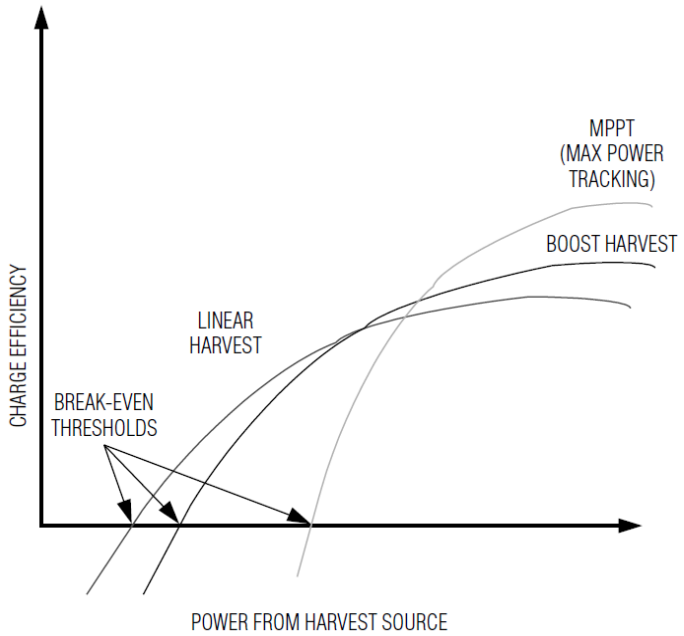

Figure 68 MPPT charge efficiency [83]

If the power from harvest source is weak then usage of boost charger and MPPT function is not effective. In this case, boost charger and MPPT consumes all power from harvest source and none energy is transferred to the output. Then is better to transfer all energy from harvester directly into the energy storage (consisting of a capacitor). Several researchers have published papers focused on advanced MPPT methods for energy harvesting for example [84][85] and [86].

4.3.5.3 Voltage adjustment by DC-DC converters

Energy from piezoelectric harvester is stored in the main storage capacitor. Now, modification of the level of output voltage is required. A DC-DC converter is an electronic circuit that converts a source of direct current (DC) from one voltage level to another. Generally, DC-DC converters can be divided into four categories: Zener diode regulators, linear regulators, charge pumps (switched capacitor DC-DC converters) and inductor-based DC-DC switching converters. For Zener diode regulator (Figure 69), the output voltage is equal to the Zener voltage which usually has a 5% tolerance [87]. Output voltage is equal to the Zener breakdown voltage and therefore cannot be easily adjusted and is fixed at only one level of voltage. Zener diodes are fabricated with breakdown voltages in the range of a few volts to a few hundred volts.

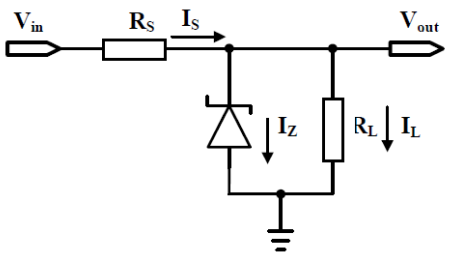

Figure 69 Zener diode regulator [88]

The linear regulator is like a resistive voltage divider network as shown in Figure 70 [88]. It is typical linear regulator using a PMOS transistor. A negative feedback network compares the output voltage against the reference voltage. When the output voltage is different from the reference voltage, the feedback network senses the differences and changes the conductivity of PMOS transistor. A linear regulator does not require any inductor, which would make it bulky and expensive.

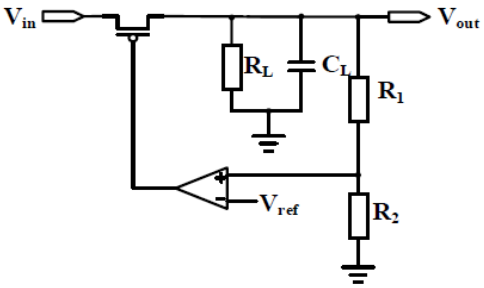

Figure 70 Linear regulator structure [88]

Charge pump DC-DC converters include capacitors to store energy temporarily and then release energy to the output [89]. Currently exists several different charge pump topologies such as Doubler, Dickson charge pump (Figure 71), Cockcroft-Walton charge pump, etc. Charge pump DC-DC converters use transistors and capacitors and allow easier integration. Charge-pumps circuits are capable of high efficiencies, sometimes as high as 90–95% and use some form of switching devices to control the connection of voltages to the capacitor.

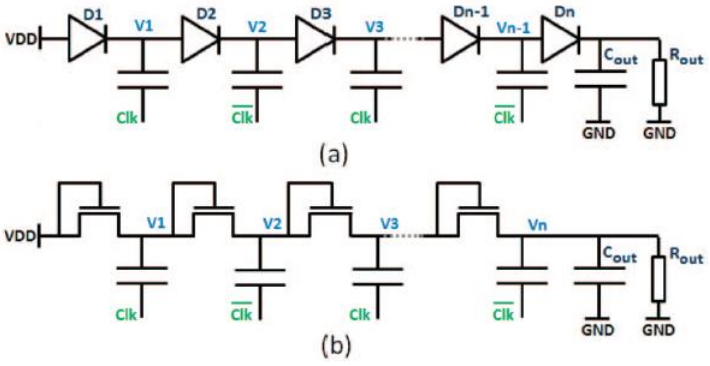

Figure 71 a) Dickson charge pump with diodes b) Dickson charge pump with CMOS. [90]

Inductor based switching converters achieve high power efficiency. We have three basic topologies such as buck converter for step down the voltage (Figure 72 a), boost converter for step up the voltage (Figure 72 b) and buck-boost converter for step up/step down the voltage (Figure 72 c).

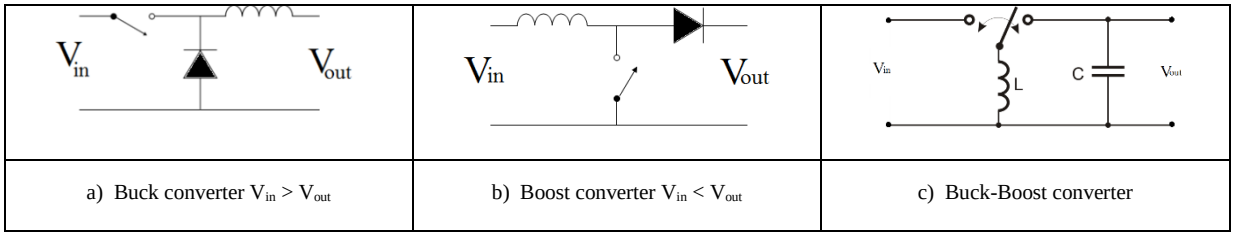

a) Buck converter $V_{in} > V_{out}$ | b) Boost converter $V_{in} < V_{out}$ | c) Buck-Boost converter

Figure 72 Basic topologies of inductor based DC-DC converters.

Different DC-DC converters and their benefits are summarised in Table 5

Table 5 Summary of DC-DC converters

Zener diode	Linear regulator	Charge pump	Inductor based
Very simple (+)	Low noise (+)	Simple (+)	High efficiency (+)
Easy to use (+)	Stable Vout (+)	Goof efficiency (+)	Bulky (+)
Fast (+)	Lower efficiency (-)	Easy integration (+)	High cost (-)
Very inefficient (-)		Noisy (-)	Noisy (-)

A few researches are focused on creating of far more sophisticated DC-DC converters, where efficiency will be very high. All these designs follow the topologies mentioned above. For example, [91] have described adaptive controller for piezoelectric harvester. Another technique is to use a flyback converter, which is inductor based buck-boost converter [92] or DC-DC boost converter with the maximum power point tracking (MPPT) [93]. This type of DC-DC converter follows the requirements on input and output voltage. All DC-DC converters demand a small amount of energy for electronics support (switch control). It is possible to either develop the DC-DC converter made from commercial components and tailor it for given application, or to buy a commercial product as an integrated circuit.

4.3.5.4 Stabilisation of output voltage

An electronic component focused on stabilisation of output voltage is designed to deliver a constant voltage to a load at its output terminals regardless of the changes in the input or incoming supply voltage. It is consisted by DC-DC-converters or by low-dropout regulators. A low-dropout or LDO regulator is a DC linear voltage regulator that can regulate the output voltage even when the supply voltage is very close to the output voltage [94]. If the input voltage comes from a battery or another LDO and has very little ripple, a standard LDO can be used in dropout to achieve a low noise output [95].

4.3.5.5 Electronics protection

It is an electronic device focused on battery charging and protection electronics for controlling undervoltage and overvoltage levels.

4.3.5.6 Power management integrated circuits

As is mentioned previously, electronics for energy harvester consist by AC/DC conversion, DC/DC converter and energy storage (illustrated in Figure 73). In recent days is possible to buy a lot of integrated circuits targeted to energy harvesting solutions. Integrated circuits include current monitoring electronics, DC-DC converters different types such as charge-pump or buck-boost charger, maximum power point tracking (MPPT) for optimal energy extraction from a variety of energy generation sources and battery charging and protection electronics for controlling undervoltage and overvoltage levels. Companies focused on this topic are for example: Texas Instruments, STMicroelectronics, Analog Devices, Spansion, and others. Next important function of few integrated power management circuits is a cold-start function. The cold-start function provides accumulation energy for main boost charger. This function is activated when all energy sources for operating of integrated circuit are depleted. Effectivity is lower than main boost charger but operates with low power.

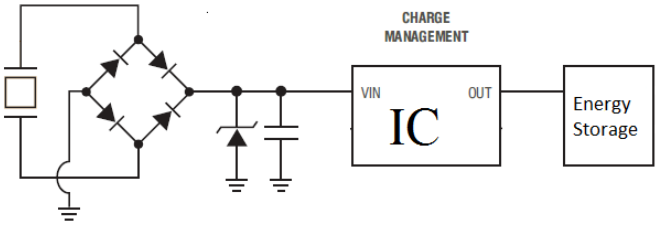

Figure 73 Block scheme of piezo harvester with power management

For example, the cold-start function is implemented in the integrated circuit bq25504 (Texas Instrument), developed for ultra-low power applications. A charger operation after a depleted storage element is attached and harvester is available is shown in Figure 74.

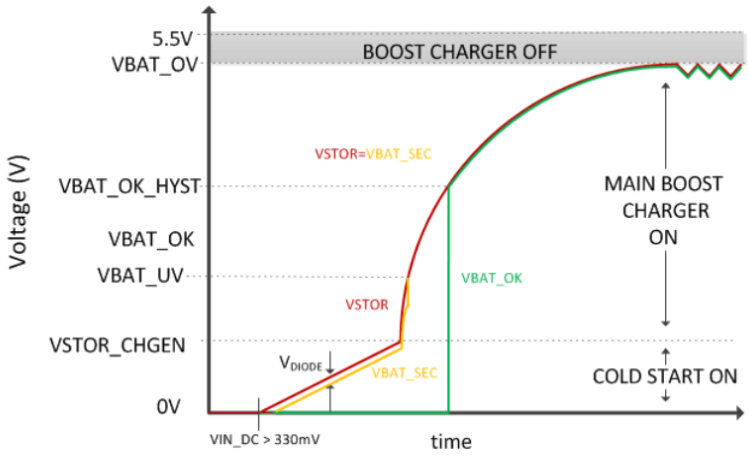

Figure 74 Charger operation after a depleted storage element is attached and harvester is available. Texas Instrument IC bq25504. [96]

If the mechanical vibration source has continuous excitation with one dominant frequency, then most of ICs with MPPT will operate with high efficiency of energy harvesting from piezoelectric device. In case of shock impacts where it is necessary to capture as much energy as possible then some type of charge pump integrated is appropriate to use only.

4.3.5.7 Examples of ICs for Vibration Energy Harvesting

Basics ICs for power management and storage energy are shown in Table 6. All parameters follow from datasheets. Design and decision (which IC do you want to use) follows from energy harvester output voltage range and kind of energy storage.

Table 6 Table of proposed ICs with basic parameters summary

IC name	min. V_{IN} [V]	max. V_{IN} [V]	MPPT	Energy Storage	Notes
LTC3588-1	2.7	20	No	Capacitors	AC input
ADP5090	0.38	3.3	Yes	Li-ion Batteries, Supercapacitors	DC input
MAX17710	0.75	5.3	No	Li-ion Batteries, Thin -film Batteries	DC input
bq25504	0.33	5.5	Yes	Li-ion Batteries, Thin-film Batteries, Supercapacitors, Capacitors	DC input

4.3.5.7.1 LTC 3588-1:

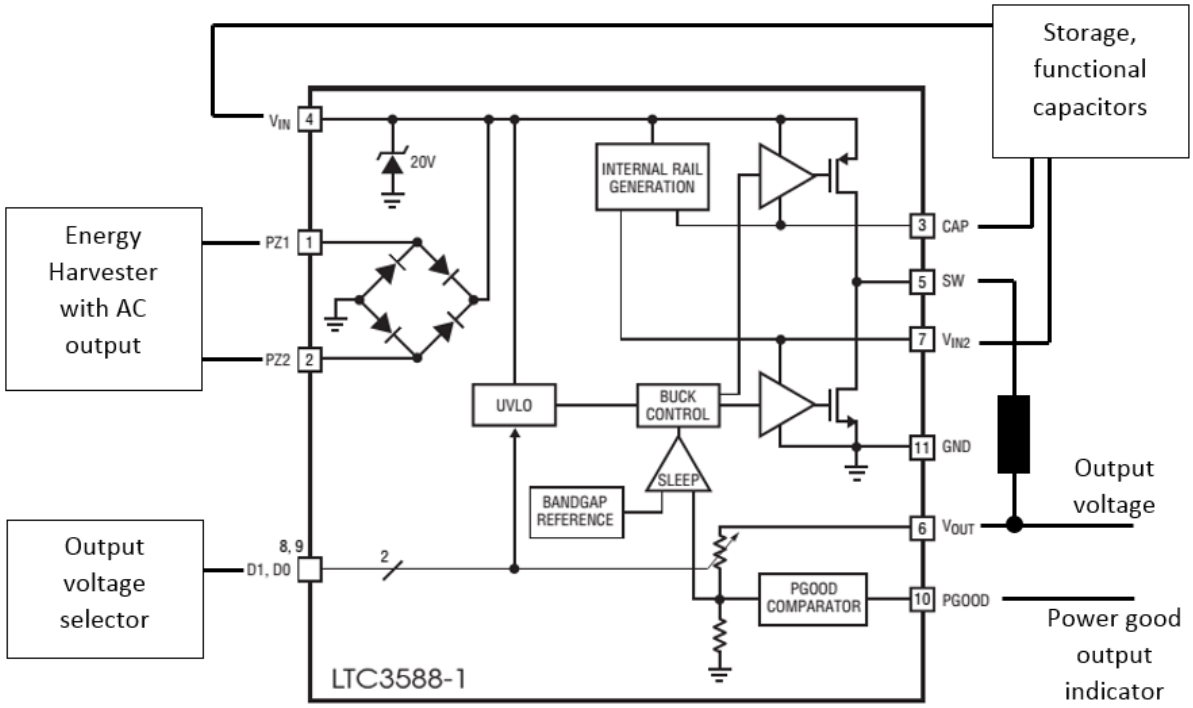

Figure 75 BOM diagram of LTC3588-1 [97]

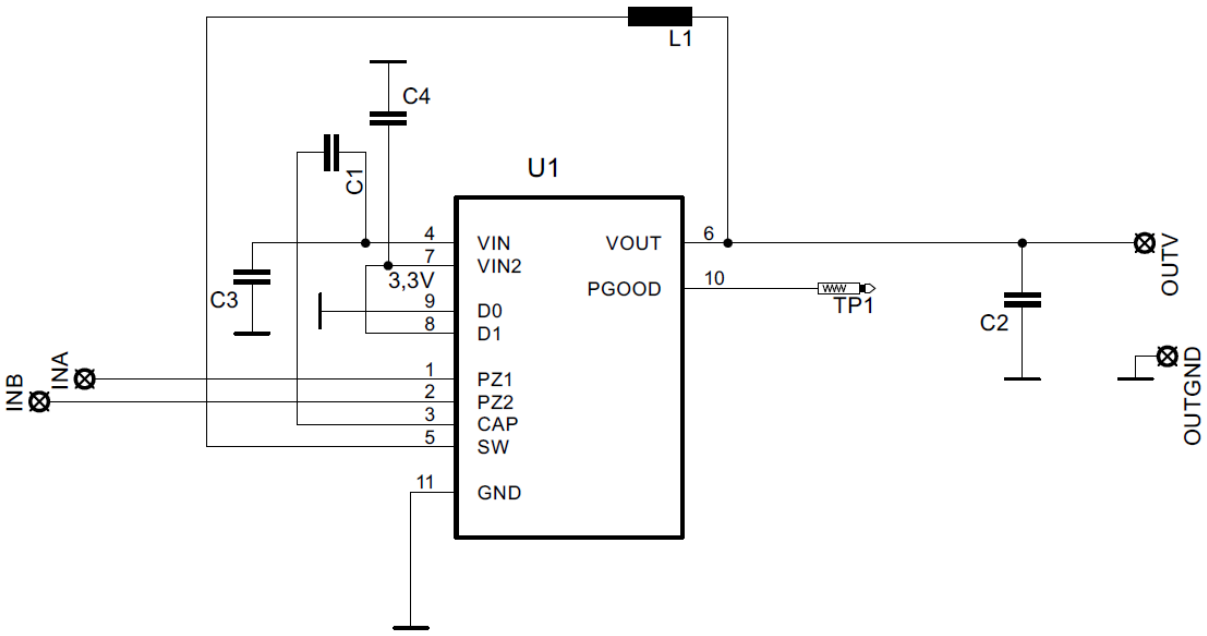

Figure 76 Electric scheme: LTC3588

Figure 77 LTC 3588-1

Brief description: The LTC3588-1 integrates a low-loss full-wave bridge rectifier, so piezo energy harvester is possible connect to IC directly. Input voltage range is from 2.7 V up to 20 V. Output voltage is possible to choose on 1.8 V, 2.5 V, 3.3 V and 3.6 V. Harvested energy can be stored on the input capacitor or the output capacitor. The LTC3588-1 does not have maximum power point tracking (MPPT) function.

4.3.5.7.2 ADP5090

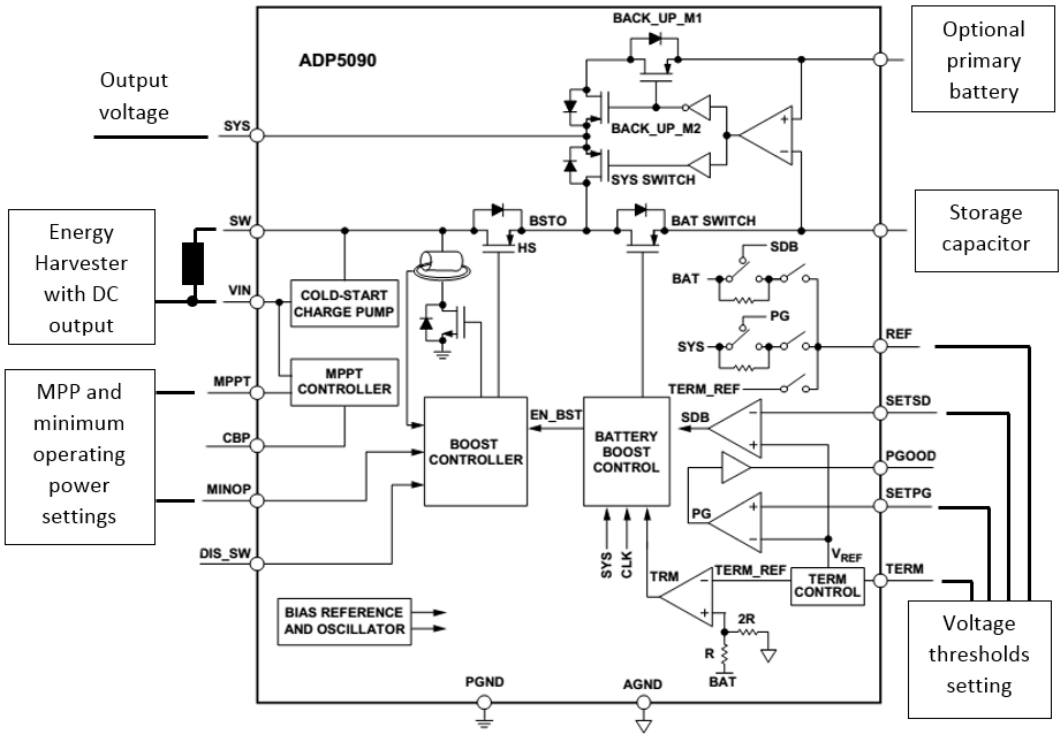

Figure 78 BOM diagram of ADP5090 [98]

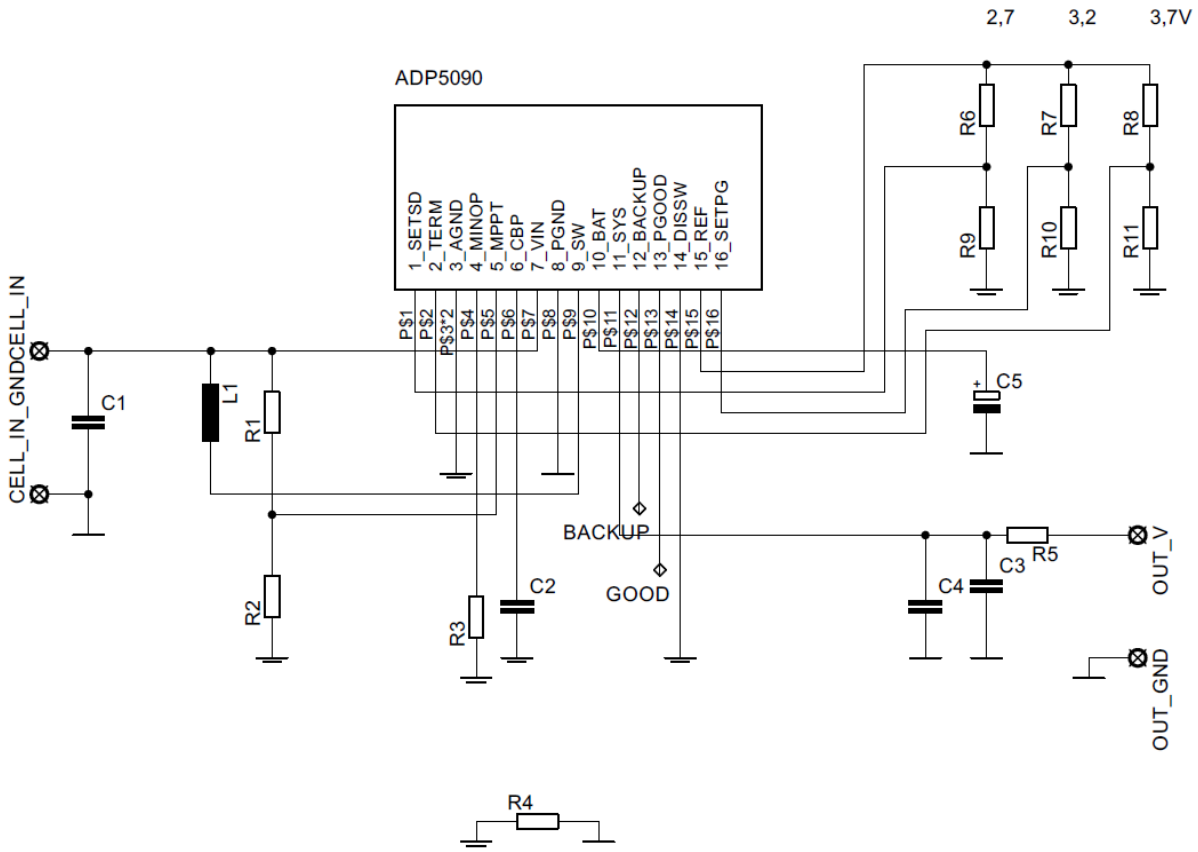

Figure 79 Electric scheme: ADP5090

a: top view. **(b) bottom view.**

Figure 80 Electric board with ADP5090

Brief description: The ADP5090 operates with input voltage range from 0.38 V up to 3.3 V. If is used battery (for supporting cold-start register) so input voltage is harvested from 0.08 V. Input voltage must be rectified on DC voltage from piezo energy harvester. Harvested energy can be stored on li-ion battery or supercapacitor. MPPT is integrated inside the IC.

4.3.5.7.3 MAX17710

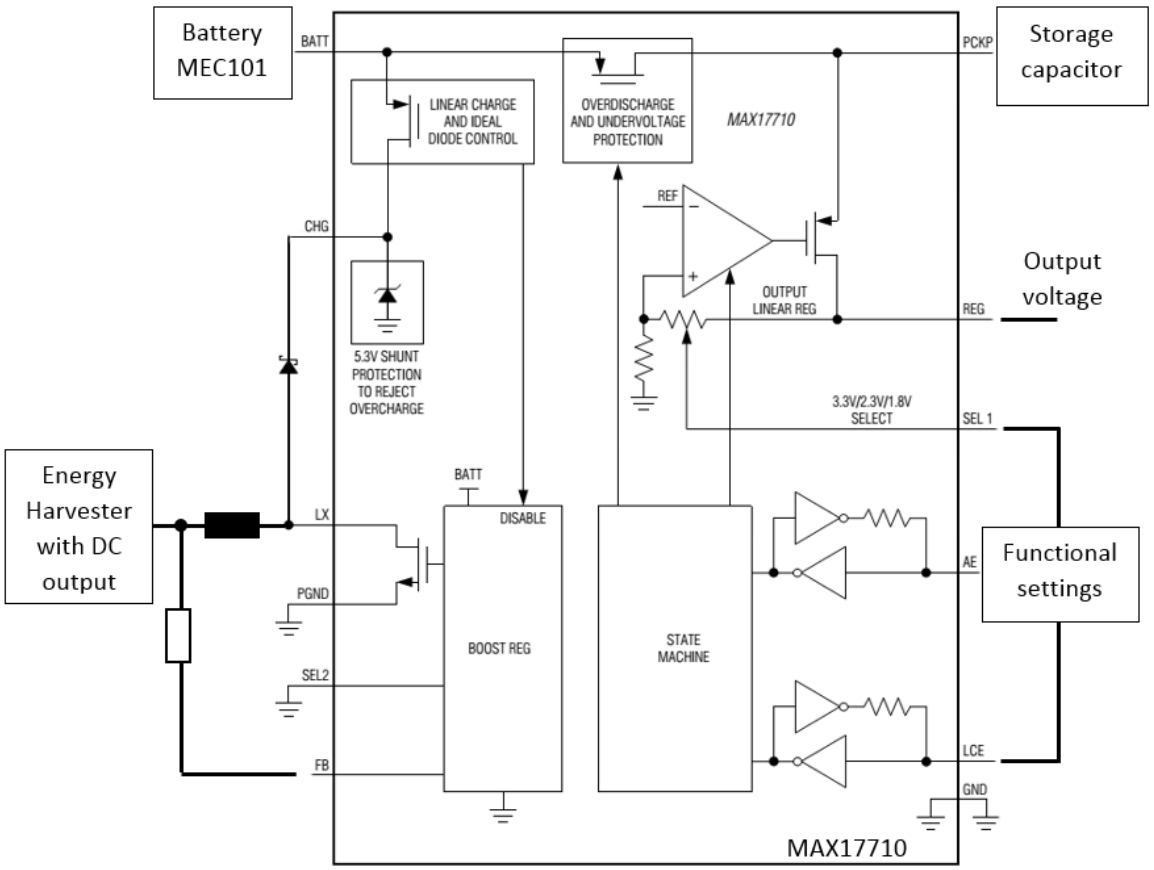

Figure 81 BOM diagram of MAX17710 [83]

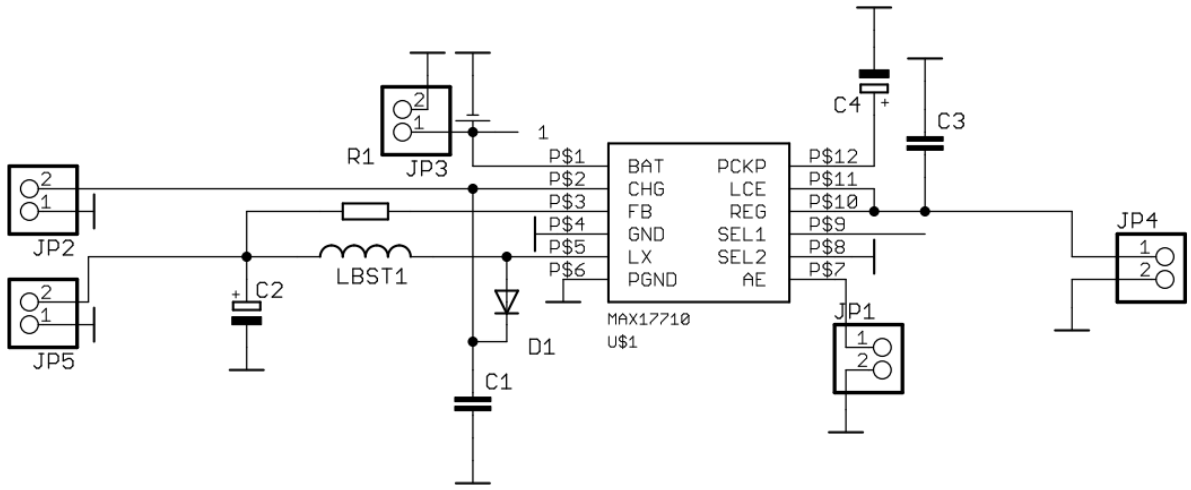

Figure 82 Electric scheme: MAX17710

Figure 83 Electric board with MAX17710

Brief description: The MAX17710 operates with input voltage range from 0.75 V up to 5.3 V. Input voltage has to be rectified on DC voltage from piezo energy harvester. Output voltage is possible to choose on 1.8 V, 2.3 V or 3.3 V. Harvested energy can be stored on li-ion battery or Thin-film battery. MPPT is not integrated inside this IC.

4.3.5.7.4 Bq25504

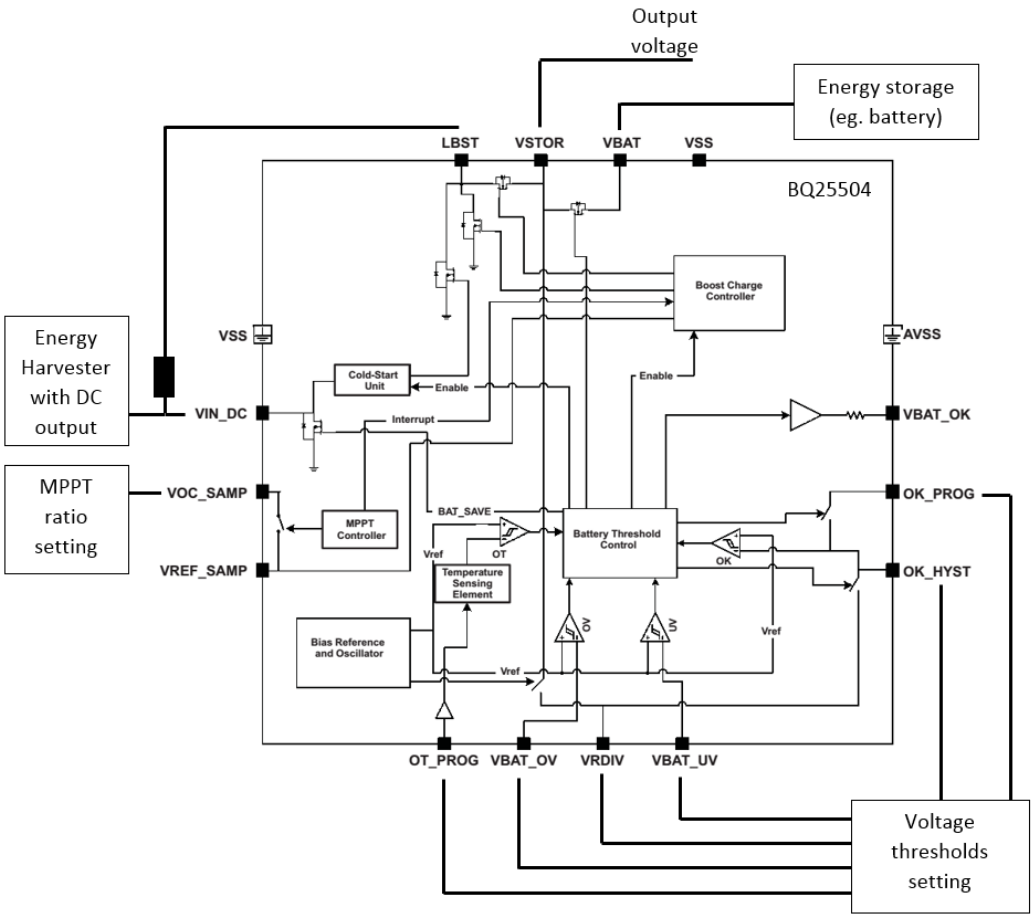

Figure 84 BOM diagram of bq25504 [96]

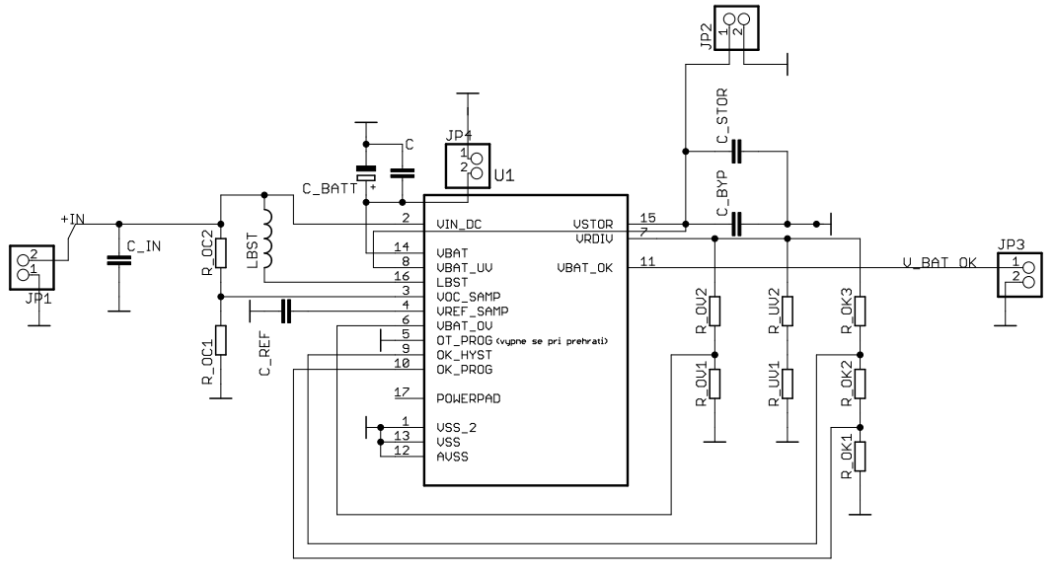

Figure 85 Electric scheme: bq25504

a: top view. **b: top view.**

Figure 86 Electric board with bq25504

Brief description: The bq25504 operates with input voltage range from 0.33 V up to 5.5 V. The IC needs 0.3 V for activation and then is possible to harvest energy down to 0.08V. Input voltage has to be rectified on DC voltage from piezo energy harvester. Harvested energy can be stored on li-ion battery, Thin-film battery, supercapacitor or conventional capacitor. MPPT is integrated inside the IC.

4.3.5.7.5 Commercial ICs Summary

All these draft proposals stem from the basic connection of ICs from datasheets, and needs to be tested and compared for given energy harvesters. The final design of the power management electronics will be decided based on the energy harvester parameters (such as output voltage range, dynamic electric resistance, number of energy harvesters) and the energy storage type and parameters (battery, super capacitor or conventional capacitor).

4.4 SOLAR PANELS

4.4.1 General solar cell properties

Photovoltaic solar panels and installations can be built in a number of different sizes and configurations to suit the application; the energy harvesting capacity is linked to the size (area) of the panels, the orientation relative to the sun and the intensity of the sunlight reaching the panels. To capture the maximum amount of energy the panels can be mounted on active mounts which track the sun, however these are complex and often a simpler, larger, array of fixed panels are used to capture the same energy. The nominal maximum power rating of crystalline silicone solar panels is approximately 150 W/m^2. Taking into account the passage of the sun throughout the day and statistics for average sunshine variations due to weather, the average power output of a panel fixed at the optimal angle is approximately 0.4kWh/m^2/day, which is 12.4kWh/m^2/month

4.4.2 Survey of potential solar cells solutions

4.4.2.1 Solar Capture Technologies solar panel designs for transport applications

Solar Capture Technologies Ltd can design and manufacture custom solar models or solar panels according to customer specifications with a range of materials, options for integrated holes and a framed or frameless design. There are numerous options available when specifying custom solar modules including: custom shaped modules to fit a product, specified sized modules to fit a product, glass fronted modules, option of low-iron toughened glass or high performance ETFE cover material, textured front modules, maximised cell area to optimise power output, framed or frameless modules, electrical outputs to meet product demands, a choice of backing substrates including tedlar and anodised aluminium, a choice of industry standard electrical connectors, bends and holes to suit end product. Some of solar modules designed by the company are shown in the figures below.

Figure 87 Solar modules [99]

4.4.2.2 Solar installation on major station

The figure below shows the PV system installed to the platform roof of Tokyo Station. The generated power (installed rated capacity) is 453 kW, which is used for lighting and air conditioning of the station. The generated energy per day in winter was found to be less than 30% of that in May, June and July. The construction cost is about four times higher than conventional construction work cost.

As around amount, the ratio of estimated utilised energy per hour to initial capital investment is about 20 MWh/100milion JPY = 0.2 Wh/JPY, that is about one twenties of other applications.

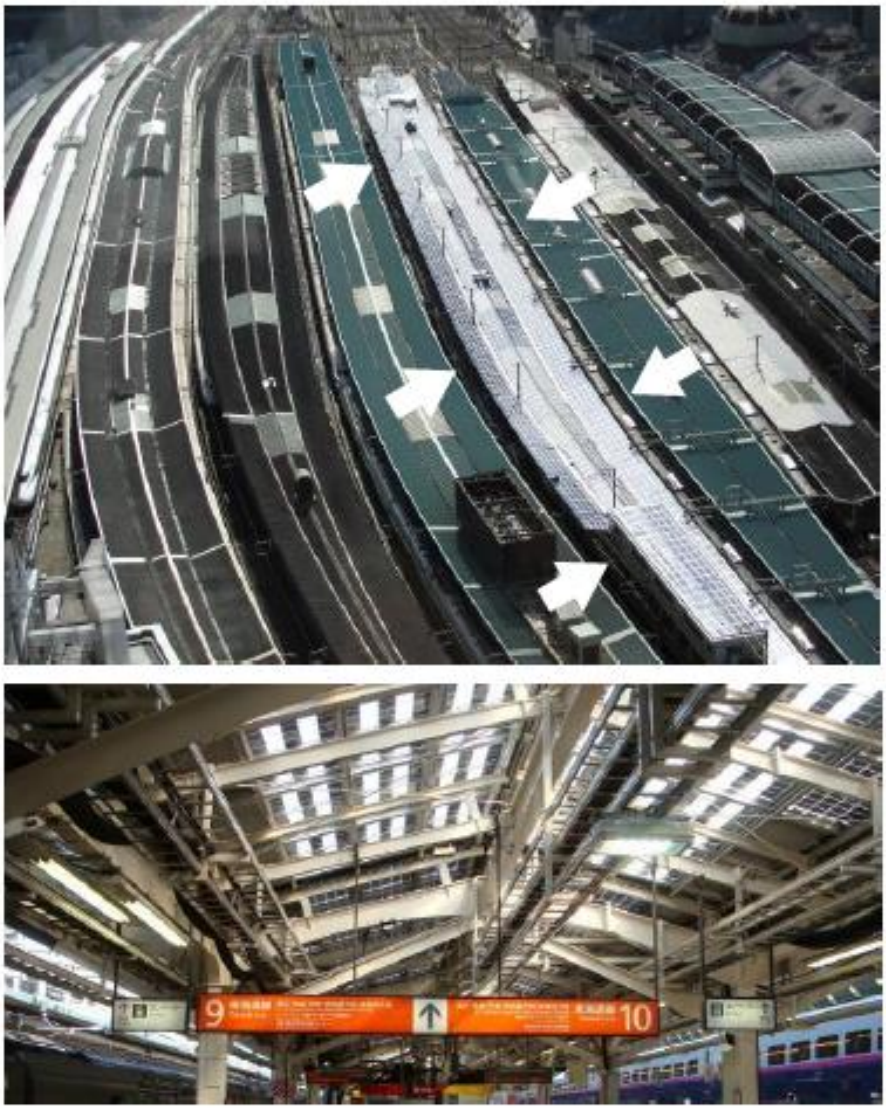

Figure 88 Photos of PV system installed to Tokyo Station [100]

4.4.2.3 Solar installation for small station

As major project of solar power introduction to the railway station, “zero emission station” was constructed at Hiraizumi station in 2012 where all electric power of the station is supplied from solar panel on a sunny day. In this station, as shown in the figure below, 78 kW photovoltaic panels were installed and residual electric power is stored to 240 kWh lithium ion battery during the daytime. The stored energy is used for lighting and air conditioning during the night.

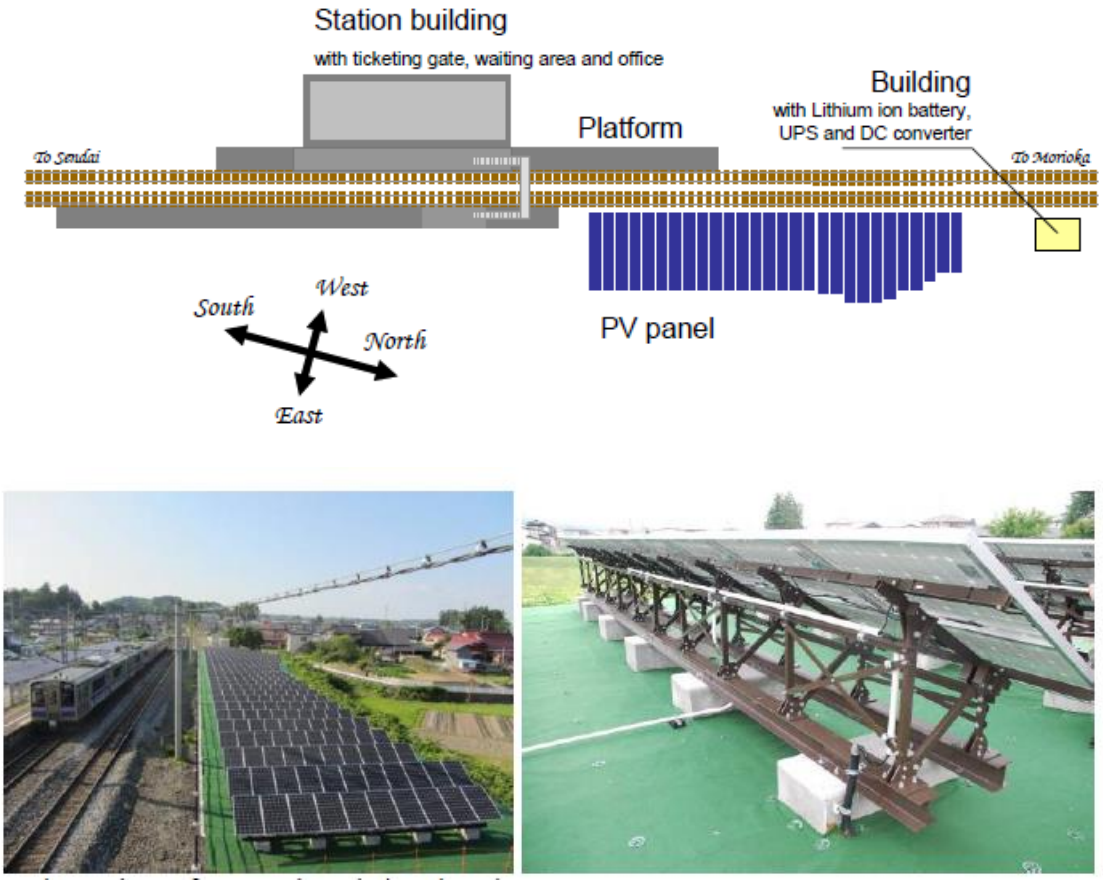

Figure 89 PV panel at Hiraizumi Station in Japan [100]**,** [101]

4.4.2.4 Tracking solar array concept design for vehicles

A PVC-array design on vehicle's roof filled with converters has been reported. Each element of the array (or a group of elements) is mounted on an axe, which may be individually driven by a low power servomotor coupled with a gear reducer, or be united by a commune lever, in the manner of a lattice window, and be driven by one motor of greater power. At least two motors are needed for one mechanism of two-axe system. An example of a two identical mechanisms system is shown on the figure below. Each mechanism drives a set of Solar Panels mounted on the Main Chassis (with bearings), driven by an Axe Motor 1. A Shifting Chassis is mounted over the bearings in the points where Solar Panels are mounted on the Main Chassis; a parallelogram mechanism, created this way, is similar to that one of a swing arm drafting lamp. The Shifting Chassis, driven by an Axe Motor 2 mounted over the Main Chassis, rotates the bearings of Solar Panel mounts, changing its angle of obliquity towards the Main Chassis.

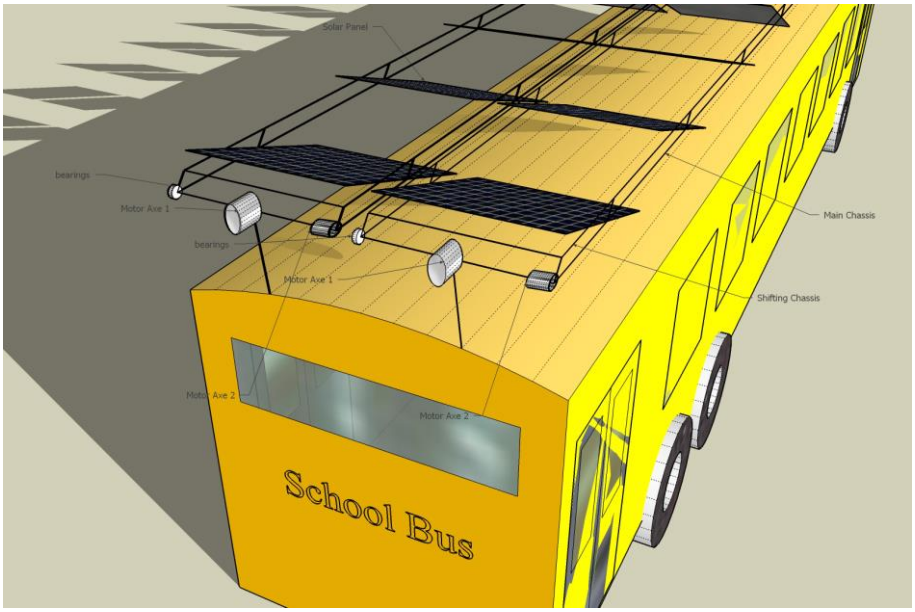

Figure 90 PV panel on vehicle's roof [102]

4.4.2.5 Solar installation for trackside monitoring application

A monitoring application with a wireless sensor network that was performed on a 95 years old riveted steel railway bridge. In order to perform an accurate assessment, strains were monitored on critical elements to catch the real loading during the passage of heavy freight trains. The wireless sensor network deployed on the bridge consisted of 8 nodes supplied with resistance strain gages and the root node connected to a solar energy rechargeable, battery powered base station. The base station, which collects all the data, was equipped with a low power computer equipped with an ARM processor. The mean power consumption is 4.5 W. The base station was mounted close to one of the abutments. Two 12 V car batteries provided the power supply. The batteries were recharged with a panel of solar cells, as shown below, was mounted on the top of the bridge.

Figure 91 Event-based strain monitoring on a railway bridge with a PV panel [103]

4.4.2.6 Greenrail – Solar equipped sleeper design

Start-up Greenrail recently presented an eco-friendly sleeper, which intends to integrate a photovoltaic (or piezoelectric) module onto an original sleeper allowing to transform the rail way in photovoltaic power stations, with a high productivity of sustainable energy[1]. Information on the power output or other parameters is not yet available, as the product is still under development.

Figure 92 Solar panel integrated to a Greenrail sleeper [104]

4.5 WIND TURBINES

4.5.1 Review of wind turbine-based solutions

4.5.1.1 Horizontal axis wind turbines

A common method of energy harvesting is to use a bladed rotor to capture energy from passing air currents and transform it into a rotary motion which can be used to drive a rotary electromagnetic generator. There are numerous commercially available products with a wide range of maximum energy harvesting capacities, the units can either be specified in terms of the maximum design power generation or the power generation over a period of time (for example a month). Wind turbines are dependent on the wind speed at any one moment and therefore their power output is variable, therefore to provide a continuous energy source require combining with other power sources and/or energy storage (such as batteries) with sufficient capacity to supply the powered equipment for a number of days when there is not sufficient wind to generate power.

One example of a range of commercially available of pole mounted horizontal axis wind turbines are shown in Figure 93 below, their energy harvesting capacity ranges from range from 30 kWh/Month to 700 kWh/Month.

[1] http://www.greenrailgroup.com

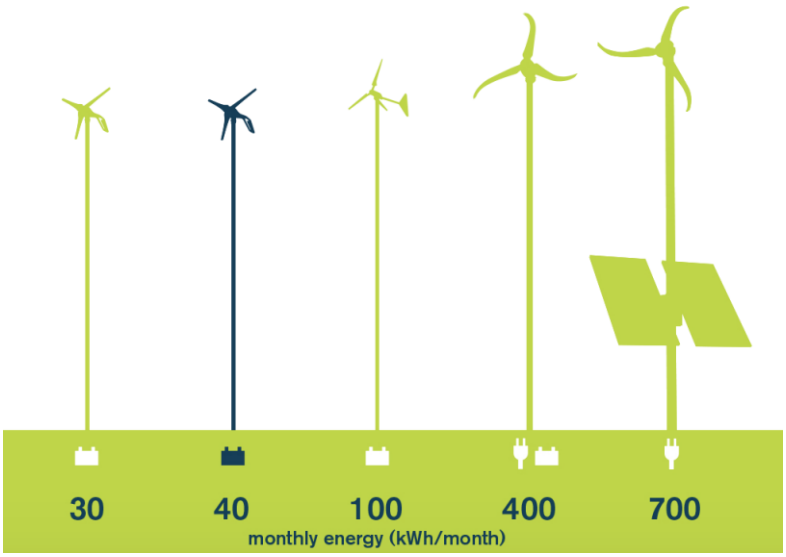

Figure 93 Pole mounted wind turbines [105]

Taking the nominal 40 kWh/Month output model as an example has an approximate energy output of 40kWh/Month with an average annual wind speed of 5.8 m/s (13 mph), although this will vary from day to day during the month, and be dependent on the geographic location. The specifications, which are represented graphically in Figure 94, are that the swept area is 1.07 m^2 with a rotor diameter of 1.17 m and the system weight is 5.9 kg. A start-up wind speed of 3.1 m/s is required, the survival wind speed is 49.2 m/s (110 mph), the wind speed operating range is 3.1-22 m/s (7-49 mph), and the optimum wind speed range is 4.5-22 m/s (10-49 mph). The output voltage could be 12, 24, and 48 VDC with a permanent magnet brushless alternator.

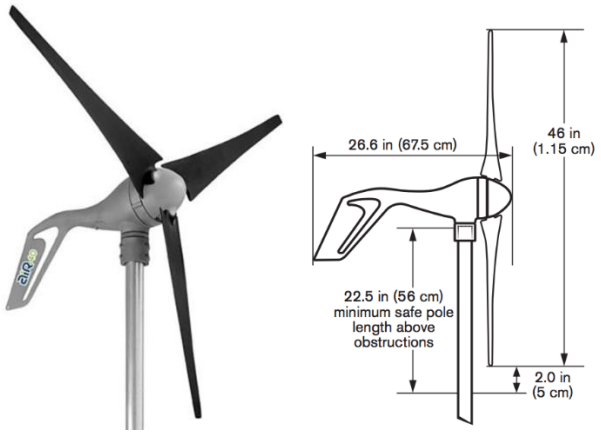

Figure 94 40 kWh/Month Pole mounted wind turbine [106]

4.5.1.2 Vertical Axis Turbine

Another configuration of commercially available wind turbine are the vertical axis turbine which use blades or buckets mounted in the same axis as the axis of rotation to deflect the wind and turn the wind energy into rotary motion to drive a electromagnetic rotary generator. The LE-v150 vertical axis turbine, as shown in the figure below as an example, it uses a proven cross ventilated 'savonius' rotor design which gives excellent power conversion for a vertical axis turbine of this size. The rotor is coupled with zero cogging axial flux alternator enabling the turbine to start up in the lightest of winds. The turbine will receive the wind from 360 degrees without the need to yaw into position and it has fully lubricated sealed bearing, so no greasing or maintenance is required. The rotor diameter is 270 mm, rotor height is 918mm, system weight is 13 kg. In this case the system output is given in momentary power output and is rated at 24 W at 8 m/s (18 mph) wind speed and the peak output is 200 W. System power output with wind speed is illustrated in the figure below. Cut-in speed is 4 m/s (9 mph), DC output voltage could be 12 V, 24 V, 48 V.

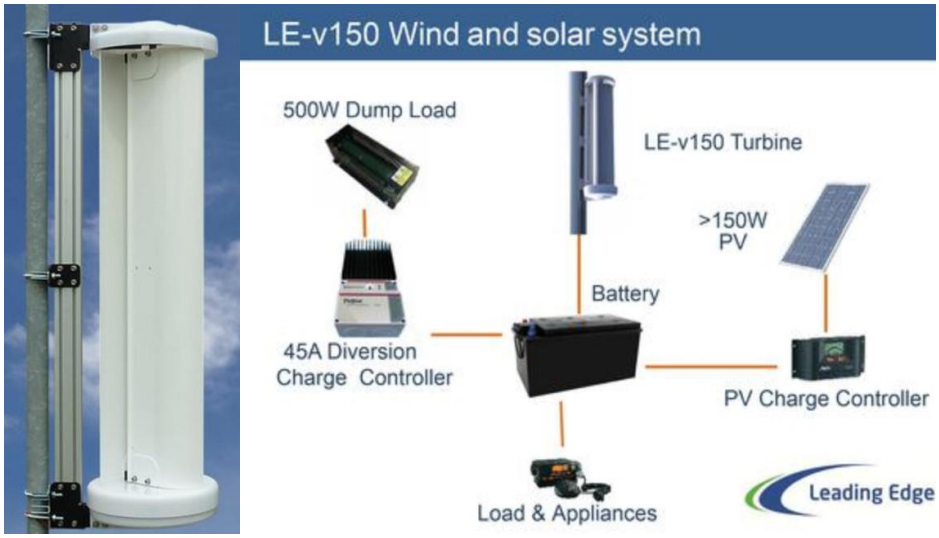

Figure 95 Vertical axis turbine [107]

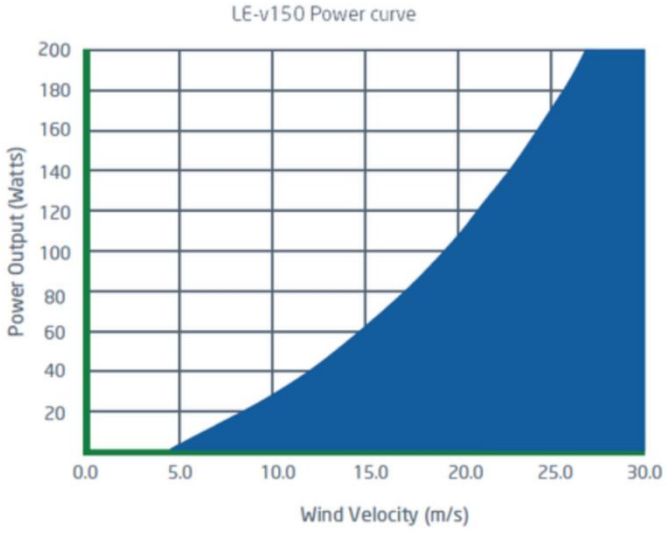

Figure 96 Power output with wind speed [107]

4.5.1.3 Novel Wind Design 1#

Researchers at Imperial College have been developing a miniature turbine-based harvester aimed specifically at duct monitoring applications. As shown in the figure below, the device comprises a 2 cm diameter shrouded turbine with an axial-flux permanent magnet (AFPM) generator integrated into the shroud. The overall cross-sectional area including the shroud is only 8 cm^2, which represents only 1.1% of the cross-section of a 1 ft diameter duct. The device has a rotor diameter of 2 cm, with an outer diameter of 3.2 cm, and generates electrical power by means of an axial-flux permanent magnet machine built into the shroud. Fabrication was accomplished using a combination of traditional machining, rapid prototyping, and flexible printed circuit board technology for the generator stator, with jewel bearings providing low friction and start up speed. Prototype devices can operate at air speeds down to 3 m/s, and deliver between 80 μW and 2.5 mW of electrical power at air speeds in the range 3–7 m/s.

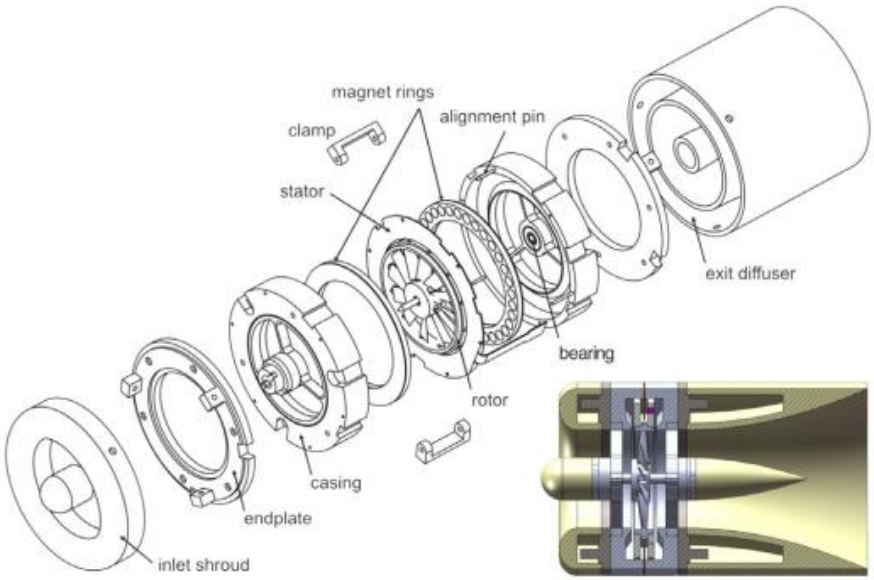

Figure 97 Wind turbine harvester 1# [108]

4.5.1.4 Novel Wind Design 2#

A novel vertical-stalk piezo-leaf generator has been reported, which could convert wind energy into electrical energy by wind-induced flapping motion. Considering of the unpredictable wind strength, the flexible and robust piezoelectric materials (PVDF) were chosen as the essential component of the device. The basic design is to clamp one edge of PVDF element to the bluff body and leave the other edge free. When the wind crosses this device, it will lead the aero-elastic instability and the periodic pressure difference will drive the piezo-leaf to bend in the downstream of the air wake, synchronously. A number of prototypes, as vertical/horizontal-stalk leaf, single /multiple layers stalk and short/long stalk were designed. From the test results, the maximum output power was observed (~300 μW, 10 MΩ load) in 8 m/s wind from a single layer vertical-stalk leaf with a short PVDF stalk. The power density approached the peak value: power per device's volume ~300 μW/cm3 and power per device's weight ~80 μW/g.

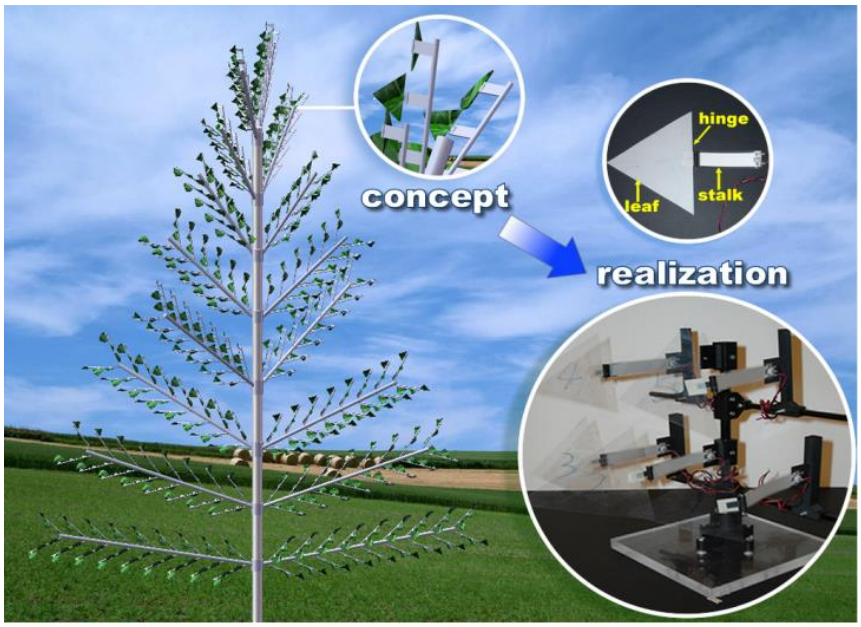

Figure 98 Wind turbine harvester 2# [109]

4.5.1.5 Novel Wind Design 3#

A piezoelectric windmill was designed for electric energy harvesting. The structure and framework of the piezoelectric windmill is similar to that of conventional windmill except it has active piezoelectric blades. As the wind flows through the windmill the active blades oscillate in turn producing electricity. The figure below shows the schematic of the piezoelectric windmill which consist of bimorph transducers arranged along the circumference. Ten bimorphs were used in this prototype. The dimensions of each individual bimorph were 60200.6 mm^3 with a free length of 53 mm. The resonance frequency and capacitance for this size of bimorph was measured to be 65 Hz and 170 nF, respectively. A detailed description of the fabrication technique is described elsewhere. The arrangement of the transducers is made such that corresponding to wind flow the piezoelectric transducer oscillates between the stoppers. The oscillatory motion is generated using the cam-shaft gear mechanism. The continuous back and forth oscillation of bimorph between the two stoppers will continuously generate electricity. The characterisation of the windmill was done inside a long square tube. Wind was blown in the tube using a fan. Wind speed was measured using EA-3010U anemometer fitted at the top of the mill. The voltage was monitored on the HP 54601A digital four-channel oscilloscope using HP 10071A probe. A full-bridge rectifier circuit using the low power diodes was fabricated and the voltage was measured across a capacitor. A power of 7.5 mW at the wind speed of 10 mph was measured across a matching load of 6.7 kΩ.

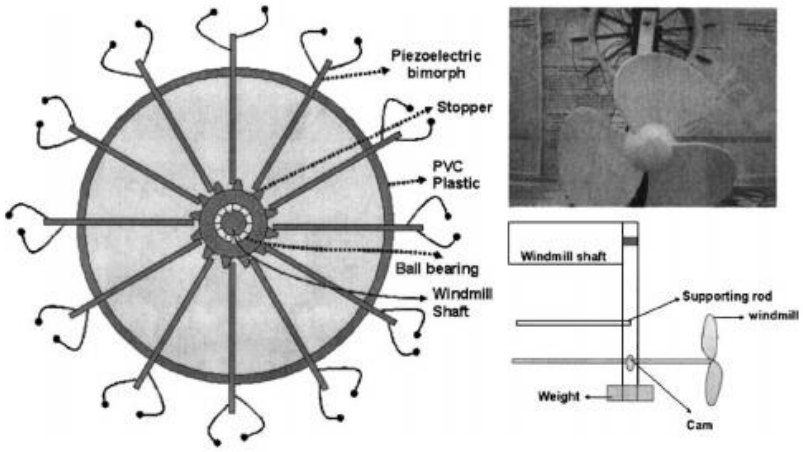

Figure 99 Wind turbine harvester 3# [110]

4.5.1.6 Novel Wind Design 4#

The T-BOX Wind Power Generator generates energy from the air currents induced by the earodynamic effects of passing trains, rather than the ambient wind. It does this without any interference with normal train operation – the device is installed between railway sleepers, and is partially buried underground. As the train passes over the device, the air currents generated from the train aerodynamics spins the turbine inside the T- box to generate electricity. The T- box contains all the mechanical components required for harnessing, storing and supplying converted power. Hence, the power generated from this device can be supplied to public facilities along the railway and also to remote areas where electricity has not yet reached. The device, differs in that it is designed to be installed within the actual railing track itself. It consists of a durable metallic cylinder with vents, which allow air to flow through and rotate turbine blades housed inside. The Hetronix wind turbine system consists of a 2.5 meter rotor system and a generator which is 35 cm in diameter. The 58 kilogram wind turbine is rated at 2000 watts @ 12.5 m/s wind.

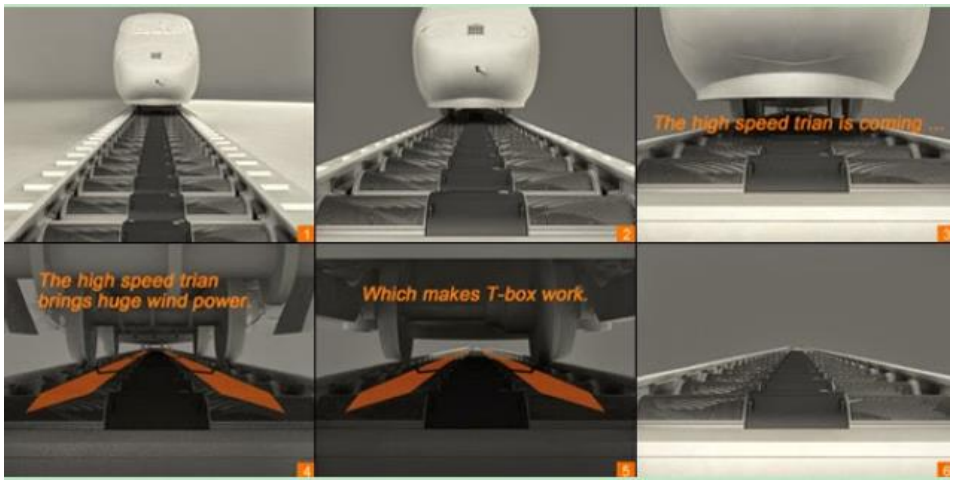

Figure 100 T-BOX wind power generator [111]

4.6 POWER MANAGEMENT AND ENERGY STORAGE

The job of power management circuitry in energy harvesting is to match the output impedance and frequency characteristics of the physical energy transduction hardware with the input electrical power limitations of the energy storage element and application electronics. How this is done has a significant effect on the overall system efficiency. In the case of a solar PV, interfacing to a lead acid battery can be accomplished with a simple diode. Vibration energy harvesters need active frequency and impedance matching, as well as low loss rectification. Sudden shocks can generate large voltage spikes that can damage unprotected circuitry. Comprehensive system design is necessary in both cases to achieve a cost effective and efficient system.

Energy storage technologies also have to be matched to the energy harvesting method and energy delivery requirements. In trackside applications, although weight might not be a problem, susceptibility to theft and installation size (potential to interfere with maintenance) have to be considered as well as capacity, temperature range and operational life in the environment.

4.6.1 Power management electronics

It is possible to develop a unique power management electronics tailored for given application or use some commercial IC. Basically, the correct choice of ICs for given harvester follows from the amplitude of voltages generated on the output of harvester device during operation. Levels of input voltages for each ICs are limited and it is possible to find different levels of these voltages for different type of ICs. Companies focused on this field are developing effective integrated circuits, which are able to operate with still declining level of input voltages. Recently it is possible to find many integrated circuits operating with input voltages lower than 100mV, where MPPT function and different types of charge boosters are integrated. Most of ICs are focused on energy harvesting from different sources such as thermal energy and solar energy so DC input voltage is required. In this case the energy harvester with AC output needs to be connected over rectifier. Nowadays it is possible to connect the EH device directly on ICs because the rectifier (a full bridge) is often integrated. It should be also noted, that charge pumps, MPPT and other higher functions require some energy for operation, which decreases the power output to the application.

4.6.2 Energy storage

Energy can be stored either in capacitors, or in batteries. While capacitors are based on electrostatic principle, batteries use an electrochemical principle for energy storage. Figure 101 shows power density as a function of energy density for different energy storage devices. Batteries have high energy density, but power density is low. On the other hand, capacitors have high power density, higher than batteries, but far lower energy density than batteries. Supercapacitors occupy area between capacitors and batteries in Figure 101. Energy harvesting uses supercapacitors or Li-Ion/Li-Polymer batteries for energy storage in most of the small-scale applications. Batteries are limited by the number of charge/discharge cycles. The charge cycles for Li-Ion batteries is around 1000. For Thin film batteries, the charge cycles could be 10000 and higher. Other important parameters to be considered are: capacity, voltage range, maximal level of discharging and charging current, leakage current, temperature range and material.

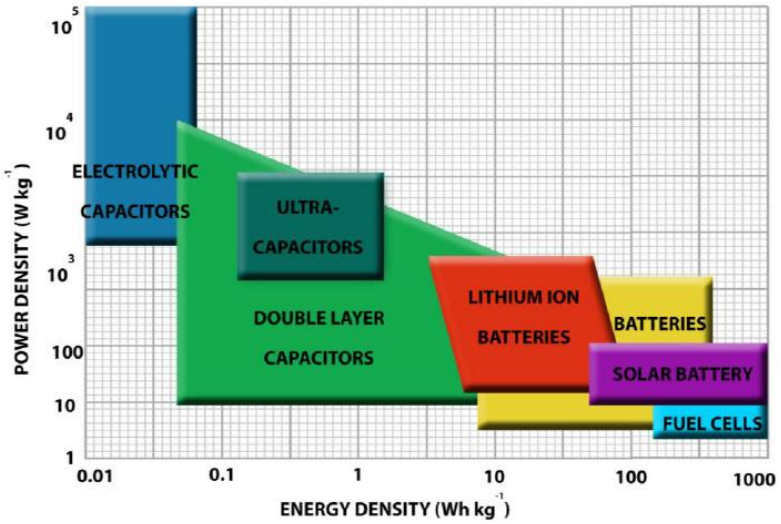

Figure 101 Power density as a function of energy density for different energy storage devices [112]

4.7 TEH DESIGN OPTIONS SUMMARY

Table 7 Summary of TEH solutions

Ambient energy source	Conversion principle	Installed on	Date	Technology Readiness	Reported Average Performance[2]	Reference
Displacement	Electromagnetic induction (Linear generator)	Road		TRL4	55 V	-
Displacement (wheel contact)	Electromagnetic induction (Linear generator)	Track		TRL 2	1.6-8 Wh/day	Concepts 1.1-1.5
Displacement (Track)	Electromagnetic induction (Linear generator)	Track		TRL 2	5-32 Wh/day	Concepts 2.1-1.3
Displacement	Generator	Sleeper	2011	TRL 4	11.08 W	[50]
Displacement	Generator	Sleeper	2012	TRL 4	1.4 W	[48]
Displacement	Generator	Sleeper	2018	TRL 5	7 W	[47]
Displacement	Piezoelectric	Sleeper	2014	TRL 4	81 µW	[51]
Displacement	Piezoelectric	Rail	2015	TRL 4	0.14 mW	[52]
Displacement	Magnetostriction	Rail	2015	TRL 4	0.25 J	[53]
Passing wheels	Variable reluctance	Rail	2013	TRL 4	20 mW	[54]
Vibrations	Electromagnetic	Sleeper	2016	TRL 2	0.27 J	[64]
Vibrations	Electromagnetic	Sleeper	2012	TRL 4	2 mW	[65]
Vibrations	Electromagnetic	Rail	2017	TRL 3	6 mW	[68], [67]
Vibrations	Piezoelectric	Rail	2016	TRL 4	4.88 mW	[69]
Vibrations	Piezoelectric	Sleeper	2014	TRL 3	21.4 mW	[45]
Vibrations	Triboelectric	-	2013	-	726.1 mW/m^2	[70]
Vibrations	Triboelectric	-	2014	-	0.4 W/m^2	[71]
Vibrations	Triboelectric	-	2014	-	104.6 W/m^2	[72]
Vibrations	Triboelectric	-	2014	-	60.2 mW/m^2	[73]
Vibrations	Triboelectric	-	2015	-	121 mW/m^2	[74]
Vibrations	Triboelectric	-	2015	-	3.7 W/m^2 @ 13.9 Hz	[75]
Solar	Photovoltaic	Trackside	-	TRL7-9	150 W/m2 0.4 kWh/m^2/day	-
Wind	Electromagnetic	Trackside	-	TRL 7-9	40 kWh/month	-
Wind	Electromagnetic	Sleeper (T-BOX)	-	-	Peak 2 kW (short duration)	-

[2] Performance is reported with respect to different units, conditions and specifications, therefore the values are not directly comparable

5 TRACKSIDE EH SYSTEM SWOT ANALYSIS

The previous chapter summarises different types of energy harvesters, exploitable in trackside environment. The mentioned designs vary from commercially available solution (mostly for solar and wind power) to non-validated design concepts. Within the scope of this project it is proposed to focus on the development of innovative TEH solutions, exploiting one of the possible electromechanical energy conversion approaches. The mechanical energy available in the trackside environment comes mainly in the form of the kinetic energy of the passing train. Small part of this energy can be scavenged to power up the required trackside application without significantly affecting the train or track dynamics.

Different amounts of energy can be theoretically scavenged depending on the placement of the harvester and its working principle. Either the kinetic energy of the train can be directly exploited by utilising a mechanism that comes to a contact with the wheels of passing train, or a contactless device can be employed, utilising a ferromagnetic property of the train wheels for variable reluctance-based energy conversion. Alternatively the train imparts kinetic energy into the track in the form of mechanical deformation of the rails and sleepers, from there it can be harvested. Energy harvesting from track displacements can either exploit directly the relative movement of the track parts (possibly including the supporting ground), or by employ a mechanical resonator, serving as an energy accumulation element (Figure 102). Some of these conversion approaches might not be universally allowed for trackside energy harvesting due to e.g. safety regulations, and others might not be able to provide the required energy e.g. for a continuous function of given electronic application, while being able to convert sufficient energy amounts for burst-mode operation.

This chapter aims to summarise the strengths and weaknesses of selected TEH solutions, together with their application opportunities and threats in order to justify the recommendations towards the selection of the final candidate for the TEH system development within the Etalon project.

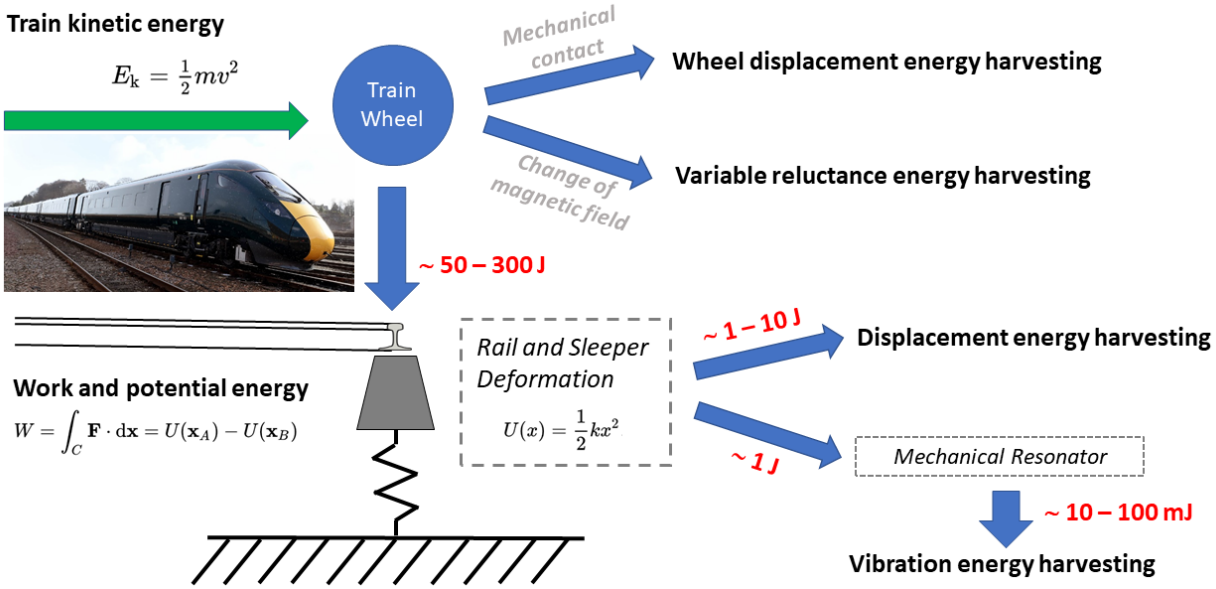

Figure 102 Energy flow of electromechanical TEH systems for a single wheel passing

The criteria on which the comparison of the TEH energy harvester components are made include:

- The power output capacity (including all train traffic and environmental factors)
    - Note: In this context power output relates to the absolute power output from the energy harvester component, it does not include any storage which might be part of the TEH system.
- Pattern of power output (consistency); continuous, intermittent short interval, intermittent long interval, period of power output
- Complexity and reliability of the energy harvester
- Impact/effect of the energy harvester on the train
- Impact/effect of the energy harvester on the track
- Complexity of the installation including fixings and supports
- Impact/effect of the installation on track inspection and maintenance
- Effect of the surrounding trackside environment
- Cost of device and installation
- Maintenance requirement and maintainability

One common issue with cables powering (and controlling) trackside equipment is that they are vulnerable to theft and interference. When the cables are removed by outside interference significant delays are caused in installing replacement cable (or splicing new sections into the cables) both due to the laying of the new cable and the verification and testing of the connections (that the cables connect the correct inputs and outputs) over potentially large distances. The advantage of local energy harvesters is that whilst they might also be vulnerable to theft, standardised modules could be quickly replaced and the connections easily verified and tested as they are in the same location.

5.1 WHEEL DISPLACEMENT-BASED HARVESTERS

5.1.1 Wheel displacement-based harvesters

Table 8 SWOT analysis – wheel displacement-based harvesters

Strengths	Weaknesses
• Large direct driving force available • Largest displacement of actuator (of concepts considered) • Relatively high power densities • Linear generator designs mechanically simple	• Dependent on energy from passing trains which is only available for short moments of time in a period (variable with traffic pattern) • Would have to be removed for rail grinding and possibly tamping • Might cause and obstruction for track maintenance • Complex mechanical motion conversion (linear to rotary) for geared designs
Opportunities	**Threats**
• Clamping directly to the rail would ensure good alignment with the wheel and not interfere with the strength of the rail. • Use of similar actuating devices currently used for other applications (e.g., lubrications systems, axle-counters, etc.)	• High impact loads on the unit • Potential for contact with wheel to cause damage to wheel or acceptance issues.

5.1.2 Track displacement harvesters

Table 9 SWOT analysis – track displacement harvesters

Strengths	Weaknesses
• No interference with the wheel or wheel-rail contact • Large direct activation force available • Displacement takes place over longer time period (than wheel contact designs) reducing shock loading.	• Activation displacement quite low • Some designs require ground/ballast anchors which are time consuming to install, rely on the track staying in correct alignment and can interfere with track alignment and support maintenance (tamping) • Dependent on energy from passing trains which is only available for short moments of time in a period (variable with traffic pattern) • Complex mechanical motion conversion (linear to rotary) for geared designs • Might cause and obstruction for track maintenance • Smart materials might suffer from early wear
Opportunities	**Threats**
• Various designs would allow harvesting of huge amounts of energy generated by the track displacements • Possible integration into new special sleeper design.	• Differential settlement of track and ground anchor might reduce relative displacement or increase it beyond tolerances.

5.2 VARIABLE RELUCTANCE HARVESTERS

Table 10 SWOT analysis – variable reluctance harvesters

Strengths	Weaknesses
• Simple design • Promising power output • No mechanical contact • No moving parts	• Sensitivity to wheel distance from the device • Design must be optimised to a ferromagnetic wheel geometry • Permanent magnets might attract unwanted ferromagnetic particles from the environment • Would have to be removed for rail grinding and possibly tamping • Might cause and obstruction for track maintenance
Opportunities	**Threats**
• Check rail (guard rail) placement might provide better performance	• Will not work with non-ferromagnetic train wheels

5.3 VIBRATION HARVESTERS

Table 11 SWOT analysis – vibration energy harvesters

Strengths	Weaknesses
• Maintenance-free solution • Full integration into sleeper possible • Track tamping-resistant	• Comparably lower power output • Contains moving parts • Power output highly dependent on track and train parameters
Opportunities	**Threats**
• Possible autonomous power source for ultra-low power devices (sensors…)	• Improving the track parameters will lower the level if input vibrations, lowering the power output

5.4 SOLAR HARVESTERS

Table 12 SWOT analysis – solar harvesters

Strengths	Weaknesses
• Abundant energy source reasonable reliable and predictable over long term (days/months) • Not dependent on train traffic • Moderate power output and continuous over long periods (but intermittent)	• Power output limited to daytime • Power output weather and seasonally dependent • Affected by local environment (shading and angle to horizons) and geographic location • Requires large energy storage capacity to cope with night-time and days of low/no power output • Solar panels effectiveness affected by dirt, snow and other opaque contaminants • Size of area required for large power outputs • Requires moderate mounting for installation
Opportunities	**Threats**
• Combine installation (same pole) with wind to offset each other's seasonal variations	• Easily adapted for different applications, therefore an attractive target for theft (perhaps discouraged with unique embedded marking for railway models) • Installation moderately vulnerable to extreme winds

5.5 WIND HARVESTERS

Table 13 SWOT analysis – wind harvesters

Strengths	Weaknesses
• Abundant energy source reasonable reliable and predictable over long term (days/months) • Not dependent on train traffic • Moderate to high power output and continuous over long periods (but intermittent)	• Power output weather and seasonally dependent • Affected by local environment (sheltering/shielding and exposure) and geographic location • Requires large energy storage capacity to cope with days of low/no power output • Requires suitable area for deployment and location with exposure to the wind • Requires significant mounting for installation (pole)
Opportunities	**Threats**
• Combine installation (same pole) with solar • Potential for vertical axis generators to be mounted close to passing trains to take advantage of the air flows generated by the train aerodynamics to provide additional supplemental power	• Easily adapted for different applications, therefore an attractive target for theft • Installation vulnerable to extreme winds

6 THEORETICAL PERFORMANCE ANALYSIS OF TEH SYSTEMS

The following energy and system analysis is directed towards a subset of the technologies described above. Some options for mechanical implementation of movement or energy conversion have been rejected:

- Geared designs. Offer high mechanical gain into large rotations of electrical generators, but it is not possible to achieve this without high contact forces, translated through mechanical gears and bearings, implying either high cost or high wear rates that we incompatible with mass deployment.
- Direct displacement piezo transducers, (not resonant piezo), due to the high forces and long lifetime, current piezo technology will not offer sufficient installation life within the cost limitations.
- Triboelectric generators may be used to replace electromagnetic transducers in future designs, but are currently insufficiently mature to include for further development in this project, where the focus is on the coupling mechanism with the track or wheel.

The included technologies offer a variety of installation types, level of development and output power. It is anticipated that appropriate solutions for trackside energy harvesting will be engineering using multiple harvester technologies.

6.1 DISPLACEMENT HARVESTER ANALYSIS

6.1.1 Potential linear displacement concept designs

In section 4.1.1.2, a series of design concepts for integrating linear generators into railway infrastructure were proposed. In this section a simulation programme in Matlab/SIMULINK is described which was developed to give a preliminary calculation of the concept systems performance. Following this the results of the simulations for each of the concepts are given, the ultimate result being the estimated power output of one device when subject to the example traffic pattern described in section 2.3.2, Expected conditions for TEH systems.

The Matlab/SIMULINK simulation consists of:

- A parameter file to initialise all the input parameters;
- A “Wheel/Track-Vertical displacement” subsystem to simulate the vertical displacement captured from the wheel flange of trains, or of the track when the train runs over, and a lever (where present) to amplify the captured displacement;
- A “Linear electric generator” subsystem to predict the electric power generated from the harvester.

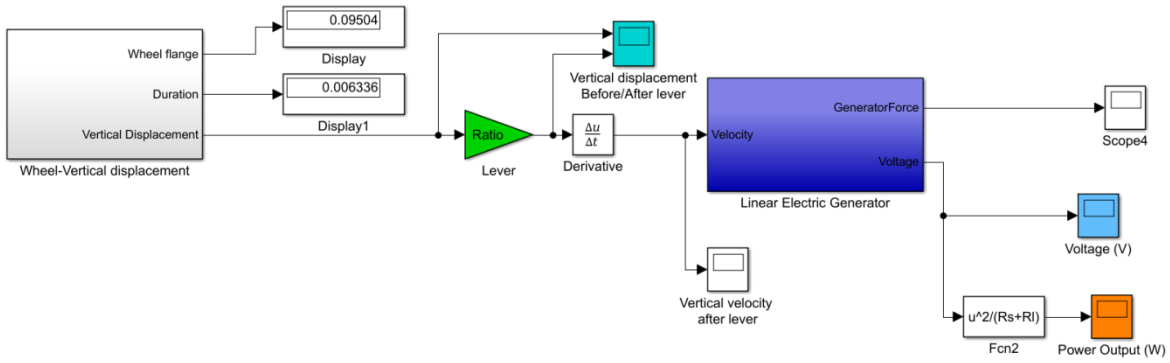

Figure 103 Simulation model in Matlab/SIMULINK

The parameters of each concept and each type/speed of train in the traffic pattern were input to the simulation programme and the estimated power output/day was calculated, in addition to other parameters such as the reaction force on the wheel or track. The results of the calculations are shown in Table 14.

Table 14 Estimated energy output of linear generators concepts integrated into railway infrastructure

Concept no	Concept drawing	Estimated displacement at the source/generator [mm]	Diameter D [mm]	Length L [mm]	Actuating force F [N] (The calculation is based on a train speed of 100 km/h)	Estimated Impact Force on the wheel/rail [N]	Estimated energy per wheel contact [J]				Estimated energy per day [Wh] (generic traffic scenario)	Energy to impact force ratio [Wh/kN]
							Express passenger train	Stopping passenger train	Loaded freight train	Un-loaded freight train		
1.1	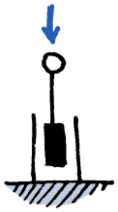	10/10	100	300	574.0	574	6.72	4.80	2.88	2.88	**1.05**	1.824
			50	90	37.6	38	0.44	0.31	0.18	0.18	**0.07**	1.761

1.2	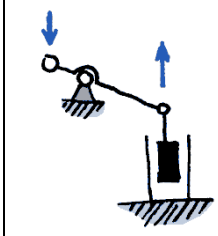	10/15	150	300	2427.3	3641	42.63	30.45	14.83	14.83	**6.00**	1.649
1.3	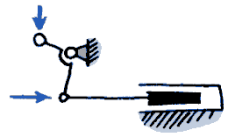	10/15	max 90	max 500	701.3	1052	12.32	8.80	4.94	4.94	**1.86**	1.764
1.4	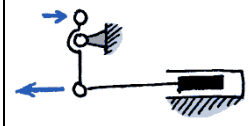	30/30	90 max	500 max	983.4	983.4	34.66	24.75	13.88	13.88	**5.22**	3.981
1.5		30/45	40	50	33	29	1.52	1.08	0.65	0.65	**0.24**	8.067
2.1		2/10	100	1000	3417.1	17086	39.9	28.50	17.10	17.10	**6.22**	0.364
2.2	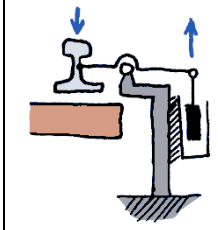	3/15	200	1000	12340	61700	215.3	153.8	86.35	86.35	**32.45**	0.395
2.3	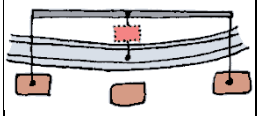	3/15	90 max	1000	3606.8	18034	63.18	45.13	27.08	27.08	**4.92**	0.273

Based on the estimated performance and other factors regarding the concept designs the following conclusions can be made:

- The estimated energy outputs of the linear generator energy harvesting concepts are promising, however, concepts 1.1 and 1.5 have a relatively low predicted output. Therefore, it is likely that an excessive number of units might have to be deployed to meet the energy harvesting targets of the application.
- The concepts which can be installed entirely within the track structure have the advantage of being relatively compact and self-contained; those that require a ground anchor would introduce complexities for installations and operation of the track. However all designs would have to consider their effect on access to the track for track maintenance.

6.2 VARIABLE RELUCTANCE HARVESTER ANALYSIS

6.2.1 Single wheel passing simulation results

A single wheel pass was simulated for a variable reluctance harvester, where the change of magnetic flux through the circuit (Figure 104) is caused by passing train wheels made of ferromagnetic material.

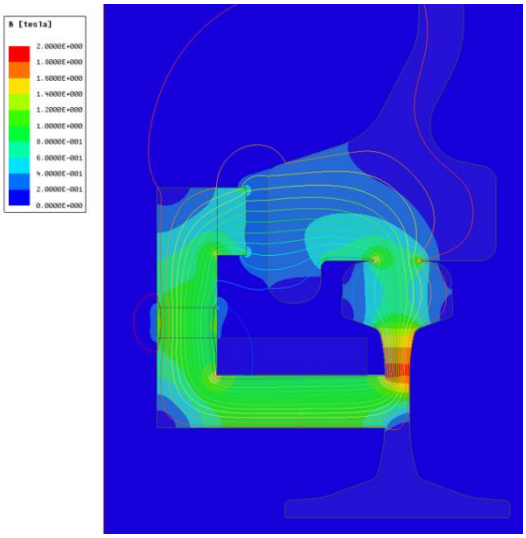

Figure 104 Magnetic flux density distribution in the variable reluctance harvester during the wheel passing

Analysis results (Figure 105) indicate that the variable reluctance harvester might present a viable TEH solution, as the energy harvested from a single wheel pass is in the range of Joules. Furthermore, this type of harvester does not affect the track dynamics, and therefore the amount of energy extracted from the passing train is not a concern.

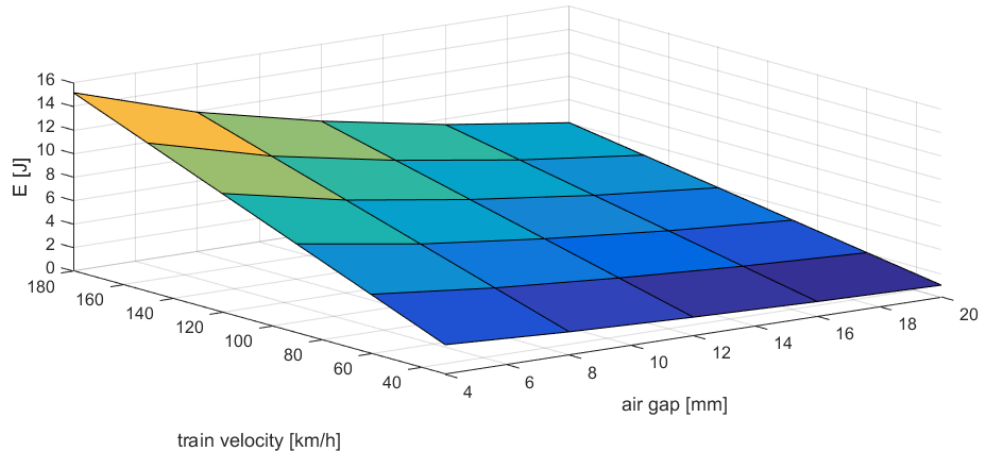

Figure 105 Harvested energy from a single wheel passing as a function of train speed and air gap length

6.2.2 Daily levels of harvested energy

Table 15 Variable reluctance harvester - daily harvested energy

			Energy harvested per wheel [J]			Total Energy [J]		
Train type	**No. of trains daily**	**Active wheels per train**	**4mm**	**12mm**	**20mm**	**4mm**	**12mm**	**20mm**
Express passenger train(8 cars, 140km.h^{-1})	6	36	11.81	7.36	4.69	2550.6	1590.0	1013.7
Stopping passenger train (4 cars,100km.h^{-1})	8	10	8.43	5.26	3.35	674.8	420.6	268.2
Loaded freight train (20 cars, 60km.h^{-1})	4	84	5.06	3.15	2.01	1700.4	1060.0	675.8
Empty freight train (20 cars, 60km.h^{-1})	4	84	5.06	3.15	2.01	1700.4	1060.0	675.8
					Sum [J]:	**6626.1**	**4130.5**	**2633.5**
					Sum [Wh]:	**1.84**	**1.15**	**0.73**

The daily estimations of harvested energy from a given scenario shows, that generally kilojoules can be harvested from the passing trains each day. This equals to an average available power output between 30 and 75 mW, depending on the wheel distance from the harvester. This amount of power can be used to continuously power up some of the low consumption electronic parts in the trackside environment.

6.3 VIBRATION HARVESTER ANALYSIS

6.3.1 Theoretical analysis using a single wheel excitation waveform

Due to the geometry of train car chassis and its variance between the different types of trains it is generally not feasible to employ an inertial harvester working in resonance operation for trackside energy harvesting solutions. Instead, an impulse (shock) excitation by the passing wheels can be exploited.

The simplified shape of an acceleration waveform coming from s a single train wheel passing was created. A constant deflection 2mm of the sleeper is assumed no matter the train speed, and the acceleration magnitudes are calculated according to the waveform width (Figure 106) to reach the set track deflection.

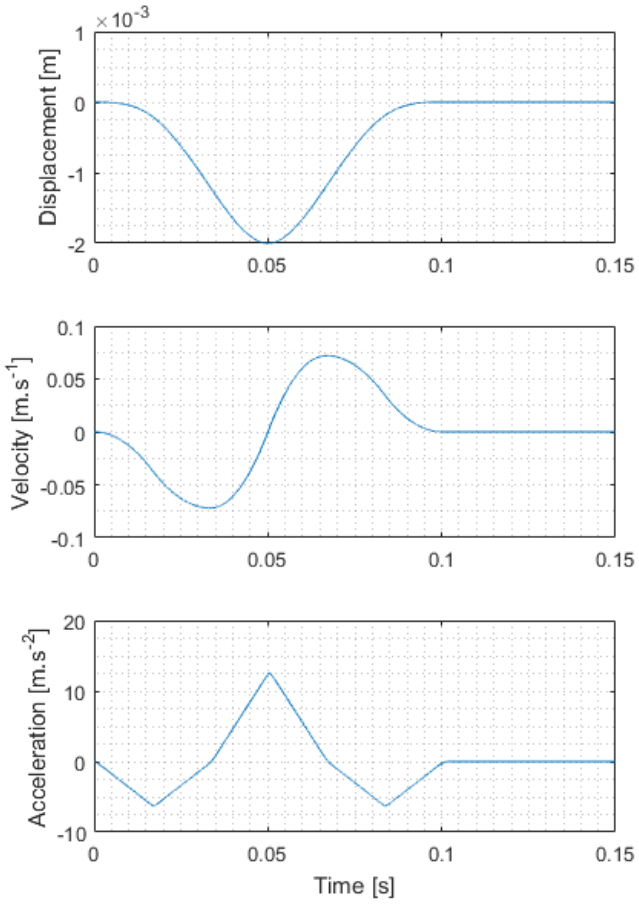

Figure 106 Displacement, velocity and acceleration simplified waveforms - single wheel pass

The energy harvested by a generic idealised linear inertial harvester from a single wheel passage is then calculated for different combinations of the harvester natural frequency setting and the

acceleration waveform width. The harvester was modelled as a spring mass damper system (as described in 4.3.1), with constant both electrical and mechanical quality factors both set to 50. The proof mass of the harvester was set to 1kg.

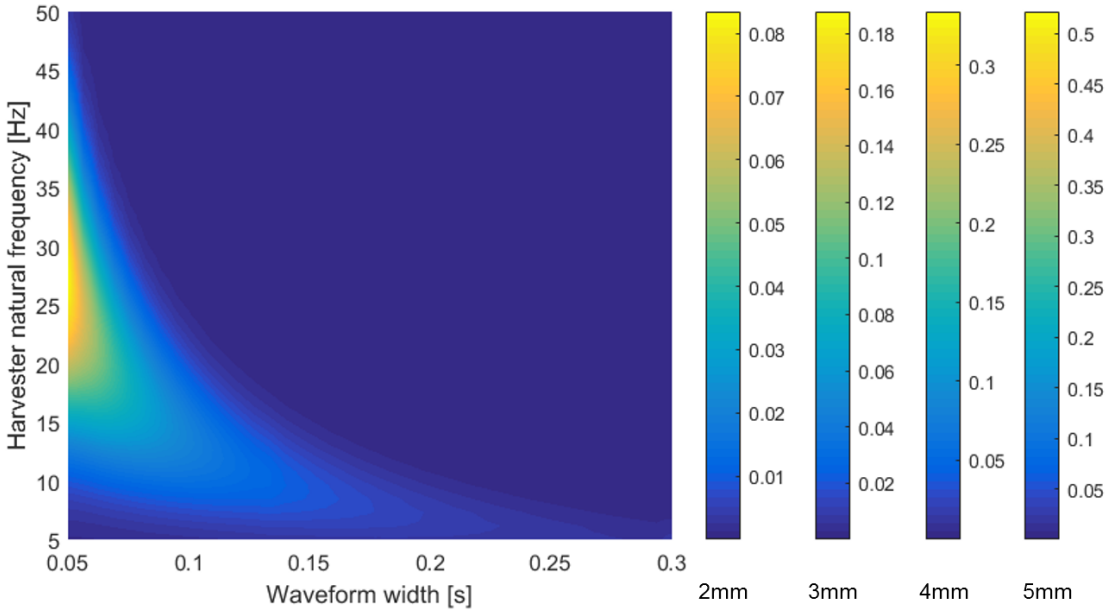

Figure 107 Harvested energy [J] from a single wheel depending on the harvester tuning and train speed (excitation pulse width) – sleeper deflections between 2-5mm

The analysis results confirm the findings of [64], as the train speed 200 km/h is associated with a waveform width of roughly 0.1 seconds. In the real train situation however, the wheels are passing in a more complicated periodic patterns, depending on rail car type.

6.3.2 Real data based analysis

In order to better evaluate the feasibility of vibration energy harvesters in the trackside environment, four measurement sets of rail sleeper acceleration and displacement from passing of different passenger trains through an unspecified track in Czech Republic were obtained and used as inputs for further analysis.

Table 16 Basic data of measured trains and track types

Train identifier	Train type	Train speed [km.h^{-1}]	Measurement point
1	Passenger – regional	90	Regular track
2	Passenger - express	141	Regular track
3	Passenger – regional	80	Railway switch
4	Passenger - express	130	Railway switch

The generic harvester model remained similar as in previous chapter, but it was updated with non-ideal transducer with non-zero inner impedance, calculated from an expected coil design. The model was then fed with real acceleration. The average power output and total harvester energy was observed for different natural frequency tunings of the harvester and different trains.

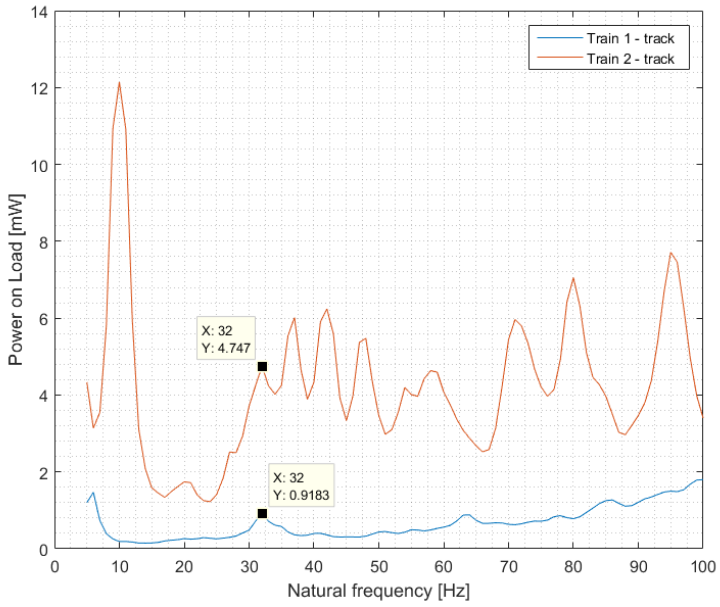

Figure 108 Harvester power output dependency on natural frequency tuning – regular track

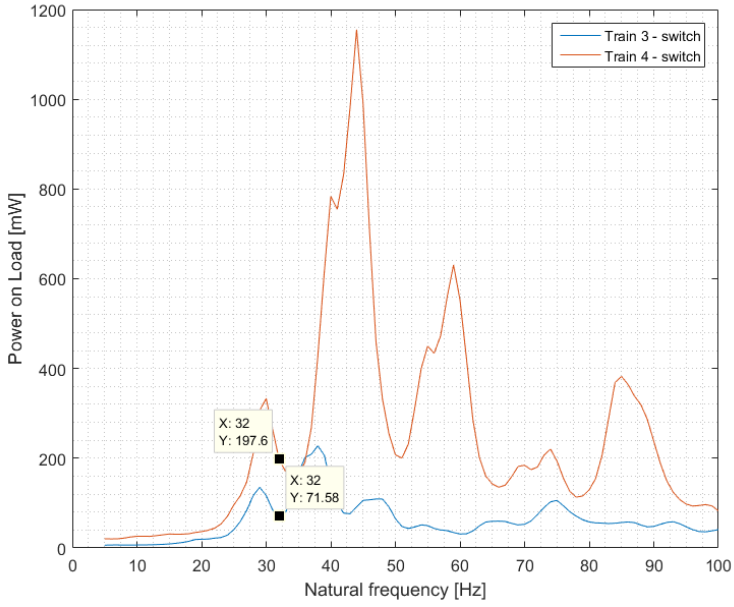

Figure 109 Harvested power dependency on harvester natural frequency - railway switch

It is clear from the results, that tuning the harvester to frequency low enough to exploit the single wheel passes as simulated in the previous subchapter is not practically feasible due to different characteristics of the excitation on the regular track and the railway switch. Instead, a harvester natural frequency tuning of 32Hz was found to provide satisfactory results for all of the measured trains, providing 0.92mW of output power on load in the worst-case scenario (Figure 110).

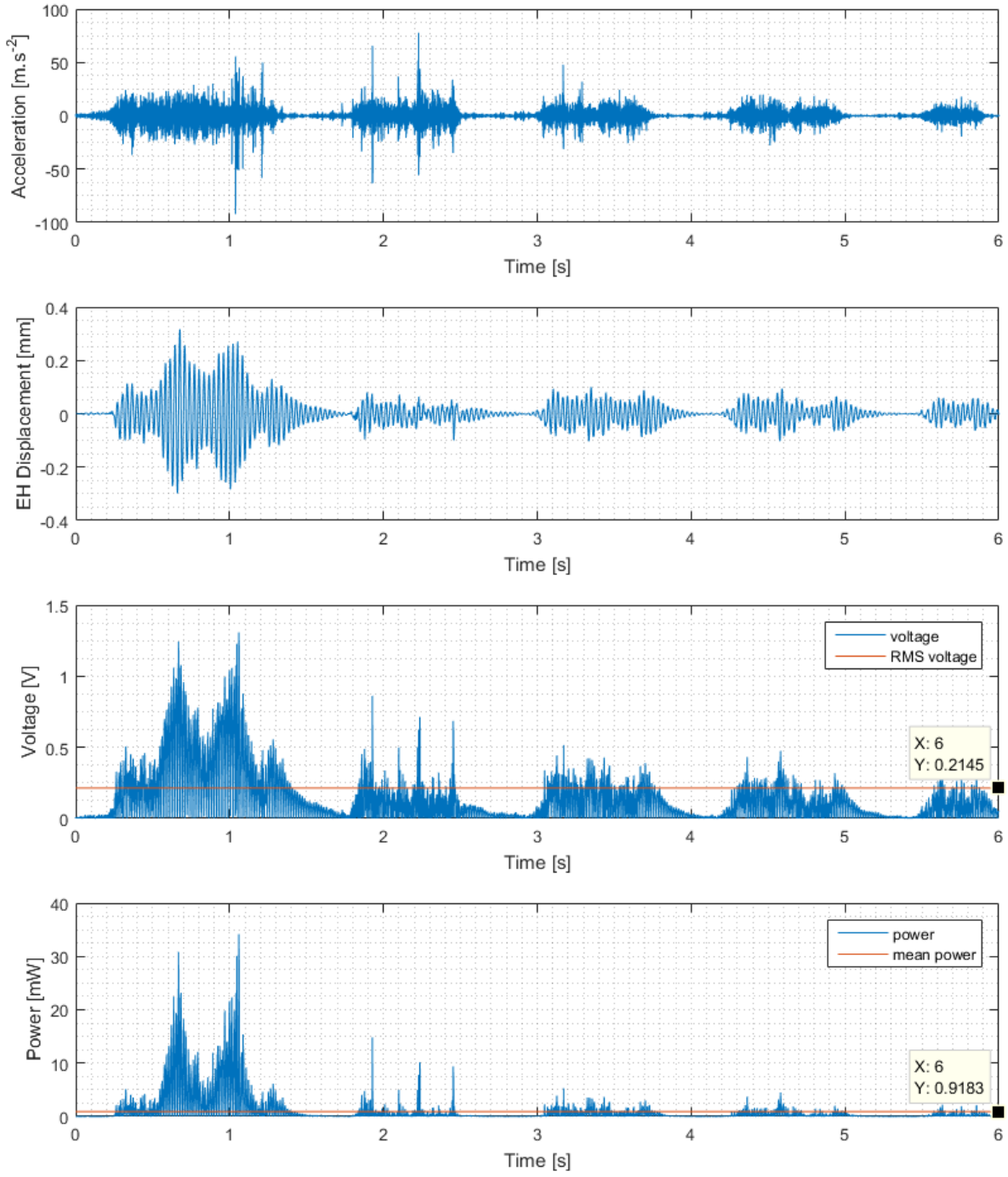

Figure 110 Simulation results from a generic TEH model tuned to 32Hz – train 1

In the best case scenario the same harvester was able to deliver 197mW of power on load (Figure 111, while being placed on the railway switch sleeper and excited by an express train. The obvious differences between these results can be explained by comparing the excitation acceleration waveforms of the two trains on the respective tracks.

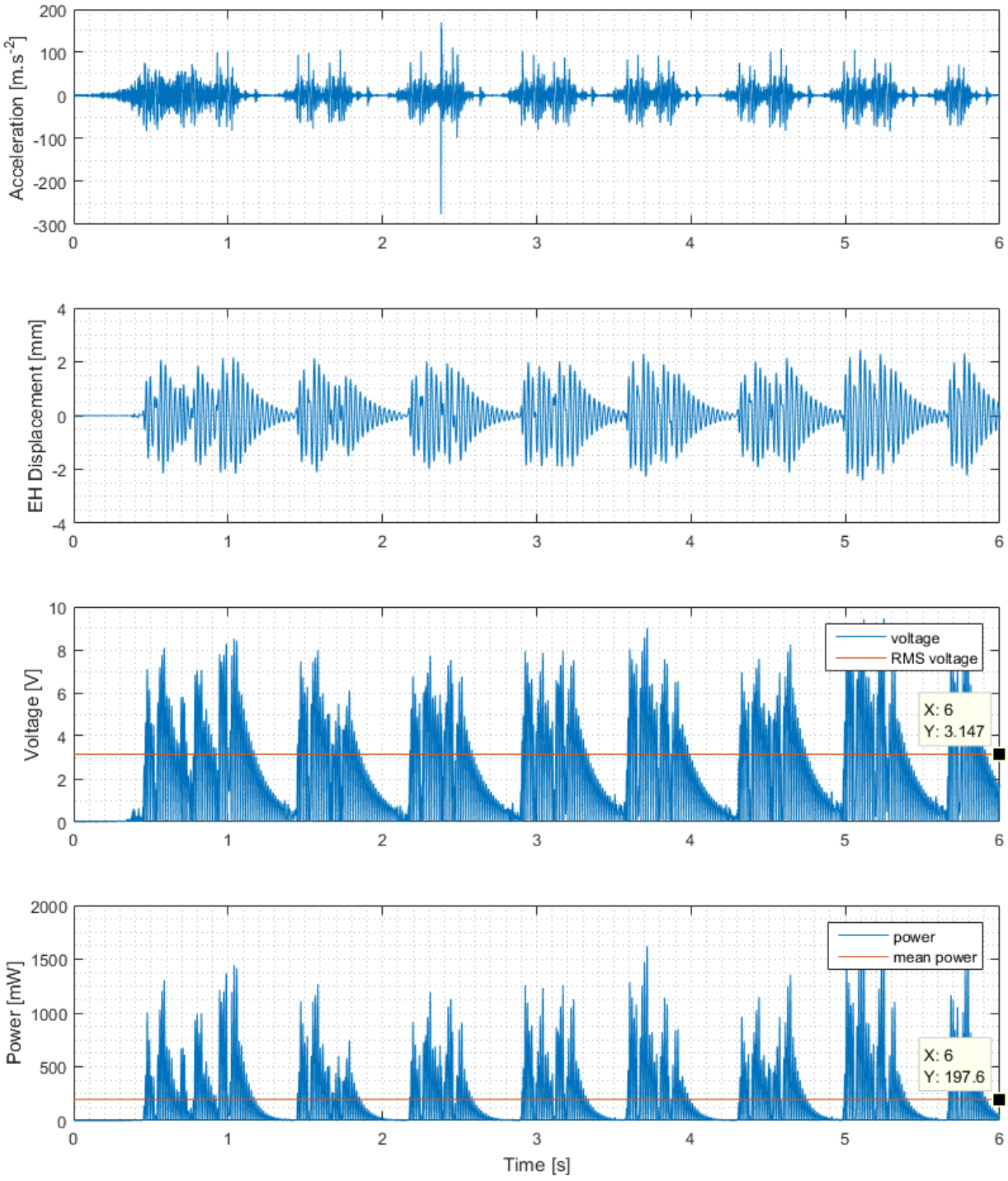

Figure 111 Simulation results from a generic TEH model tuned to 32Hz – train 4

The results from all simulated trains are summarised in the following table:

Table 17 Simulated vibration energy harvester performance for different trains passing

Train identifier	Harvester natural frequency [Hz]	Load impedance [Ω]	RMS voltage on load [V]	Average power on load [mW]	Total harvested energy [mJ]
1	32	50	0.2	0.9	5.5
2			0.5	4.7	19.9
3			1.9	71.6	629.9
4			3.1	197.6	1185.6

6.3.3 Daily energy harvesting prospects for vibration energy harvesters

This section provides a rough estimation of energy levels available from a vibration energy harvesting device, outlined in the previous section. The results were estimated from the obtained real life measurements and their extrapolation to fit the generic scenario of 22 trains of four different types passing through the track during one day, as described in 2.3.2.

In order to compare the estimation with more optimistic results, a different approach was analysed as well. The results presented in [64], where a harvester is tuned specifically for different speeds of passing trains, were extrapolated and used for a new estimation. Even though this approach is not practically feasible due to multiple needed natural frequencies of the harvester, the results still remain in range of joules of energy, harvested during the whole day.

Table 18 Vibration energy harvester - daily harvested energy

	Number of trains daily	Realistic scenario: energy on load per train [mJ]	Realistic scenario: total harvested energy on load [mJ]	Optimistic scenario: energy on load per train [mJ]	Optimistic scenario: total energy harvested on load [mJ]
Express passenger train (8 cars, 140 km.h^{-1})	6	35	210	105	630
Stopping passenger train (4 units, 100 km.h^{-1})	8	8	64	35	280
Loaded freight train (20 cars, 60 km.h^{-1})	4	14	56	40	160
Empty freight train (20 cars, 60km.h^{-1})	4	10	40	25	100
Sum [mJ]:			**370**	Sum [mJ]:	**1170**
Sum [mWh]:			**0.102**	Sum [mWh]:	**0.325**

6.4 SOLAR SYSTEMS ANALYSIS

The performance of commercial solar panels in terms of how much power they generate for each unit of sunlight is well established, the nominal maximum power rating of crystalline silicone solar panels is approximately 150 W/m^2, however the amount of power a solar installation will generate depends on the orientation of the panels and other factors such as weather. There is significant experience with solar energy harvesting therefore there are readily available and established tools for taking all the factors into account to estimate the power generation of a solar panel installation. The general maximum amount of energy in sunlight reaching the earth is 1,000 watts per square metre (m^2) of surface area (normal to the incident light). Crystalline silicone solar panels are about 15% efficient at turning solar energy into electricity, therefore the nominal maximum power rating of solar panels is 150 W/m^2. Various calculation tools exist in order to assist in order to estimate the actual power generated by an installation, taking into account the time of year, angle of the sun and average sunlight variations due to weather. As an example the estimated power output for a fixed solar panel of 1 m^2 (150 W output) located in central Europe is shown in Table 19 using the Geographical Assessment of Solar Resource and Performance of Photovoltaic Technology calculation tool provided by the European Commission, Join Research Centre, Institute for Energy and Transport, Photovoltaic Geographical Information System (PVGIS).

Table 19 Estimation of power generation performance for a 1m^2 150W solar panel. [113]

Fixed system: inclination=35°, orientation=0° Estimated losses due to temperature and low irradiance: 7.7% (using local ambient temperature) Estimated loss due to angular reflectance effects: 3.0% Other losses (cables, inverter etc.): 14.0% Combined PV system losses: 23.0%				
Month	Average daily electricity production (kWh)	Average monthly electricity production (kWh)	Average **daily** sum of global **irradiation per square meter** (kWh/m2)	Average sum of global **irradiation per square meter** (kWh/m2)
Jan	0.14	4.51	1.16	35.8
Feb	0.27	7.51	2.16	60.3
Mar	0.45	14.0	3.77	117
Apr	0.59	17.7	5.10	153
May	0.58	18.1	5.15	160
Jun	0.62	18.5	5.55	166
Jul	0.59	18.4	5.40	167
Aug	0.55	17.1	4.97	154
Sep	0.47	14.1	4.11	123
Oct	0.33	10.2	2.78	86.3
Nov	0.17	5.00	1.36	40.7
Dec	0.12	3.77	0.97	30.1
Yearly average	**0.408**	**12.4**	**3.55**	**108**
Total for year		**149**		**1290**

These figures are for a location in central Europe the average amount of energy received by a location varies across Europe and the world. The average annual direct normal irradiation by sunlight across Europe are shown in Figure 112 Average annual direct normal irradiation by sunlight in Europe below, the location in above would be on the boundary between the lightest green and yellow areas.

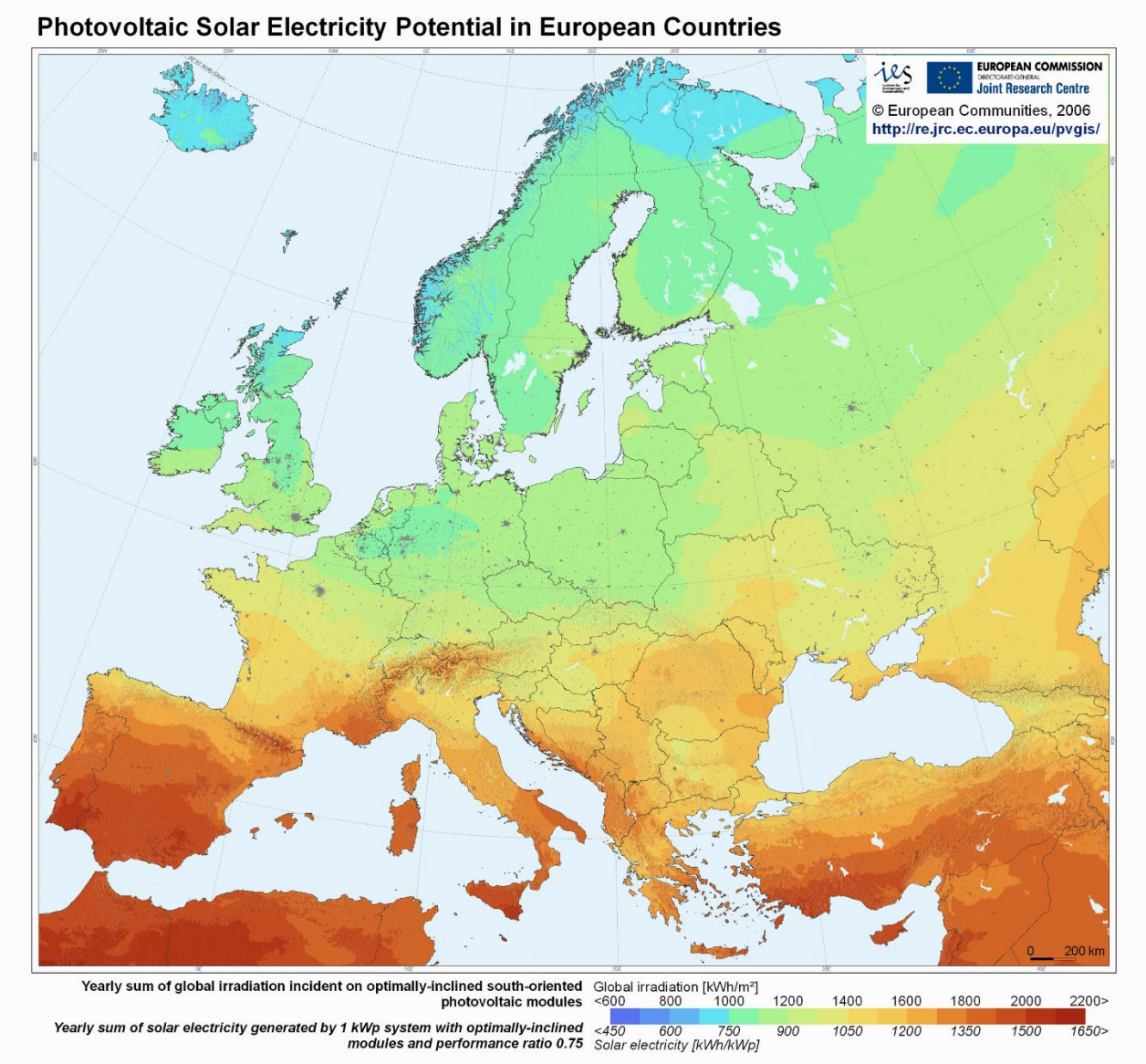

Figure 112 Average annual direct normal irradiation by sunlight in Europe

To design a solar installation for a system powered entirely by solar, the month with the lowest average solar power collection would need to be considered, along with the average power requirement for that month at the location, then a large enough array of panels specified for the installation to meet the power requirement. An energy storage system with enough capacity to capture and store the power in excess of the monthly average, and provide continuous power over

night and on days when solar power output is below average. Alternatively a solar installation could be combined with another form of energy harvesting. In addition a check would have to be made that the location was suitable for the installation in term of space for the installation and factors affecting the amount of sunlight received and the installation design modified accordingly or alternative forms of energy harvesting used.

6.5 WIND HARVESTERS ANALYSIS

The performance of wind turbines in terms of how much power they generate for a given wind speed is well established and is part of the manufacturers specifications. When selecting a wind turbine of appropriate power output for an application it is important to match the average energy harvested over a long period with the average power consumption of the application The specification of the system must also ensure sufficient energy storage capacity to capture and store the power in excess of the monthly average, and provide continuous power on days when wind turbine power output is below average. Due to wind turbines being an established form of energy harvesting/power generation in other applications there is established data for the long term energy harvesting performance of wing turbines which can be used to select the appropriate product for the application. As an example Figure 113 shows the estimated monthly energy output for the nominal 40 kWh/month horizontal axis wind turbine shown as an example in section 4.5.1.1, this gives a more precise estimate of the expected monthly energy output of the device (compared to the nominal rating) based on the average annual wind speed at the location. Figure 114 shows the annual wind speed at 50 m elevation for different areas across Europe allowing the average wind speed at a location to be estimated, however this data is intended for electricity supply grind sized installations where the 50 m elevation is more relevant, for trackside installations more detailed information for each location should be considered. The data from the average monthly output of the wind turbine (for average annual wind speed) and average annual wind speed at the location being considered (including local factors affecting wind speed) can be used to select a commercial wind turbine with the appropriate power output for an application.

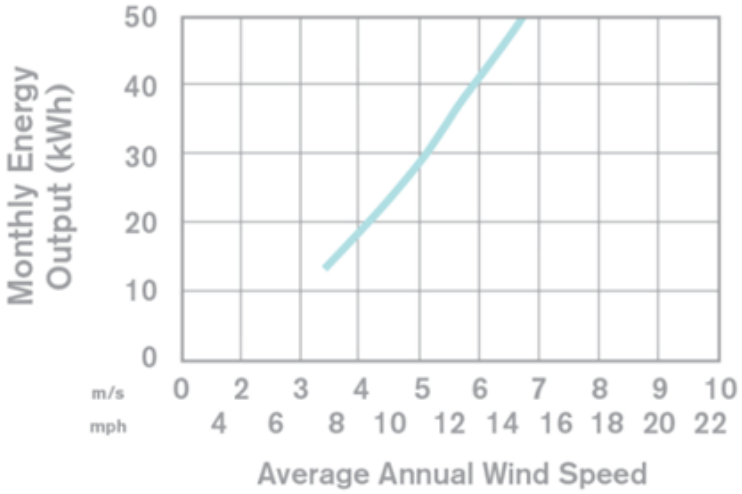

Figure 113 Variation of average monthly energy output estimates for a nominal 40kWh/month wind turbine with average wind speed [106]

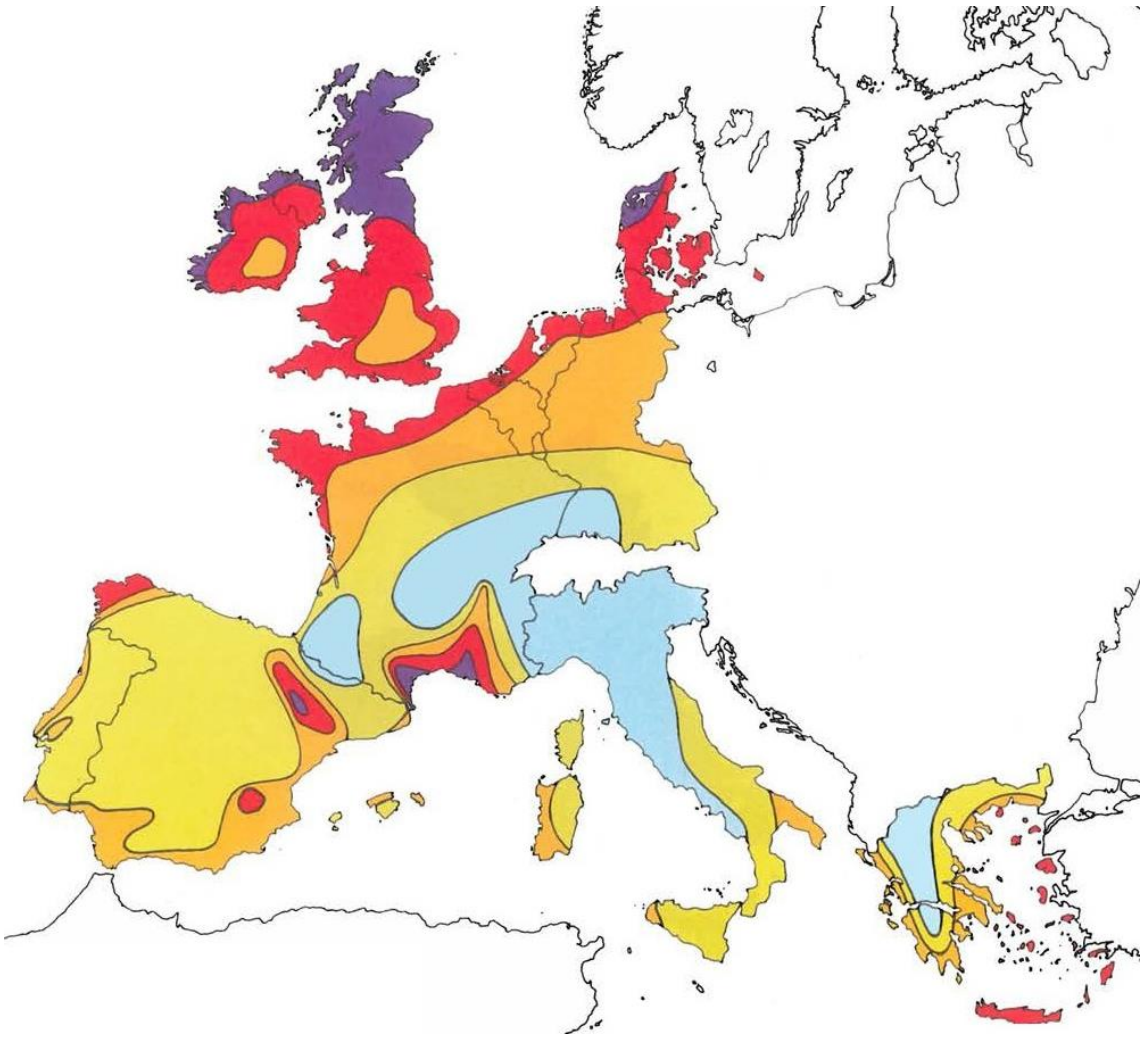

	Sheltered terrain	Open Plain	Hills and Ridges
	> 6	> 7,5	> 11,5
	5.0-6.0	6,5 - 7,5	10,0 - 11,5
	4.5-5.0	5,5 - 6,5	8,5 - 10,0
	3.5-4.5	4,5 - 5,5	7,0 - 8,5
	< 3.5	< 4,5	< 7

Figure 114 Average wind speed at 50m elevation for different areas across Europe (m/s²) [114]

Comparison between average wind speed Figure 114 and average sunlight Figure 112 shows that the trends in available energy for wind and solar for different locations are generally opposite, therefore either wind energy harvesting could be used in areas where solar is less effective (and vice-versa). Alternatively dual wind/solar installations could be considered for some installations so that the strengths of one type of energy harvesting can compensate for the weaknesses of the others.

6.6 COMPARISON

The different energy harvester types analysed in sections above can provide very varying daily amounts of energy, depending on the exact environmental conditions. As was mentioned in 4.7, the comparison of different principles is not straightforward and the performance is not being reported in consistent way, as the number of variables involved is high. For that reason a comparison using conditions set in 2.3.2 as a generic scenario for TEH, is presented in this section to obtain at least a basic understanding of the capabilities of different types of TEHs in given conditions, set to match a Central European railway with medium traffic density of 22 trains per day.

Table 20 Comparison of estimated power outputs for different types of energy harvesters

Harvester type	Estimated daily power output [Wh]
Displacement	0.07-32.45
Variable Reluctance	0.83-1.74
Vibration	1.02×10^{-4} - 3.25×10^{-4}
Solar panel	408
Wind harvester	1300

The results indicate, that the mature technologies, such as solar panels and wind turbines, can theoretically provide high energy outputs for trackside applications. These results might not be easily matched by other energy harvesting approaches without upscaling the harvesters or using redundant devices. However, other energy harvesting approaches might prove feasible in applications, where the use of solar or wind devices is limited for some reason.

7 DISCUSSION

To give the reader some sense of the information communication density that might be achieved with these technologies, we can stipulate a basic message size, band rate and transmission power common to many low power sensor radios running at 2.4 GHz (e.g. 802.15.4, more information on this topic is to be found in deliverable report D3.1of work package WP3 within this project [115]), to derive an energy per message. In order to assess the usefulness of an energy harvesting technology we can then estimate the number of messages per day (or per train) that could be supported by a given energy harvester.

This analysis excludes any consideration of antenna efficiency and range – this will need work on efficient antenna design for trackside applications to establish a reliable range.

Conservatively, and using information from WP3, 50 mW is necessary to transmit at 2.4 GHz and 100kbd (approximately 10000bytes per second) using “low power” methods.

Therefore, to transmit 100bytes requires (50mW x 100/10000) J (assuming that 100bytes is sufficient to convey a secure message).

Total energy required for **one secure message** could be approximately **0.5 mJ**. 1 message per second is 0.5 mW continuously. From this basis, an energy harvester producing 1 W continuously can support 2000 messages/s (more than the radio channel can support), if the power consumption of the object controller functionality is neglected.

8 CONCLUSIONS AND RECOMMENDATIONS FOR FUTURE TRACKSIDE ENERGY HARVESTING SYSTEM DESIGN

The objective of this conclusion is to summarise the work carried out identifying and characterising energy harvesting technologies and concepts with potential relevance to Trackside Energy Harvesting. There are too many factors and variables in terms of power output (related to scales of energy harvester installations and variation in power production profile depending on location and conditions), and power requirements (related to object controller design and duty), to make specific or general recommendations for non-specific applications. However the information contained in this report can be used as a general guide for developing outline specification and initial designs for an energy harvesting installation to meet a specific set of requirements, although the TRL of each technology or concept, and breadth of data available for each, should be taken into account. This situation is in line with the expected outcomes and Work Package 4 work plan. The conclusions below are highly relevant to further work that would be carried out in Task 4.4 to develop and deliver proofs of the most promising concepts discussed in this report.

Different technologies that could potentially be used for harvesting energy on the trackside, in the railway environment, have been identified and analysed in the previous sections. These include both conceptual designs and prototypes specifically developed for such applications, as well as mature technologies (e.g., solar cells, wind turbines, etc.), which have been validated in other applications, and could be transferred to railway applications through typical technology and knowledge transfer methodology.

The following sub-sections summarise the specific conclusions for the considered types of energy harvesting systems, and makes general conclusions of this investigation with respect to requirements and further implementation, which will be taken into consideration for further research and developments on this topic within the ETALON project.

8.1 DISPLACEMENT HARVESTERS

- The potential energy that could be harvested from displacements at the level of track and wheel-rail interaction is significant, and different systems have already been designed and tested at prototype level. In addition, novel concepts using linear generators to convert the mechanical energy into electrical energy have been proposed.
- The most promising energy sourcing solutions are:
  - *Displacement of actuating element of energy harvester by contact with the wheel. The advantages of these solutions are that the complexity is lower and their integration is simpler. The main disadvantage relates to the contact and impact forces imposed on the wheel, which would have to be extremely well managed to comply with the current standards and requirements in this area:*
  - *Track elements displacement (i.e., rail and sleepers). The advantages of these solutions are that the forces that could be used to drive the energy harvester are very high, and the impact of the harvesters on the track elements is relatively low. The major disadvantages relate to*

higher complexity of these systems, and significant impact on rail operation, especially on maintenance processes.

- The identified solutions for converting the mechanical energy of the displacements induced by the wheel or track to electrical energy are based on different physical principles, including:
  - *Electromagnetic induction;*
  - *Piezoelectric;*
  - *Magnetostrictive.*
- The solutions based on electromagnetic induction could be classified in two different categories:
  - *Rotary generators using geared solutions, which were intensively researched in the last decade, particularly in the US and in China. Prototypes based on both wheel contact and track displacements have been tested on real track and the potential amount of harvested energy is relevant. However, the geared mechanisms appear to be complicated, costly and the feasibility is uncertain (no information reported so far). Considering all these, and for avoiding duplication with ongoing advanced research, ETALON will not focus further on these types of harvesters.*
  - *Linear generator solutions were proposed and investigated at conceptual level by UNEW; the advantages are the relatively high potential power output (compared to other train/track displacement solutions) and the mechanical simplicity compared to solutions relying on gear systems. The potential disadvantages include managing the shock loading caused by, and reacted on wheels. Both wheel contact and rail displacements were considered as primary sources of energy, and the potential harvested energies initially estimated are promising, i.e.:*
    - *0.07 – 6.0 Wh/day in the case of the system using the wheel-contact;*
    - *6.22 – 32.45 Wh/day in the case of the system using the rail displacement.*
- The solutions based on piezoelectric energy conversion are potentially mechanically simple, although locations directly underneath sleepers may impact on maintenance. Energy outputs are significantly lower per installation than other conversion types, however, and the lifetime of the piezo material may be short, due to mechanical wear

The solutions based on magnetostrictive linear harvesters suffer from similar constraints as the piezo harvesters, and although output figures are not available it is believed that output energy is similar to piezo harvesters. Direct coupling between the rail and ballast may be vulnerable to maintenance and track dynamics, as well as exposing the active components to high levels of wear. The risk in this technology is considered too high, relative to other methods, to progress at this time. Considering the above conclusions, solutions using **linear generators** (based on both wheel contact and rail displacement) **will be further investigated** by UNEW within ETALON. The main considered further activities include:

- Further simulations and calculations to estimate the energy that could be harvested by different design and installation concepts;
- System design, including modelling, prototype manufacture, installation, and further operation and maintenance aspects;
- Development of appropriate power management and storage solution;
- Production of prototype;
- Testing of prototype;
- Analysis of tests' results.

The main identified **challenges** include:

- Integration on the track system (flexible and simple installation, low impacts on track and wheel, low impacts on maintenance, etc.);
- Low-medium complexity of design solution, hence feasible cost of the system, simple installation, increased reliability, etc.
- Managing the shock loading caused by, and reacted on wheels

8.2 VARIABLE RELUCTANCE HARVESTERS

- The energy output potential for variable reluctance harvesters is significantly high. There is a potential for a storage of the harvested energy and for ensuring a long-time operation of smart object controller during the day.
- The effect of magnetic flux change caused by a passing ferromagnetic wheel can be effectively used by a variable reluctance TEH, which can be easily integrated onto a rail.
- The output power significantly depends on a train speed and on the geometry of the ferromagnetic train wheel.

Considering these aspects, the **variable reluctance harvesters will be further investigated** by BUT within the ETALON project. The main considered further activities include:

- Further simulations and calculations to estimate the energy that could be harvested by different designs;
- System design, including installation, and further operation and maintenance aspects;
- Testing of prototype;
- Analysis of tests' results.

The main identified **challenges** include:

- Integration on the track system (flexible and simple installation with railway approvals, low impact on maintenance…);
- Relying on ferromagnetic property of the train wheels;
- Issues related to a possible build-up of ferromagnetic particle contamination.

8.3 VIBRATION ENERGY HARVESTERS

- Vibration energy harvesting devices can generally be used only in a specific domain with stable vibration frequency operation or with very high excitation acceleration. The second case is observed in a trackside environment, where a vibration TEH mostly cannot be used in the resonance operation mode.
- Vibration harvesters provide autonomous source of energy for several specific monitoring and diagnostics applications, such as bridge monitoring of structure health monitoring systems. This kind of EH devices is used to power the ultra-low power electronics with required power inputs in range of 10 μW – 100 mW.

- The scaled-up design of these devices brings many difficulties in acceleration feedbacks and operation modes, which are not acceptable for the vibrating base structure.
- Vibration TEHs can be designed as maintenance free devices, generating electricity only as trains pass. For continuous power generation this technology is not effectively applicable.
- The vibration TEH can be easily integrated inside a sleeper.

Considering the conclusions above, the use of **vibration energy harvesters** for powering the smart trackside devices **will be further investigated** by BUT within ETALON. The main considered further activities include:

- Further simulations and modelling to compare the energy that can be harvested by different designs of vibration TEHs;
- Design of the vibration TEH system prototype, including power management and storage solution;
- Prototype of customised solution; and development of appropriate power management and storage solution;
- Testing of prototype;
- Analysis of tests' results.

The main identified **challenges** include:

- Low power output harvested only during passage of a train;
- Improving the track parameters will further decrease the power output of vibration EH;
- Complexity of the designs containing oscillating parts, hence possibly affecting the reliability and the cost of the solution.

8.4 SOLAR ENERGY HARVESTERS

- The PV cells / solar panels are mature technologies, widely accepted and used in various applications and industries.
- These high TRL solutions (TRL9) include solar panel installations which can be scaled from small to large physical area and small to large power outputs.
- The PV cells / solar panels offer predictable (over long time scales) energy harvesting which is not dependent on the passage of railway traffic.
- Although solar panel power production is intermittent, when producing power they can provide a continuous (but fluctuating) power output over many hours.

Considering the above conclusions, the use of **solar energy harvesting solutions** for powering the new smart generation of object controllers **will be further investigated** by UNEW within ETALON. The main considered further activities include:

- Assist specialised manufacturer in producing a tailored customised solution;
- Prototype of customised solution; and development of appropriate power management and storage solution;
- Testing of prototype;
- Analysis of tests' results.

The main identified **challenges** include:

- Integration in the trackside environment (flexible and simple installation with railway approvals);
- Reliability and feasibility of the customised solar panel in railway environment;
- Issues of surface contamination build-up affecting performance.

8.5 WIND ENERGY HARVESTERS

- Wind turbines are mature technologies, widely accepted and used in various applications and industries.
- These high TRL solutions (TRL9) include a range of physical sizes from small to large generators with small to large power outputs, this means that a unit with the appropriate average output can be selected for the required application.
- Wind turbines offer predictable (over long time scales) energy harvesting which is not dependent on the passage of railway traffic.
- Although wind turbine power production is intermittent, when producing power they can provide a continuous (but fluctuating) power output over many hours.

Considering the above conclusions, **the use of wind energy harvesting solutions** could be considered suitable for powering the new generation of smart object controllers. However the energy harvesting and power output characteristics of these devices are already well established, which means that the main outstanding issue for the TEH application would be the approvals of designs of installation. Therefore, at this point in time it is not expected that application of these energy harvesters to the powering of new generation of smart object controllers will be further investigated within ETALON.

The main identified **challenges** include:

- Integration in the trackside environment (flexible and simple installation with railway approvals);
- Reliability and feasibility of wind turbines in a railway environment and developing an archive of power generation data

8.6 GENERAL CONCLUSIONS

- The performance of the technologies identified in literature and industry sources were estimated through different methods, using different parameters, specifications and units of measure or parameters. Therefore, in most of the cases, the reported or estimated performance of the different technologies are not directly comparable, so a general assessment was performed. The general assessment considered not only ‘performance’ related to energy harvesting potential, but also key aspects regarding their feasibility, estimated costs, and issues related to the integration of these technologies with respect to impacts on rail operation, maintenance, interaction and compatibilities with rail elements, etc.

- In general, the novel and emerging technologies specifically designed (or that could be designed) for trackside energy harvesting applications involve major interactions with the rail elements, and, therefore, have a significant impact on operations and, especially, maintenance activities.

The table below sets out approximate energy output, either per wheel (trackside harvesters) or per day (environmental harvesters such as solar or wind) and provides a summary of the other factors and the intended further development and assessment in subsequent tasks and work packages of ETALON in a trackside energy harvester prototype for each technology/concept. These technologies can then be compared against the requirements (undefined here) of a given application. A more complex analysis of OC design is required to identify the actual power requirements including the power requirements of logic outputs/inputs, information processing etc, and data transmission.

Table 21 Summary of conclusions on the potential use of different energy harvesting systems for powering trackside object controllers.

Technology	TRL	Performance		Feasibility aspects				Potential for powering the OC	Further work in ETALON (T4.4)	
		Available quantitative data	Qualitative assessment	System complexity	Installation and integration issues/effect	Maintainability	LCC		YES/NO	Description
Displacement harvester Rotary generators using geared solutions	3-4	1.6 J/wheel [49] 0.31 Wh/day	High	High	Medium	Unknown	Unknown	Medium	NO	In development, no access to research, avoid duplication of effort
Displacement harvester Linear generator solutions	0-1	0.31-154 J/wheel (depending on design) 0.07 – 30 Wh/day (depending on design)	High	Medium	Medium	Medium	Medium	High	YES	Design, simulations, prototype and testing
Variable reluctance harvester	1-2	2.01-11.81 J/wheel 0.73-1.84 Wh/day (depending on design and other variables)	High	Low	Low	High	Low	Medium	YES	Simulations, design, prototype manufacture, testing and analysis

Vibration harvester	2-3	0.53-1.66 mJ/wheel 0.10-0.33 mWh/day (depending on the design and track variables)	Medium	Medium	Low	High	Low	Medium	YES	Design, simulations, prototype and testing
Solar Solar panels	8-9	100-600 Wh/day/m^2 (Average for central Europe depending on time of year)	High	Low	Low	Medium	Medium	High	YES	Specification of prototype panel installation and measurement of output
Wind Commercial wind turbines	8-9	1.3 kWh/day (for 1m2 swept area of turbine, variable/intermittent, average based on estimated monthly average)	High	Low	Low	Medium	Low	High	NO	Established technology, sufficient data exists for estimating output/specifying installation

REFERENCES

[1] E. E. Aktakka and K. Najafi, “A Micro Inertial Energy Harvesting Platform With Self-Supplied Power Management Circuit for Autonomous Wireless Sensor Nodes,” *IEEE J. Solid-State Circuits*, vol. 49, no. 9, pp. 2017–2029, Sep. 2014.

[2] Z. Hadas, V. Vetiska, R. Huzlik, and V. Singule, “Model-based design and test of vibration energy harvester for aircraft application,” *Microsyst. Technol.*, vol. 20, no. 4–5, pp. 831–843, Jan. 2014.

[3] Y.-J. Yoon, W.-T. Park, K. H. H. Li, Y. Q. Ng, and Y. Song, “A study of piezoelectric harvesters for low-level vibrations in wireless sensor networks,” *Int. J. Precis. Eng. Manuf.*, vol. 14, no. 7, pp. 1257–1262, 2013.

[4] Z. Hadas, J. Kurfurst, C. Ondrusek, and V. Singule, “Artificial intelligence based optimization for vibration energy harvesting applications,” *Microsyst. Technol.*, vol. 18, no. 7–8, pp. 1003–1014, Feb. 2012.

[5] C. R. Bowen, H. A. Kim, P. M. Weaver, and S. Dunn, “Piezoelectric and ferroelectric materials and structures for energy harvesting applications,” *Energy Environ. Sci.*, vol. 7, no. 1, 2014.

[6] M. Pozzi, A. Canziani, I. Durazo-Cardenas, and M. Zhu, “Experimental characterisation of macro fibre composites and monolithic piezoelectric transducers for strain energy harvesting,” in *Smart Structures (NDE)*, 2012, p. 834832.

[7] P. Cahill, N. A. N. Nuallain, N. Jackson, A. Mathewson, R. Karoumi, and V. Pakrashi, “Energy Harvesting from Train-Induced Response in Bridges,” *J. Bridg. Eng.*, vol. 19, no. 9, p. 4014034, 2014.

[8] A. K. Batra and A. Alomari, *Power Harvesting via Smart Materials*. SPIE PRESS, 2017.

[9] N. Standard, “IEEE Standard on Piezoelectricity,” *East*, p. 74, 1988.

[10] C.-K. Lee and F. C. Moon, “Modal Sensors/Actuators,” *J. Appl. Mech.*, vol. 57, no. 2, p. 434, 1990.

[11] R. Ambrosio, A. Jimenez, J. Mireles, M. Moreno, K. Monfil, and H. Heredia, “Study of Piezoelectric Energy Harvesting System Based on PZT,” *Integr. Ferroelectr.*, vol. 126, no. 1, pp. 77–86, Jan. 2011.

[12] A. Daniels, M. Zhu, and A. Tiwari, “Evaluation of Piezoelectric Material Properties for a Higher Power Output From Energy Harvesters With Insight Into Material Selection Using a Coupled Piezoelectric- Circuit – Finite Element Method,” vol. 60, no. 12, pp. 2626–2633, 2013.

[13] S. Priya, “Criterion for material selection in design of bulk piezoelectric energy harvesters,” *IEEE Trans. Ultrason. Ferroelectr. Freq. Control*, vol. 57, no. 12, pp. 2610–2612, 2010.

[14] S. G. Kim, S. Priya, and I. Kanno, “Piezoelectric MEMS for energy harvesting,” *MRS Bull.*, vol. 37, no. 11, pp. 1039–1050, 2012.

[15] H. Li, C. Tian, Z. D. Deng, H. Li, C. Tian, and Z. D. Deng, “Energy harvesting from low frequency applications using piezoelectric materials Energy harvesting from low frequency applications using piezoelectric materials,” vol. 41301, no. 2014, pp. 0–20, 2015.

[16] L. T.-E. Nyamayoka, G. A. Adewumi, and F. L. Inambao, “Design of a prototype generator based on piezoelectric power generation for vibration energy harvestin,” *J. Energy South. Africa*, vol. 28, no. 4, Dec. 2017.

[17] A. Čeponis, D. Mažeika, and V. Bakanauskas, “Trapezoidal Cantilevers with Irregular Cross-Sections for Energy Harvesting Systems,” *Appl. Sci.*, vol. 7, no. 12, p. 134, Jan. 2017.

[18] S. Kumar, R. Srivastava, and R. K. Srivastava, “Design and analysis of smart piezo cantilever beam for energy harvesting,” *Ferroelectrics*, vol. 505, no. 1, pp. 159–183, Dec. 2016.

[19] O. Rubes and Z. Hadas, “Designing, modelling and testing of vibration energy harvester with nonlinear stiffness,” in *Smart Sensors, Actuators, and MEMS VIII*, 2017, p. 102460W.

[20] Y. C. Shu and I. C. Lien, “Analysis of power output for piezoelectric energy harvesting systems,” *Smart Mater. Struct.*, vol. 15, no. 6, pp. 1499–1512, Dec. 2006.

[21] S. Boisseau, G. Despesse, and B. A. Seddik, *Small-Scale Energy Harvesting*. InTech, 2012.

[22] S. P. Beeby, M. J. Tudor, and N. M. White, “Energy harvesting vibration sources for microsystems applications,” *Meas. Sci. Technol.*, vol. 17, no. 12, pp. R175–R195, Dec. 2006.

[23] B. Bhattacharya, “Terfenol and Galfenols : Smart Magnetostrictive Metals for Intelligent Transduction,” *Dir. Mag. (Indian Inst. od Technol. Kanpur)*, vol. 7, no. 2, pp. 35–40, 2005.

[24] V. Berbyuk and J. Sodhani, “Towards modelling and design of magnetostrictive electric generators,” *Comput. Struct.*, vol. 86, no. 3–5, pp. 307–313, Feb. 2008.

[25] T. Fan and Y. Yamamoto, “Vibration-induced energy harvesting system using Terfenol-D,” in *2015 IEEE International Conference on Mechatronics and Automation (ICMA)*, 2015, pp. 2319–2324.

[26] V. Berbyuk, “Vibration energy harvesting using Galfenol-based transducer,” vol. 8688, p. 86881F, 2013.

[27] S. Matsusaka, H. Maruyama, T. Matsuyama, and M. Ghadiri, “Triboelectric charging of powders: A review,” *Chem. Eng. Sci.*, vol. 65, no. 22, pp. 5781–5807, 2010.

[28] Z. L. Wang, L. Lin, J. Chen, S. Niu, and Y. Zi, *Triboelectric Nanogenerators*. 2016.

[29] S. Niu, S. Wang, L. Lin, Y. Liu, Y. S. Zhou, Y. Hu, and Z. L. Wang, “Theoretical study of contact-mode triboelectric nanogenerators as an effective power source,” *Energy Environ. Sci.*, vol. 6, no. 12, p. 3576, 2013.

[30] T. Jiang, X. Chen, K. Yang, C. Han, W. Tang, and Z. L. Wang, “Theoretical study on rotary-sliding disk triboelectric nanogenerators in contact and non-contact modes,” *Nano Res.*, vol. 9, no. 4, pp. 1057–1070, 2016.

[31] W. R. Harper, “The Volta Effect as a Cause of Static Electrification,” *Proc. R. Soc. A Math. Phys. Eng. Sci.*, vol. 205, no. 1080, pp. 83–103, Jan. 1951.

[32] A. F. Diaz and R. M. Felix-Navarro, “A semi-quantitative tribo-electric series for polymeric materials: The influence of chemical structure and properties,” *J. Electrostat.*, vol. 62, no. 4, pp. 277–290, 2004.

[33] Y. Zi, S. Niu, J. Wang, Z. Wen, W. Tang, and Z. L. Wang, “Standards and figure-of-merits for quantifying the performance of triboelectric nanogenerators,” *Nat. Commun.*, vol. 6, no. September, pp. 1–8, 2015.

[34] F.-R. Fan, Z.-Q. Tian, and Z. Lin Wang, “Flexible triboelectric generator,” *Nano Energy*, vol. 1, no. 2, pp. 328–334, Mar. 2012.

[35] G. Zhu, C. Pan, W. Guo, C. Y. Chen, Y. Zhou, R. Yu, and Z. L. Wang, “Triboelectric-generator-driven pulse electrodeposition for micropatterning,” *Nano Lett.*, vol. 12, no. 9, pp. 4960–4965, 2012.

[36] G. Zhu, J. Chen, Y. Liu, P. Bai, Y. S. Zhou, Q. Jing, C. Pan, and Z. L. Wang, “Linear-grating triboelectric generator based on sliding electrification,” *Nano Lett.*, vol. 13, no. 5, pp. 2282–2289, 2013.

[37] S. Wang, L. Lin, Y. Xie, Q. Jing, S. Niu, and Z. L. Wang, “Sliding-triboelectric nanogenerators based on in-plane charge-separation mechanism,” *Nano Lett.*, vol. 13, no. 5, pp. 2226–2233, 2013.

[38] S. Niu, Y. Liu, S. Wang, L. Lin, Y. S. Zhou, Y. Hu, and Z. L. Wang, “Theory of sliding-mode triboelectric nanogenerators,” *Adv. Mater.*, vol. 25, no. 43, pp. 6184–6193, 2013.

[39] Y. Yang, H. Zhang, J. Chen, Q. Jing, Y. S. Zhou, X. Wen, and Z. L. Wang, “Single-electrode-based sliding triboelectric nanogenerator for self-powered displacement vector sensor system,” *ACS Nano*, vol. 7, no. 8, pp. 7342–7351, 2013.

[40] S. Niu, Y. Liu, S. Wang, L. Lin, Y. S. Zhou, Y. Hu, and Z. L. Wang, “Theoretical investigation and structural optimization of single-electrode triboelectric nanogenerators,” *Adv. Funct. Mater.*, vol. 24, no. 22, pp. 3332–3340, 2014.

[41] S. Wang, Y. Xie, S. Niu, L. Lin, and Z. L. Wang, “Freestanding triboelectric-layer-based nanogenerators for harvesting energy from a moving object or human motion in contact and non-contact modes,” *Adv. Mater.*, vol. 26, no. 18, pp. 2818–2824, 2014.

[42] S. Wang, S. Niu, J. Yang, L. Lin, and Z. L. Wang, “Quantitative measurements of vibration amplitude using a contact-mode freestanding triboelectric nanogenerator,” *ACS Nano*, vol. 8, no. 12, pp. 12004–12013, 2014.

[43] S. Niu, Y. Liu, X. Chen, S. Wang, Y. S. Zhou, L. Lin, Y. Xie, and Z. L. Wang, “Theory of freestanding triboelectric-layer-based nanogenerators,” *Nano Energy*, vol. 12, pp. 760–774, 2015.

[44] K. Kalantar-zadeh, *Sensors*. Boston, MA: Springer US, 2013.

[45] W. Wang, R.-J. Huang, C.-J. Huang, and L.-F. Li, “Energy harvester array using piezoelectric circular diaphragm for rail vibration,” *Acta Mech. Sin.*, vol. 30, no. 6, pp. 884–888, Dec. 2014.

[46] Z. Zhang, X. Zhang, Y. Rasim, C. Wang, B. Du, and Y. Yuan, “Design, modelling and practical tests on a high-voltage kinetic energy harvesting (EH) system for a renewable road tunnel based on linear alternators,” *Appl. Energy*, vol. 164, pp. 152–161, Feb. 2016.

[47] X. Zhang, Z. Zhang, H. Pan, W. Salman, Y. Yuan, and Y. Liu, “A portable high-efficiency electromagnetic energy harvesting system using supercapacitors for renewable energy applications in railroads,” *Energy Convers. Manag.*, vol. 118, pp. 287–294, 2016.

[48] J. J. Wang, G. P. Penamalli, and L. Zuo, “Electromagnetic energy harvesting from train induced railway track vibrations,” *Proc. 2012 8th IEEE/ASME Int. Conf. Mechatron. Embed. Syst. Appl. MESA 2012*, vol. 11787, pp. 29–34, 2012.

[49] T. Lin, Y. Pan, S. Chen, and L. Zuo, “Modeling and field testing of an electromagnetic energy harvester for rail tracks with anchorless mounting,” *Appl. Energy*, vol. 213, pp. 219–226, Mar. 2018.

[50] A. Pourghodrat, “Energy Harvesting Systems Design for Railroad Safety,” p. 89, 2011.

[51] Y. Tianchen, Y. Jian, S. Ruigang, and L. Xiaowei, “Vibration energy harvesting system for railroad safety based on running vehicles,” *Smart Mater. Struct.*, vol. 23, no. 12, 2014.

[52] J. Wang, Z. Shi, H. Xiang, and G. Song, “Modeling on energy harvesting from a railway system using piezoelectric transducers,” *Smart Mater. Struct.*, vol. 24, no. 10, p. 105017, 2015.

[53] J. Kaleta, K. Kot, R. Mech, and P. Wiewiorski, “The Use of Magnetostrictive Cores for the Vibrations Generation and Energy Harvesting from Vibration, in the Selected Frequencies of Work,” *Key Eng. Mater.*, vol. 598, pp. 75–80, Jan. 2014.

[54] M. Kroener, S. K. T. Ravindran, and P. Woias, “Variable reluctance harvester for applications in railroad monitoring,” *J. Phys. Conf. Ser.*, vol. 476, no. 1, 2013.

[55] J. Smilek and Z. Hadas, “Improving power output of inertial energy harvesters by employing principal component analysis of input acceleration,” *Mech. Syst. Signal Process.*, vol. 85, pp. 801–808, Feb. 2017.

[56] Z. Hadas, V. Singule, and C. Ondrusek, “Optimal Design of Vibration Power Generator for Low Frequency,” *Solid State Phenom.*, vol. 147–149, pp. 426–431, 2009.

[57] Z. Hadas and R. Lan, “Modelling and Verification of Piezoelectric Vibration Energy Harvester,” in *Advances in Intelligent Systems and Computing*, vol. 393, 2016, pp. 305–310.

[58] J. Song and Y. K. Tan, “Energy consumption analysis of ZigBee-based energy harvesting wireless sensor networks,” in *2012 IEEE International Conference on Communication Systems, ICCS 2012*, 2012, pp. 468–472.

[59] P. Kamalinejad, C. Mahapatra, Z. Sheng, S. Mirabbasi, V. C. M. Leung, and Y. L. Guan, “Wireless energy harvesting for the Internet of Things,” *IEEE Commun. Mag.*, vol. 53, no. 6, pp. 102–108, Jun. 2015.

[60] C. Cepnik, R. Lausecker, and U. Wallrabe, “Review on Electrodynamic Energy Harvesters—A Classification Approach,” *Micromachines*, vol. 4, no. 2, pp. 168–196, Apr. 2013.

[61] M. Kim, J. Dugundji, and B. L. Wardle, “Efficiency of piezoelectric mechanical vibration energy harvesting,” *Smart Mater. Struct.*, vol. 24, no. 5, p. 55006, May 2015.

[62] A. Khaligh, P. Zeng, and C. Zheng, “Kinetic Energy Harvesting Using Piezoelectric and Electromagnetic Technologies #x2014;State of the Art,” *Ind. Electron. IEEE Trans.*, vol. 57, pp. 850–860, 2010.

[63] Z. Hadas, J. Smilek, and O. Rubes, “Analyses of electromagnetic and piezoelectric systems for efficient vibration energy harvesting,” in *Proceedings of SPIE - The International Society for Optical Engineering*, 2017, vol. 10246.

[64] V. G. Cleante, M. J. Brennan, G. Gatti, and D. J. Thompson, “Energy harvesting from the vibrations of a passing train: Effect of speed variability,” *J. Phys. Conf. Ser.*, vol. 744, no. 1, 2016.

[65] Z. Hadas, V. Vetiska, V. Singule, O. Andrs, J. Kovar, and J. Vetiska, “Energy Harvesting from Mechanical Shocks Using A Sensitive Vibration Energy Harvester,” *Int. J. Adv. Robot. Syst.*, vol. 9, p. 1, 2012.

[66] “ReVibe Energy.” [Online]. Available: https://revibeenergy.com.

[67] M. Gao, P. Wang, Y. Wang, and L. Yao, “Self-Powered ZigBee Wireless Sensor Nodes for Railway Condition Monitoring,” pp. 1–10, 2017.

[68] M. Gao, P. Wang, Y. Cao, R. Chen, and D. Cai, “Design and Verification of a Rail-Borne Energy Harvester for Powering Wireless Sensor Networks in the Railway Industry,” *IEEE Trans. Intell. Transp. Syst.*, vol. 18, no. 6, pp. 1596–1609, 2017.

[69] M. Y. Gao, P. Wang, Y. Cao, R. Chen, and C. Liu, “A rail-borne piezoelectric transducer for energy harvesting of railway vibration,” *J. Vibroengineering*, vol. 18, no. 7, pp. 4647–4663, 2016.

[70] J. Chen, G. Zhu, W. Yang, Q. Jing, P. Bai, Y. Yang, T. C. Hou, and Z. L. Wang, “Harmonic-resonator-based triboelectric nanogenerator as a sustainable power source and a self-powered active vibration sensor,” *Adv. Mater.*, vol. 25, no. 42, pp. 6094–6099, 2013.

[71] X. Wen, W. Yang, Q. Jing, and Z. L. Wang, “Harvesting Broadband Kinetic Impact Energy from Mechanical Triggering/Vibration and Water Waves,” *ACS Nano*, vol. 8, no. 7, pp. 7405–7412, 2014.

[72] W. Yang, J. Chen, Q. Jing, J. Yang, X. Wen, Y. Su, G. Zhu, P. Bai, and Z. L. Wang, “3D stack integrated triboelectric nanogenerator for harvesting vibration energy,” *Adv. Funct. Mater.*, vol. 24, no. 26, pp. 4090–4096, 2014.

[73] J. Yang, J. Chen, Y. Liu, W. Yang, Y. Su, and Z. L. Wang, “Triboelectrification-based organic film nanogenerator for acoustic energy harvesting and self-powered active acoustic sensing,” *ACS Nano*, vol. 8, no. 3, pp. 2649–2657, 2014.

[74] X. Fan, J. Chen, J. Yang, P. Bai, Z. Li, and Z. L. Wang, “Ultrathin, rollable, paper-based triboelectric nanogenerator for acoustic energy harvesting and self-powered sound recording,” *ACS Nano*, vol. 9, no. 4, pp. 4236–4243, 2015.

[75] L. Zhang, L. Jin, B. Zhang, W. Deng, H. Pan, J. Tang, M. Zhu, and W. Yang, “Multifunctional triboelectric nanogenerator based on porous micro-nickel foam to harvest mechanical energy,” *Nano Energy*, vol. 16, pp. 516–523, 2015.

[76] Y. K. Ramadass and A. P. Chandrakasan, “An Efficient Piezoelectric Energy Harvesting Interface Circuit Using a Bias-Flip Rectifier and Shared Inductor,” *IEEE J. Solid-State Circuits*, vol. 45, no. 1, pp. 189–204, Jan. 2010.

[77] Y. C. Shu, I. C. Lien, and W. J. Wu, “An improved analysis of the SSHI interface in piezoelectric energy harvesting,” *Smart Mater. Struct.*, vol. 16, no. 6, pp. 2253–2264, 2007.

[78] S. Lu and F. Boussaid, “A highly efficient P-SSHI rectifier for piezoelectric energy harvesting,” *IEEE Trans. Power Electron.*, vol. 30, no. 10, pp. 5364–5369, 2015.

[79] A. Badel, D. Guyomar, E. Lefeuvre, and C. Richard, “Efficiency Enhancement of a Piezoelectric Energy Harvesting Device in Pulsed Operation by Synchronous Charge Inversion,” *J. Intell. Mater. Syst. Struct.*, vol. 16, no. 10, pp. 889–901, Oct. 2005.

[80] D. Guyomar, A. Badel, E. Lefeuvre, and C. Richard, “Materials and Conversion Improvement by Nonlinear Processing,” vol. 52, no. 4, pp. 584–595, 2005.

[81] E. Lefeuvre, A. Badel, C. Richard, L. Petit, and D. Guyomar, “A comparison between several vibration-powered piezoelectric generators for standalone systems,” *Sensors Actuators, A Phys.*, vol. 126, no. 2, pp. 405–416, 2006.

[82] E. Lefeuvre, A. Badel, A. Benayad, L. Lebrun, C. Richard, and D. Guyomar, “A comparison between several approaches of piezoelectric energy harvesting,” *J. Phys. IV*, vol. 128, pp. 177–186, Sep. 2005.

[83] “Datasheet: MAX17710.” [Online]. Available: https://datasheets.maximintegrated.com/en/ds/MAX17710.pdf.

[84] X.-D. Do, S.-K. Han, and S.-G. Lee, “Optimization of piezoelectric energy harvesting systems by using a MPPT method,” *2014 IEEE Fifth Int. Conf. Commun. Electron.*, pp. 309–312, 2014.

[85] J. Yi, F. Su, Y. H. Lam, W. H. Ki, and C. Y. Tsui, “An energy-adaptive MPPT power management unit for micro-power vibration energy harvesting,” *Proc. - IEEE Int. Symp. Circuits Syst.*, pp. 2570–2573, 2008.

[86] C. Lu, C.-Y. Tsui, and W.-H. Ki, “Vibration Energy Scavenging System With Maximum Power Tracking for Micropower Applications,” *IEEE Trans. Very Large Scale Integr. Syst.*, vol. 19, no. 11, pp. 2109–2119, 2011.

[87] B. M. Lee, “Application Note 82 November 1999 Understanding and Applying Voltage References Application Note 82 AN82-2,” *Translator*, no. November, pp. 1–12, 1999.

[88] C. Wang, “an Ultra-Low Power Voltage Regulator System for Wireless Sensor Networks Powered By Energy Harvesting,” p. 137, 2014.

[89] G. Palumbo, D. Pappalardo, and M. Gaibotti, “Charge pump circuits: power consumption optimization - a summary,” *IEEE Circuits Syst. Mag.*, vol. 4, no. 3, pp. 0–3, 2004.

[90] J. Heitz, V. Frick, N. Dumas, N. Weber, C. Lallement, and L. Hébrard, “Modeling and optimization of a latched charge pump loaded by a resistive circuit,” *Analog Integr. Circuits Signal Process.*, vol. 83, no. 3, pp. 353–367, 2015.

[91] G. K. Ottman, H. F. Hofmann, A. C. Bhatt, and G. A. Lesieutre, “Adaptive piezoelectric energy harvesting circuit for wireless remote power supply,” *IEEE Trans. Power Electron.*, vol. 17, no. 5, pp. 669–676, 2002.

[92] S. Boisseau, P. Gasnier, M. Perez, C. Bouvard, M. Geisler, A. B. Duret, G. Despesse, and J. Willemin, “Synchronous Electric Charge Extraction for multiple piezoelectric energy harvesters,” *Conf. Proc. - 13th IEEE Int. NEW Circuits Syst. Conf. NEWCAS 2015*, no. i, pp. 8–11, 2015.

[93] G. Chowdary and S. Chatterjee, “A 300-nW sensitive, 50-nA DC-DC converter for energy harvesting applications,” *IEEE Trans. Circuits Syst. I Regul. Pap.*, vol. 62, no. 11, pp. 2674–2684, 2015.

[94] C. Gillott, “Third Edition,” *Evolution (N. Y).*, 1998.

[95] M. Day, “Understanding Low Drop Out (LDO) Regulators,” *Texas Instruments, Dallas*, pp. 1–6, 2002.

[96] “Datasheet: bq25504.” [Online]. Available: http://www.ti.com/lit/ds/symlink/bq25504.pdf.

[97] “Datasheet: LTC3588-1.” [Online]. Available: http://www.analog.com/media/en/technical-documentation/data-sheets/35881fc.pdf.

[98] “Datasheet: ADP5090.” [Online]. Available: http://www.analog.com/media/en/technical-documentation/data-sheets/ADP5090.pdf.

[99] “Solar Capture Technologies.” [Online]. Available: http://www.solarcapturetechnologies.com/.

[100] H. Hayashiya, H. Itagaki, Y. Morita, Y. Mitoma, T. Furukawa, T. Kuraoka, Y. Fukasawa, and T. Oikawa, “Potentials, peculiarities and prospects of solar power generation on the railway premises,” in *2012 International Conference on Renewable Energy Research and Applications (ICRERA)*, 2012, pp. 1–6.

[101] H. Hayashiya, S. Kikuchi, K. Matsuura, M. Hino, M. Tojo, T. Kato, M. Ando, T. Oikawa, M. Kamata, and H. Munakata, “Possibility of energy saving by introducing energy conversion and energy storage technologies in traction power supply system,” in *2013 15th European Conference on Power Electronics and Applications (EPE)*, 2013, pp. 1–8.

[102] P. Vorobiev and Y. Vorobiev, “Automatic sun tracking solar electric systems for applications on transport,” in *2010 7th International Conference on Electrical Engineering Computing Science and Automatic Control*, 2010, pp. 66–70.

[103] N. Popovic, G. Feltrin, K.-E. Jalsan, and M. Wojtera, “Event-driven strain cycle monitoring of railway bridges using a wireless sensor network with sentinel nodes,” *Struct. Control Heal. Monit.*, vol. 24, no. 7, p. e1934, Jul. 2017.

[104] “Greenrail Group.” [Online]. Available: http://www.greenrailgroup.com/en/rd-2/.

[105] “Wholesale Solar.” [Online]. Available: https://www.wholesalesolar.com/4913034/primus-windpower/wind-turbines/primus-windpower-air-40-12v-1-ar40-10-12.

[106] “Primus Windpower.” [Online]. Available: http://www.primuswindpower.com/wind-power-products/air-40-turbine/.

[107] “Leading Edge - Vertical Axis Turbine.” [Online]. Available: https://www.leadingedgepower.com/shop/store/wind-turbines/vertical-axis-wind-turbines/le-v150-vertical-axis-turbine-1121392.html.

[108] D. A. Howey, A. Bansal, and A. S. Holmes, “Design and performance of a centimetre-scale shrouded wind turbine for energy harvesting,” *Smart Mater. Struct.*, vol. 20, no. 8, p. 85021, Aug. 2011.

[109] S. Li and H. Lipson, “Vertical-Stalk Flapping-Leaf Generator for Wind Energy Harvesting,” in *Volume 2: Multifunctional Materials; Enabling Technologies and Integrated System Design; Structural Health Monitoring/NDE; Bio-Inspired Smart Materials and Structures*, 2009, pp. 611–619.

[110] S. Priya, “Modeling of electric energy harvesting using piezoelectric windmill,” *Appl. Phys. Lett.*, vol. 87, no. 18, p. 184101, Oct. 2005.

[111] “T-BOX Wind Power Generator.” [Online]. Available: http://t-boxwindpowergenerator.blogspot.co.uk/2014/12/t-box-wind-power-generator-report.html.

[112] S. Holmberg, A. Perebikovsky, L. Kulinsky, and M. Madou, “3-D Micro and Nano Technologies for Improvements in Electrochemical Power Devices,” *Micromachines*, vol. 5, no. 2, pp. 171–203, Apr. 2014.

[113] “Photovoltaic Geographical Information System - Interactive Maps.” [Online]. Available: http://re.jrc.ec.europa.eu/pvgis/apps4/pvest.php.

[114] I. Troen and E. Lundtang Petersen, *European wind atlas*. 1989.

[115] “Trade-off analysis for on-board and track-side communication systems,” *Etal. Proj. Deliv. Rep.*, vol. WP3, no. D3.1, 2018.